OPTIMAL FORMS OF RECTANGULAR-BASE, SHALLOW SHELLS WITH RESPECT TO BUCKLING

by

David T. Young

Dissertation submitted to the Faculty of the
Virginia Polytechnic Institute and State University
in partial fulfillment of the requirements for the degree of
DOCTOR OF PHILOSOPHY
in
Civil Engineering

APPROVED:

R. H. Plaut, Chairman

R. M. Baker

L. W. Johnson

M. Holzer

A. E. Somers

June, 1985

Blacksburg, Virginia

2/3/86 MCR

OPTIMAL FORMS OF RECTANGULAR-BASE, SHALLOW SHELLS WITH RESPECT TO BUCKLING

by

David T. Young

(ABSTRACT)

Thin, elastic, shallow shells having uniform thickness and rectangular boundaries are investigated. The boundary conditions are either simply supported or clamped, and the shell is subjected to a uniformly distributed load applied over either the full shell area or a central region. The thickness, material properties, edge lengths, and surface area of the shell are specified, and the objective is the determination of the shell shape which will maximize the buckling load.

Marguerre's two, coupled, non-linear equations of equilibrium are used to describe prebuckling deformations and stresses. Considering small vibrations about the equilibrium state, two, coupled, linear equations of motion are derived. Subsequently, by recognizing that at buckling the lowest frequency of vibration goes to zero, the buckling equations are obtained. Finally, the Lagrange multiplier technique is employed to formulate an augmented objective function, and the calculus of variations is applied in order to derive the governing set of equations. The resulting system of equations is solved numerically by the finite difference method.

Results for shells with various surface areas are presented. For each surface area the investigation is performed on shells having either

clamped or simply supported boundary conditions and either a square or a rectangular boundary. The applied uniform load covers either the full shell area or a partial central region. The shell form, buckling load, and buckling modes of the optimal forms are compared with those of the reference form (double sine) having the same surface area, and changes are noted. Also, comparisons with respect to forms, buckling load, and type of buckling are made between the optimal form of a shell subjected to a full uniform load and the optimal form of the same shell subjected to a partial uniform load.

In some cases, the buckling load of the optimal form is sensitive to imperfections in the form or in the loading distribution as well as to changes in the design. In these cases, some of the apparent advantages of the optimum form may be diminished. Thus, the frequencies of vibration at buckling, the corresponding buckling modes, and the presence of adjacent equilibrium states are monitored in order to evaluate the sensitivity of the optimal form to imperfections and to design changes.

ACKNOWLEDGMENTS

I wish to express my sincere gratitude to my advisor, Dr. Ray Plaut, for his many hours of guidance and consultation. His advice and expertise with respect to this dissertation were essential and are genuinely appreciated. Of equal importance were his suggestions and encouragements with respect to professional and personal matters.

I also express my appreciation to the members of my committee, Drs. R. M. Barker, S. M. Holzer, L. W. Johnson, and A. E. Somers, for their support of the research and for their critical reviews of the manuscript. Dr. Johnson was instrumental in the development and application of the numerical analysis techniques, and Dr. Somers provided assistance with respect to the use of the computer facilities.

I gratefully acknowledge the financial support provided by Dr. Plaut through a graduate research assistantship under National Science Foundation Grant No. CEE-8210222. Also, the Civil Engineering Department is acknowledged for providing an opportunity for study and additional financial assistance.

Finally, I wish to thank my family for their love and continued interest. But my deepest thanks is given to , , and , to whom this work is dedicated, for providing me with much needed love and support and with an unending source of inspiration.

TABLE OF CONTENTS

LIST OF TABLES

LIST OF FIGURES

Chapter 1

INTRODUCTION

For thousands of years shell forms have appeared in man's structures. In the earliest days of construction the "shell" was used for shelters, for utilitarian structures, and above all for symbolic structures such as tombs, temples, and monuments. From such a simple beginning, the understanding of shell behavior has progressed from experimenting with a few, practical forms to that of mathematically modelling many complicated forms. Coincidentally, the ability to analyze various shell forms has resulted in the application of the shell to a wider variety of structural problems ranging from soft drink cans to space vehicles.

Regardless of the specific application, the shell has certain features that are beneficial to the engineer, contractor, and architect. Engineers and contractors design and build shell structures because of the inherent ability of these structures to cover large areas while requiring a minimum amount of construction material and no intermediate supports. Many architects find the shell shapes aesthetically pleasing on the exterior, and the absence of interior supports creates more options for interior design.

The increase in the popularity of shell forms has brought about certain problems that unfortunately are overlooked by many designers. The development of shell theory has resulted in the production of design aids for certain standardized forms. Thus, the designer is

not required to fully understand the more advanced theory associated with more complicated shell forms and, therefore, he does not use them. He is able to take a "least work" approach to the design. This type of design is not always preferable or safe. In addition to eliminating the chance for a more aesthetically pleasing design, the design aids may be applied to a range of shell dimensions for which they are invalid.

Additional problems with respect to shell behavior have resulted from such "play safe" designs. In the last twenty-five years, the spans of shells have become very large. This fact combined with requirements for economical construction and for material reduction has resulted in thickness to curvature ratios equalling 1:500 and less [1]. Consequently, where the "old" shells (ratios of 1:150 and greater) had a thickness dictated by the requirements of construction technology, and hence had a great reserve of strength and stability, the new shells have no such reserve. Designing the "new" shells by the "old" techniques may be inadequate without considering stability. Thus, the most important factor influencing the shell thickness and the shell form itself may well be the buckling resistance of the shell [2].

1.1 Objectives

The objectives of this study are summarized as follows:

(1) To determine the effect of the shell form upon the buckling load. By allowing the shell form to vary while keeping all other shell parameters constant, the shell form is determined which maximizes the buckling load.

(2) To generate the optimal forms of shells having different values of parameter sets (surface area, aspect ratio, boundary conditions, and region under load), and to compare the various parameter sets with respect to optimal form and buckling load.

(3) To monitor the type of buckling associated with each optimal form in order to evaluate the sensitivity of the buckling load to imperfections.

(4) To formulate the problems described above by using optimization techniques and the calculus of variations so as to permit a solution through mathematical analysis from an optimization point of view.

(5) To approximate the mathematical analysis mentioned in (4) by use of a numerical technique and to develop a computer program to generate the problem solution.

(6) To review the pertinent literature so as to offer a background for this study, to inform the reader of related work, and to offer suggestions for further research related to this study.

1.2 Purpose and Scope

Shell optimization problems are classified according to the function(s) being optimized. In this study three investigations are conducted with respect to the optimization of shell forms. First, the effect of buckling upon the shell form is evaluated; that is, for a given volume of material, the shell form is determined which has the

greatest buckling load. Secondly, the effects of full uniform load versus partial uniform load upon various shell forms are evaluated. Finally, optimal shells are evaluated to determine sensitivity to imperfections.

To obtain solutions to the problems mentioned above, the governing equations are formulated and boundary conditions are determined. Prebuckling deformations and stresses are described by Marguerre's two, coupled, non-linear equations of equilibrium. By applying small vibrations about the equilibrium state and linearizing, the two linear equations of motion are obtained. Separating variables in the motion equations results in the vibration equations. Then, by recognizing that at buckling the lowest frequency of vibration goes to zero [3-5], the buckling equations are obtained. The Lagrange multiplier technique is employed to form an augmented objective function, and the calculus of variations is applied to determine the governing set of equations. Finally, the boundary conditions are determined by evaluating the strain-displacement and stress-strain relationships and through a variational process.

The solution procedure consists of an iterative finite difference technique. For a given set of shell parameters including thickness, edge lengths, material properties, and surface area, the applied load intensity and shell form are permitted to vary. For a specified shell form, a load is applied and the equilibrium deformations and stresses and the lowest frequency of vibration are determined. As the load is increased incrementally, the lowest frequency goes to zero, and the load corresponding to the zero frequency is the buckling load.

Once these results are obtained, the optimality equation is used to obtain a new shell form. The procedure is then repeated in order to determine the buckling load of this new form and generate yet another shell form. The optimal form is obtained when no increase in buckling load is achieved by generating additional forms.

Certain restrictions are placed upon the shells being considered in order to make the problems tractable. Thin, elastic, shallow shells supported along a rectangular boundary in a horizontal plane are considered. The boundary conditions are either clamped or simply supported, and in either case the in-plane displacements at the boundaries are assumed to be zero. Shells having curved edges are not treated. The applied load is a static, transverse, uniform load located over either the full shell area or a central rectangular region.

The results of this study are presented in three categories. First, the optimal forms are presented for three shells having different surface areas. For each surface area, results are given for both clamped and simply supported boundary conditions and for square or rectangular boundaries. The shapes and buckling loads of each optimal form are compared to those of a reference form (double-sine) having the same surface area and boundary conditions. Changes in form and in buckling load are noted. Secondly, three shells having different surface areas are optimized under a full uniform load and under a partial uniform load for both clamped and simply supported boundary conditions. The optimal form and corresponding buckling load are compared to those of the standard form, and changes are noted. Finally, the type of buckling (limit point, bifurcation point, or

bimodal) for each optimal form is monitored, and the effects of imperfections and design changes upon the buckling load are noted.

1.3 Literature Review

A brief review of pertinent literature in the areas of shell stability and structural optimization is presented in the sections that follow. The number of articles and books available on these topics is substantial, and certainly all of them cannot be listed here. However, a number of publications are described in an effort to review a representative sample of the literature and to provide the reader with reference lists that will assist in further review.

1.3.1 Stability of Shells

To the layman and to many engineers, buckling is a somewhat mysterious phenomenon. In response to this mystique, several papers present a general overview of stability. Bushnell [6] attempts to convey to the reader an intuitive understanding of shell instability and leaves the development of equations predicting instability to other sources [7-9]. He covers a wide variety of related topics ranging from the basics of buckling behavior to suggested design methods. He also offers literature reviews on several aspects of shell stability including stiffened panels and modal interaction and provides an extensive reference list to assist in further review. The contribution of stability to the total design is outlined by Medwadowski [10,11] who, in [10], provides a discussion of the buckling phenomenon and the methods of investigating buckling. Also included in [10] is a review of the papers presented at the 1979 World Congress on Shell and Spatial

Structures (First Theme) in Madrid, Spain. All papers address the buckling of shell and spatial structures. The factors influencing shell buckling--shell geometry, method of support, material distribution, nature and manner of loading--are discussed in [12,13].

In the past three decades, several factors--the advent of the computer, improvements to numerical solution techniques, a better understanding of non-linear theories, more sophisticated application of shell structures--have permitted the constant growth of research in the area of shell stability. Originally, many investigations were performed on spherical shells of revolution. Several papers investigate the phenomenon of snap-buckling of spherical shells of revolution under uniform lateral load [14-17] or under a concentrated load at the apex [18,19]. Classical solutions for the buckling of spherical shells of revolution are presented [20,21]. These results compare well with results obtained by finite differences [22-24] and by series expansions [25-27]. A good review of research on buckling of spherical caps is given by Fung and Kaplan [27].

As more emphasis was placed on the development of space and marine vehicles, some of the research effort shifted to the analysis of shallow, isotropic shells on a rectangular planform. Haydl [28] conducted a theoretical investigation of the non-linear behavior of thin shells under uniform lateral load and having a constant initial curvature. Rushton [29], on the other hand, evaluated the buckling of thin shells under uniform lateral load and having a non-constant initial curvature. A dynamic relaxation method was employed to obtain solutions for shells having square or rectangular planform and simply

supported or clamped boundaries. A non-linear analysis was performed [30] on doubly curved shells (spherical, parabolic) subjected to uniform lateral loading. The solution to the snap-through buckling problem was obtained through the use of the finite difference and the Newton-Raphson techniques, and the load deflection curves were plotted. Archer and Hsueh [31,32] also employed the finite difference and Newton-Raphson techniques to evaluate the buckling of spherical shells subjected to uniform transverse load. Results were plotted in a series of load-deflection curves. Marshall and Rhodes [33] presented a theoretical analysis for the snap-through buckling of thin shells having clamped or simply supported edges and subjected to a uniform or concentrated load. Results were presented graphically. In a more general sense, Volmir [34] investigated the buckling of shallow shells under uniform transverse load using the "assumed mode type" approximate solutions. It should be noted that many of the papers mentioned in this paragraph include results for cylindrical shells. Being much simpler to model and analyze, cylindrical shells provide the test cases for the verification of the analysis of some of the more complicated problems.

In recent years, the finite element analysis of shell buckling and the analysis of buckling of orthotropic shells have received much attention. Although not directly related to this study, a few papers discussing shells on rectangular planform are mentioned below for the benefit of the reader. For additional information, Gallagher [35] conducts a survey of finite element models used in the non-linear analysis of shell structures. Finite element formulations are presented

which result in displacement or stiffness models [36,37] and mixed models [38-42]. The results of the mixed model are compared to displacement model results [39], and load-deflection curves are presented for cylindrical and spherical shells having clamped and simply supported boundary conditions [39-42]. Also, a good review of finite element work in the area of non-linear analysis of shells is presented [39,40]. The application of finite elements is presented for the non-linear analysis of cylindrical shells [43-47] and spherical shells [48,49]. Finally, the snap-buckling of thin, laterally loaded spherically curved shells made of reinforced plastic is investigated [50-55]. Results for uniform or concentrated load, simply supported or clamped boundaries, and various aspect ratios are presented in the form of load-deflection curves [55].

1.3.2 Optimal Design of Shells

The area of structural optimization has been actively researched in the past three decades [56-62]. Research activity continues to increase as evidenced by the number of recent conferences on the subject. A NATO Advanced Study Institute on Optimization of Distributed Parameter Structures was held in Iowa in 1980 [63]. A NATO Advanced Study Institute on large-scale optimization problems was held in Belgium in 1980. An International Symposium on Optimal Structural Design was held in Arizona in 1981 [64], and a Euromech Colloquium on Optimization Methods in Structural Design was held in West Germany in October, 1982.

Much attention has been given to the optimal design of shells. One category of shell optimization involves stiffened or reinforced shells in which the objective is the determination of the optimum relationship between shell thickness, stiffener spacing and stiffener size [65-73]. Many investigations have been conducted in which the form of the shell is held constant but the thickness of the shell material is redistributed in order to minimize stress [74-98]. Some studies [99-101] have been conducted in which the shell has a uniform thickness, but the shell form is varied in order to minimize the weight, while satisfying stress constraints. Another group of papers [99,100,102-110] addresses the optimization of pressure vessel heads in which membrane theory is almost always used. The thickness is constant, and the optimum shape is determined within a restricted class of functions.

The optimal design of shells in which buckling is a constraint has also received some attention. Examples of such studies [111-114] include the determination of the opening angle of a spherical shell subjected to uniform pressure and the optimum form and cross-sectional thickness of a cylindrical shell subjected to pure bending [111]; the determination of the minimum weight of a cylindrical shell subjected to combined bending and torsion [114]; the determination of the maximum load bearing capacity of a certain class of shapes having constant thickness [112]; and the determination of the minimum weight of axisymmetric shells under non-uniform axisymmetric pressure subjected to constraints on bifurcation instability and allowable stresses [113].

Several other papers provide further insight into the variety of problems encountered in the optimal design of shells. These studies address the optimum design of cooling towers [115-116]; the optimum cross-section contour of a cylinder having constant thickness and subjected to bending and torsion [117]; the optimum design of cylindrical bins [118]; and the optimum design of airplane wings [119].

More specifically related to this work are the studies in which the objective is the optimization of the shell form (shape) with respect to certain constraints while the shell thickness remains constant. Although this particular class of problems has been a popular topic for research in the last few years, modifying the shell form has long been recognized as a means of altering the shell strength. Medwadowski [2,11] discusses the factors that influence the form of a shell, and he traces the development of shell theory and the history of the traditional forms [2]. In the period of shell construction before analytical solutions were fully established, the effects of varying the shell form on the shell behavior were monitored through experimentation on models [120-122]. This approach was used in a great majority of the shell projects of the renowned designer, Dr. Hans Isler [123,124]. One noted exception to the experimental approach was that of well-known shell builder Felix Candela whose works displayed a dazzling variety of shapes. Candela recognized that by using doubly ruled surfaces he could create more aesthetically pleasing and stronger shell forms of which the hyperbolic paraboloid is the most famous [125,126].

As the theories for the optimization of shell forms have been developed, investigations have been performed which consider a variety of constraints. Some of the topics are natural extensions of similar work performed on the optimal design of arches [127-131], whereas others are more original in scope. The optimal form of shells with circular or triangular planform was determined in order to eliminate bending and minimize a surface integral of membrane stresses [132]. For shells on point-like supports, the form was determined which eliminated bending stress and placed the shell in a membrane stress situation [133]. Stadler [134] performed a multicriteria optimization in order to determine the shell form which simultaneously minimized the shell mass and strain energy. Haug [135] and Day [136] determined the optimum form of shells using an approach in which the optimization criterion was the state of stress. Plaut, Johnson, and Parbery [137] and Plaut and Johnson [3,138] determined the optimal forms of thin, shallow, elastic shells having uniform surface area, constant thickness, and circular boundaries. The optimization criteria included the maximum fundamental frequency [137], the maximum buckling load [138], and the maximum enclosed volume [3].

In summary, articles and books have been reviewed which are related to this dissertation. Much work has been done in the area of shell stability, but relatively little research has been performed on the stability of shells having rectangular planform and having no curvature along the boundaries. Also, extensive work has been done in the area of the optimum design of shells, but comparably little research has been performed on the determination of optimum shell forms.

Although a few articles addressed the effect of the shell form upon the buckling resistance of the shell, no publications were found that investigated the determination of the shell form that maximizes the buckling load for shells that have rectangular planform and no curvature along the boundaries.

CHAPTER 2

PROBLEM DEFINITION

This chapter contains a description of the shallow, elastic shell under investigation. Particular attention is given to describing the shell form, the applied load, the boundary conditions, and other shell parameters.

2.1 Description of the Shell Form

The initial configuration of the shell is shown in Figure 2.1. The boundaries are rectangular, and the initial form may or may not be described by a known geometric shape (double-sine, circular, or parabolic). In any case, however, there is no curvature along the boundaries. The X, Y, and Z axes are aligned according to the right-hand rule and have displacements, U, V, W, associated with them, respectively. The shell lies above the X-Y plane. The cross-section through the center of the shell is shown in Figure 2.1b. The initial configuration of the shell at any point (X,Y) is given by WO(X,Y), and the vertical displacement at equilibrium is given by W(X,Y). WO(X,Y) is positive in the positive Z direction, whereas W(X,Y) is positive in the negative Z-direction.

2.2 Description of the Applied Load

The shell is subjected to two types of uniform, transverse loads (Figures 2.2a, 2.2b). The full uniform load (Figure 2.2a) and the partial uniform load (Figure 2.2b) are symmetric, act downward, and

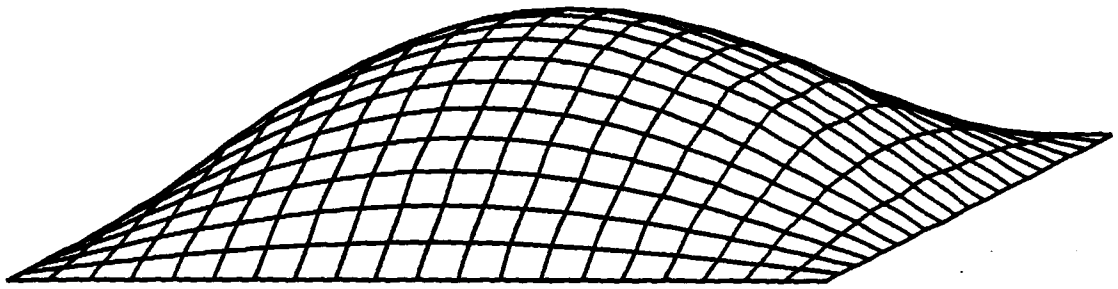

(a) Perspective of the Shell

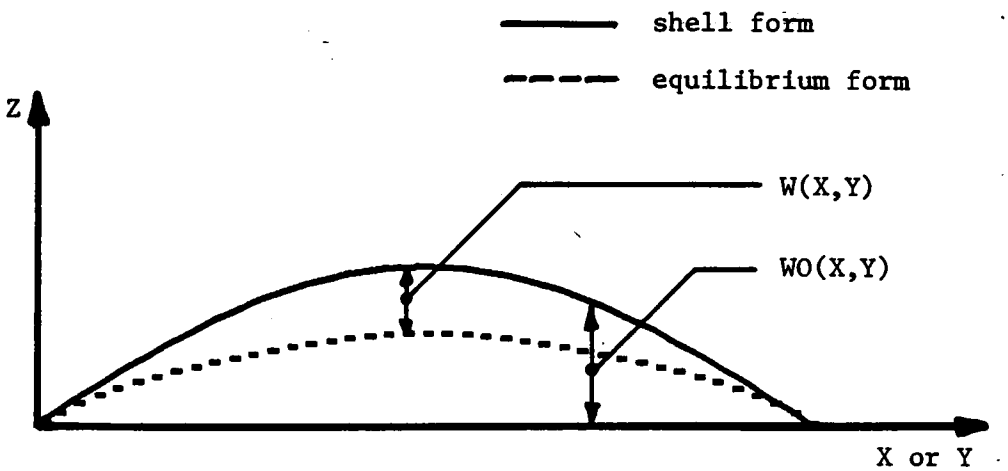

(b) Cross Section Through the Shell Center

Figure 2.1: Description of the Shallow Shell

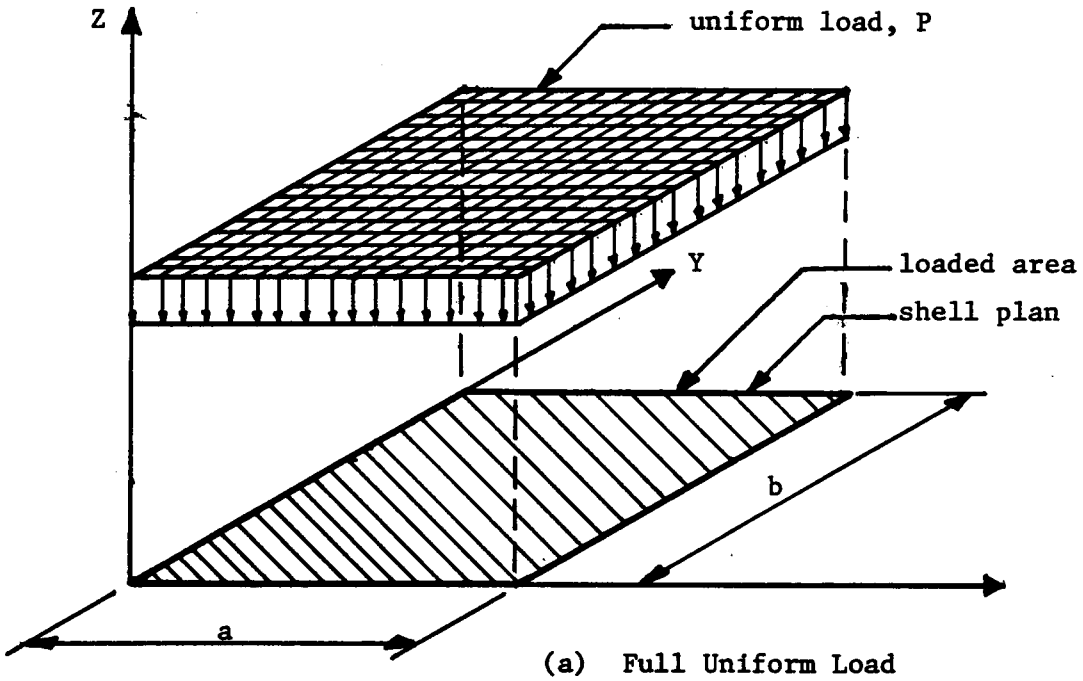

(a) Full Uniform Load

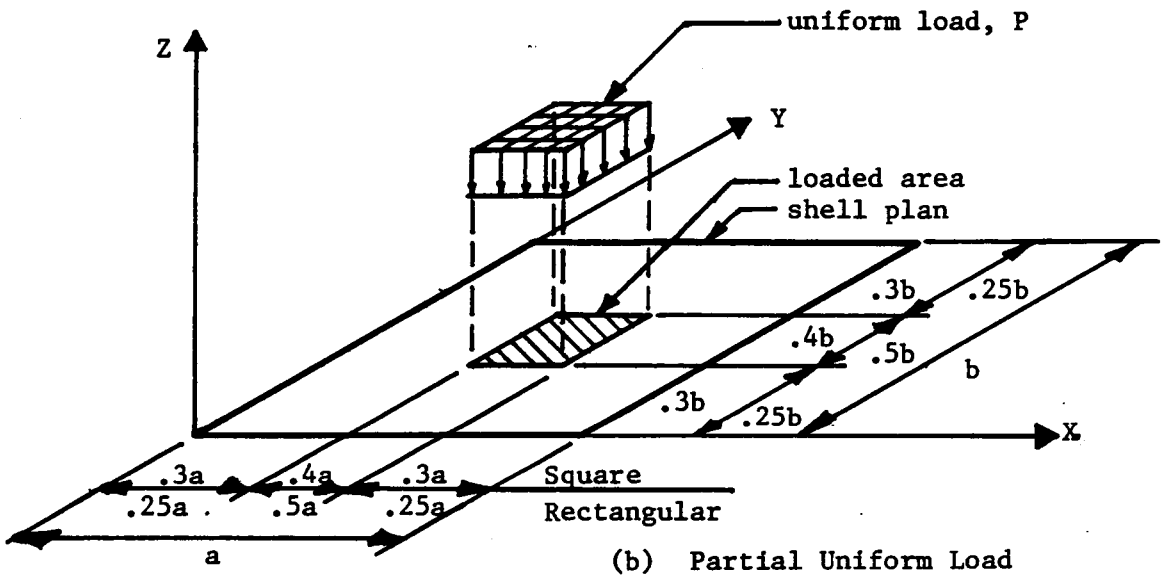

(b) Partial Uniform Load

Figure 2.2: Description of the Applied Load

are assigned initial magnitudes which permit the determination of the buckling load through iteration. It should be noted that the magnitude of the applied load itself is used in solving the finite difference equilibrium equations instead of using a mesh point load calculated from tributary areas. A more detailed explanation of this fact is offered in Chapter 3.

2.3 Description of the Boundary Conditions

The boundary conditions on the shell are either clamped (Figure 2.3a) or simply supported (Figure 2.3b). The displacements and the corresponding derivatives which are equal to zero along each boundary are indicated in the appropriate figures. Since the tangential displacements are zero along the boundaries for each case, the in-plane (membrane) stresses along the boundaries are not equal to zero and must be accounted for in the problem solution. These boundary conditions for stresses are derived and discussed in detail in Chapter 3.

2.4 Description of the Shell Parameters

Certain shell parameters (material properties, thickness, and edge lengths) are non-dimensionalized during the analysis. Thus, the actual magnitudes of these constants have no direct effect on the solutions but only appear in some non-dimensional parameters. However, in order to compare with the results of other investigations, the following values are assigned:

E = Elastic Modulus = 29 ksi

ν = Poisson's Ratio = 0.30

h = Shell Thickness = 1.00 in

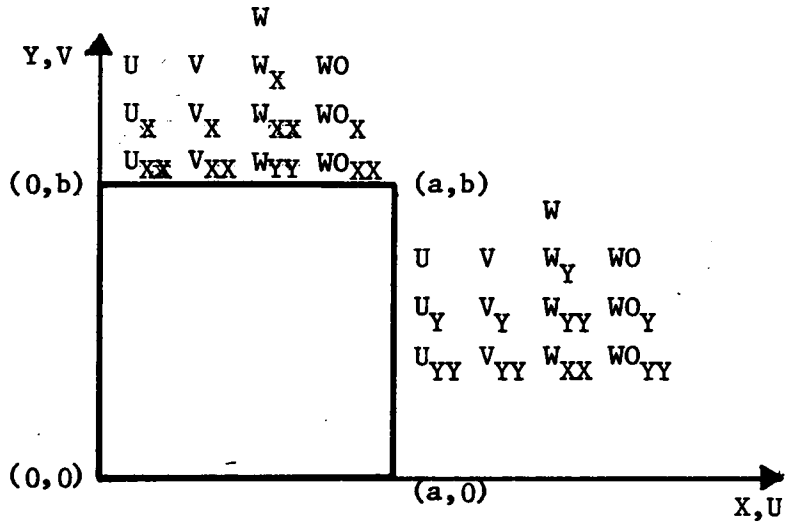

(a) Simply Supported

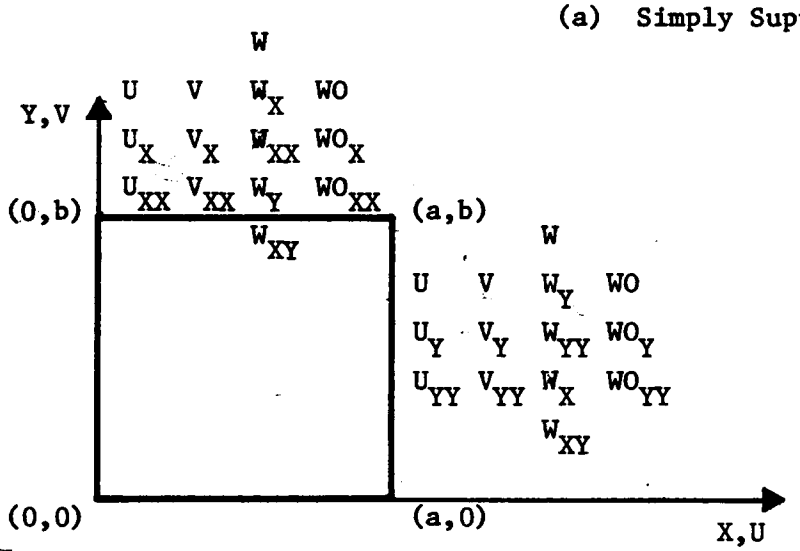

(b) Clamped

Figure 2.3: Description of the Boundary Conditions

a = Edge Length in x-direction = 20 ft

b = Edge Length in y-direction = 20 ft (square), 30 ft (rectangular)

The numerical results are not restricted to these values of E, ν, h, a, and b.

The shell surface area is also held constant during a particular problem solution. However, after the solution to one problem has been obtained, the surface area is changed, and an altogether new problem is solved. Non-dimensionalization of the surface area (as discussed in Chapter 3) results in a surface area coefficient which, in conjunction with a constant thickness, serves as an indicator of the volume of shell material. This surface area coefficient, β^2, provides the method of classifying the shells being optimized in this investigation.

CHAPTER 3

PROBLEM FORMULATION

The general theories of plates [139-142] and shells [139,141-148] are well-studied and well-documented, and the references listed offer a small, representative sample of the literature available on these topics. The reader is advised to refer to the bibliography given by Flügge [143] for a brief review of the fundamental publications on general shell theory. These basic concepts provide the foundation for the formulation described in the sections that follow.

3.1 Derivation of the Equilibrium and Compatibility Equations

The analysis of shell buckling requires the ability to determine the displacements and stresses at equilibrium just prior to buckling. Linear analysis (small-deflection theory) is inadequate in this respect, and a non-linear analysis (large-deflection theory) is required. The formulation of the non-linear equations of shell equilibrium can be accomplished by using the equations of plate equilibrium and then including initial deflection terms to generate the shell equations.

The equations of plate equilibrium are given by [140]

$$D\nabla^4 \cdot W - N_x \cdot \frac{\partial^2 W}{\partial X^2} - 2 \cdot N_{xy} \cdot \frac{\partial^2 W}{\partial X \partial Y} - N_y \cdot \frac{\partial^2 W}{\partial Y^2} = P \tag{3.1}$$

$$\frac{\partial N_x}{\partial X} - \frac{\partial N_{xy}}{\partial Y} = 0 \tag{3.2}$$

$$\frac{\partial N_y}{\partial Y} - \frac{\partial N_{xy}}{\partial X} = 0 \tag{3.3}$$

where

D = plate stiffness, $\frac{Eh^3}{12(1-\nu^2)}$

∇^4 = biharmonic operator, $\frac{\partial^4}{\partial X^4} + 2 \cdot \frac{\partial^4}{\partial X^2 \partial Y^2} + \frac{\partial^4}{\partial Y^4}$

W = transverse displacement, downward

P = transverse uniform load

When in-plane terms are neglected, one obtains the linear equation [140]

$$D \cdot \nabla^4 W = P \tag{3.4}$$

However, for the shell problems, the in-plane terms are retained and equations (3.1) - (3.3) are used. By utilizing Airy's stress function, $\phi(X,Y)$, equation (3.1) is modified and equations (3.2) and (3.3) are satisfied automatically. Letting

$$N_x = h \frac{\partial^2 \phi}{\partial Y^2} \quad , \quad N_y = h \frac{\partial^2 \phi}{\partial X^2} \quad , \quad N_{xy} = - h \frac{\partial^2 \phi}{\partial X \partial Y} \tag{3.5}$$

and substituting (3.5) into (3.1) yields

$$D\nabla^4 W - h \left[\frac{\partial^2 \phi}{\partial Y^2} \cdot \frac{\partial^2 W}{\partial X^2} + \frac{\partial^2 \phi}{\partial X^2} \cdot \frac{\partial^2 W}{\partial Y^2} - 2 \cdot \frac{\partial^2 \phi}{\partial X \partial Y} \cdot \frac{\partial^2 W}{\partial X \partial Y} \right] = P \tag{3.6}$$

Equation (3.6) represents plate equilibrium in terms of $W(X,Y)$ and $\phi(X,Y)$. In order to solve for these two unknowns, another equation is required which relates stresses to displacements. This equation of compatibility is derived by expressing the strain-displacement relations as [140]

$$\varepsilon_x = \frac{\partial U}{\partial X} + \frac{1}{2}\left(\frac{\partial W}{\partial X}\right)^2 \tag{3.7a}$$

$$\varepsilon_y = \frac{\partial V}{\partial Y} + \frac{1}{2}\left(\frac{\partial W}{\partial Y}\right)^2 \tag{3.7b}$$

$$\gamma_{xy} = \frac{\partial U}{\partial Y} + \frac{\partial V}{\partial X} + \frac{\partial W}{\partial X} \cdot \frac{\partial W}{\partial Y} \tag{3.7c}$$

where

$\varepsilon_x, \varepsilon_y$ = in-plane normal strains

γ_{xy} = in-plane shearing strain

U,V = in-plane displacements in the X and Y directions, respectively.

Differentiating and combining (3.7a,b,c) to eliminate U and V gives

$$\frac{\partial^2 \varepsilon_x}{\partial Y^2} + \frac{\partial^2 \varepsilon_y}{\partial X^2} - \frac{\partial^2 \gamma_{xy}}{\partial X \partial Y} = \left(\frac{\partial^2 W}{\partial X \partial Y}\right)^2 - \frac{\partial^2 W}{\partial X^2} \cdot \frac{\partial^2 W}{\partial Y^2} \,. \tag{3.8}$$

The stress-strain relations are given by [140]

$$\varepsilon_x = \frac{1}{E}(\sigma_x - \nu \sigma_y) \tag{3.9a}$$

$$\varepsilon_y = \frac{1}{E}(\sigma_y - \nu \sigma_x) \tag{3.9b}$$

$$\gamma_{xy} = \frac{1}{G} \tau_{xy} \tag{3.9c}$$

in which

σ_x, σ_y = in-plane normal stresses

τ_{xy} = in-plane shearing stress

G = shearing modulus = $\frac{E}{2(1+\nu)}$.

Recognizing that

$$\sigma_x = \frac{N_x}{h} \quad , \quad \sigma_y = \frac{N_y}{h} \quad , \quad \tau_{xy} = \frac{N_{xy}}{h} \tag{3.10}$$

and substituting (3.5), (3.9) and (3.10) into (3.8) results in the compatibility equation

$$\nabla^4\phi = E\left[\left(\frac{\partial^2 W}{\partial X \partial Y}\right)^2 - \frac{\partial^2 W}{\partial X^2}\cdot\frac{\partial^2 W}{\partial Y^2}\right] \tag{3.11}$$

Equations (3.6) and (3.11) are known as von Karman's equations and are utilized in the analysis of plates having large deflections. In addition to the references mentioned at the beginning of this chapter, other references offer further insight into the large-deflection theory of plates [149-161], and more specifically offer a better understanding of the development and application of the von Karman equations [162-170].

The development of the non-linear shell equilibrium equations is accomplished by generalizing equations (3.6) and (3.11) to include the initial deflection (shape), $\overline{WO}$, which is in the same direction as the deflection, W, under load. Substituting

$$W \rightarrow W + \overline{WO} \tag{3.12}$$

into equations (3.6) and (3.11) gives the following equations:

$$D\cdot\nabla^4 W = h\left[\frac{\partial^2\phi}{\partial Y^2}\cdot\left(\frac{\partial^2(W+\overline{WO})}{\partial X^2}\right) + \frac{\partial^2\phi}{\partial X^2}\cdot\left(\frac{\partial^2(W+\overline{WO})}{\partial Y^2}\right) - 2\cdot\frac{\partial^2\phi}{\partial X\partial Y}\cdot\left(\frac{\partial^2(W+\overline{WO})}{\partial X\partial Y}\right)\right] + P \tag{3.13}$$

$$\nabla^4\phi = E\cdot\left[\left(\frac{\partial^2(W+\overline{WO})}{\partial X\partial Y}\right)^2 - \left(\frac{\partial^2(W+\overline{WO})}{\partial X^2}\right)\cdot\left(\frac{\partial^2(W+\overline{WO})}{\partial Y^2}\right)\right] \tag{3.14}$$

Expanding (3.13) results in

$$D\cdot\nabla^4 W = h\left[\frac{\partial^2\phi}{\partial Y^2}\cdot\left(\frac{\partial^2 W}{\partial X^2}+\frac{\partial^2\overline{WO}}{\partial X^2}\right)+\frac{\partial^2\phi}{\partial X^2}\cdot\left(\frac{\partial^2 W}{\partial Y^2}+\frac{\partial^2\overline{WO}}{\partial Y^2}\right)-2\cdot\frac{\partial^2\phi}{\partial X\partial Y}\cdot\left(\frac{\partial^2 W}{\partial X\partial Y}+\frac{\partial^2\overline{WO}}{\partial X\partial Y}\right)\right]+P \tag{3.15}$$

which is the non-linear equation of equilibrium for the plate with initial deflection. As in the case of the flat plate, the compatibility equation must be derived. The strain-displacement relations for the initially deflected plate are given by [171]

$$\varepsilon_x = \frac{\partial U}{\partial X}+\frac{1}{2}\cdot\left(\frac{\partial W}{\partial X}\right)^2-\frac{1}{2}\cdot\left(\frac{\partial W}{\partial X}\right)\cdot\left(\frac{\partial\overline{WO}}{\partial X}\right) \tag{3.16a}$$

$$\varepsilon_y = \frac{\partial V}{\partial Y}+\frac{1}{2}\cdot\left(\frac{\partial W}{\partial Y}\right)^2-\frac{1}{2}\cdot\left(\frac{\partial W}{\partial Y}\right)\cdot\left(\frac{\partial\overline{WO}}{\partial Y}\right) \tag{3.16b}$$

$$\gamma_{xy} = \frac{\partial U}{\partial Y}+\frac{\partial V}{\partial X}+\left(\frac{\partial W}{\partial X}+\frac{\partial\overline{WO}}{\partial X}\right)\cdot\left(\frac{\partial W}{\partial Y}+\frac{\partial\overline{WO}}{\partial Y}\right)-\frac{\partial\overline{WO}}{\partial X}\cdot\frac{\partial\overline{WO}}{\partial Y} \tag{3.16c}$$

Differentiating and combining (3.16a,b,c) to eliminate U and V yields

$$\frac{\partial^2\varepsilon_x}{\partial Y^2}+\frac{\partial^2\varepsilon_y}{\partial X^2}-\frac{\partial^2\gamma_{xy}}{\partial X\partial Y}=\left(\frac{\partial^2 W}{\partial X\partial Y}\right)^2+2\cdot\frac{\partial^2 W}{\partial X\partial Y}\cdot\frac{\partial^2\overline{WO}}{\partial X\partial Y}-\frac{\partial^2 W}{\partial X^2}\cdot\frac{\partial^2 W}{\partial Y^2}-\frac{\partial^2 W}{\partial X^2}\cdot\frac{\partial^2\overline{WO}}{\partial Y^2}-\frac{\partial^2 W}{\partial Y^2}\cdot\frac{\partial^2\overline{WO}}{\partial X^2} \tag{3.17}$$

Substituting equations (3.5), (3.9), and (3.10) into (3.17) gives the following compatibility equation:

$$\nabla^4\phi = E\left[W_{xy}^2+2W_{xy}\,\overline{WO}_{xy}-W_{xx}\,W_{yy}-W_{xx}\,\overline{WO}_{yy}-W_{yy}\,\overline{WO}_{xx}\right] \tag{3.18}$$

Note that equation (3.18) is expressed in a format that is different from that used in the first part of this section. The new format will

be used for the remainder of this paper and is described as follows:

$$A_{ij} = \frac{\partial^2 A}{\partial i \partial j} \tag{3.19}$$

Equations (3.15) and (3.18) are known as Marguerre's equations, and are the two non-linear, coupled equations of equilibrium and compatibility for a plate having initial deflection. Modifying equations (3.15) and (3.18) to agree with the sign convention described in Chapter 2 (see Figure 2.2; i.e., $WO = -\overline{WO}$) produces the following equations describing the equilibrium and compatibility of a shallow shell:

$$D\nabla^4 W = h\,[\phi_{yy} \cdot (W_{xx} - WO_{xx}) + \phi_{xx}\,(W_{yy} - WO_{yy}) - 2\phi_{xy}\,(W_{xy} - WO_{xy})] + P \tag{3.20}$$

$$\nabla^4 \phi = E\,[W_{xy}^2 - 2W_{xy}\,WO_{xy} - W_{xx}\,W_{yy} + W_{xx}\,WO_{yy} + W_{yy}\,WO_{xx}] \tag{3.21}$$

In addition to the references given at the beginning of this section, other references offer further insight into the development of Marguerre's equations [171] and into the theories and applications of non-linear shell analysis [172-179].

For ease of computation, it is desirable to non-dimensionalize the equilibrium equations (3.20) and (3.21). By dividing each variable by a certain reference variable, the problem becomes independent of edge lengths, material properties, and thickness. The following non-dimensionalized variables are used:

$$x = \frac{X}{a}\ ,\quad y = \frac{Y}{a}\ ,\quad \chi = \frac{\phi}{\alpha}\ ,\quad w = \frac{W}{\Lambda}\ ,\quad wo = \frac{WO}{\Lambda}\ ,\quad p = \frac{P}{\gamma} \tag{3.22}$$

where

$$\alpha = \frac{D}{h} = \frac{Eh^2}{12(1-\nu^2)} \tag{3.23a}$$

$$\Lambda = \frac{h}{\sqrt{12(1-\nu^2)}} \tag{3.23b}$$

$$\gamma = \frac{Dh}{a^4 \cdot \sqrt{12(1-\nu^2)}} \tag{3.23c}$$

in which $0 \leq x \leq 1$, $0 \leq y \leq c$, and

$$c = \frac{b}{a} \tag{3.24}$$

Note that all of the non-dimensionalized variables are represented in lower case letters. Substituting the above variables into equations (3.20) and (3.21) produces the non-dimensionalized equilibrium and compatibility equations of a shallow shell which are given by

$$\nabla^4 w - p - \chi_{yy} \cdot \theta_{xx} - \chi_{xx} \cdot \theta_{yy} + 2\chi_{xy} \cdot \theta_{xy} = 0 \tag{3.25}$$

$$\nabla^4 \chi - w_{xy}^2 + 2w_{xy} \cdot wo_{xy} + w_{xx} \cdot w_{yy} - w_{xx} \cdot wo_{yy} - w_{yy} \cdot wo_{xx} = 0 \tag{3.26}$$

where

$$\theta = w - wo \tag{3.27}$$

3.2 Derivation of the Equations of Motion

The equations of motion are derived by applying a small, dynamic displacement, $\tilde{W}$, and stress, $\tilde{\phi}$, about the equilibrium configuration for which the displacements and stresses are given as W and ϕ, respectively. Making these substitutions into equations (3.20) and (3.21), linearizing by eliminating higher order terms in $\tilde{W}$ and $\tilde{\phi}$, and expanding the

linear ∇^4 operator by

$$\nabla^4(W + \tilde{W}) = \nabla^4 W + \nabla^4 \tilde{W} \tag{3.28a}$$

$$\nabla^4(\phi + \tilde{\phi}) = \nabla^4 \phi + \nabla^4 \tilde{\phi} \tag{3.28b}$$

yields the following equations of motion:

$$D \cdot \nabla^4 \tilde{W} - h \cdot [\phi_{yy} \cdot \tilde{W}_{xx} - \phi_{xx} \cdot \tilde{W}_{yy} - \tilde{\phi}_{yy} \cdot \theta_{xx} - \tilde{\phi}_{xx} \cdot \theta_{yy} + 2 \cdot \phi_{xy} \cdot \tilde{W}_{xy} + 2 \cdot \tilde{\phi}_{xy} \cdot \theta_{xy}] + \mu \cdot \tilde{W}_{TT} = 0 \tag{3.29}$$

$$\nabla^4 \tilde{\phi} - E \cdot [2 \cdot \tilde{W}_{xy} \cdot W_{xy} + 2 \cdot \tilde{W}_{xy} \cdot WO_{xy} + \tilde{W}_{yy} \cdot W_{xx} + \tilde{W}_{xx} \cdot W_{yy} - \tilde{W}_{xx} \cdot WO_{yy} - \tilde{W}_{yy} \cdot WO_{xx}] = 0 \tag{3.30}$$

Note that D'Alembert's principle has been applied to the equilibrium equation (3.29) to account for dynamic forces by adding the inertia force, $\mu \cdot \tilde{W}_{TT}$, in which

μ = density = mass per unit area of the shell surface (3.31)

T = time

Non-dimensionalizing equations (3.29) and (3.30) by using the same variables described previously produces the two coupled, linear equations of motion which are expressed as

$$\nabla^4 \tilde{w} - \chi_{yy} \cdot \tilde{w}_{xx} - \chi_{xx} \cdot \tilde{w}_{yy} - \tilde{\chi}_{yy} \cdot \theta_{xx} - \tilde{\chi}_{xx} \cdot \theta_{yy} + 2 \cdot \chi_{xy} \cdot \tilde{w}_{xy} + 2 \cdot \tilde{\chi}_{xy} \cdot \theta_{xy} - \tilde{w}_{tt} = 0 \tag{3.32}$$

$$\nabla^4 \tilde{\chi} - 2 \cdot \tilde{w}_{xy} \cdot w_{xy} + 2 \cdot \tilde{w}_{xy} \cdot wo_{xy} + \tilde{w}_{yy} \cdot w_{xx} + \tilde{w}_{xx} \cdot w_{yy} - \tilde{w}_{xx} \cdot wo_{yy} - \tilde{w}_{yy} \cdot wo_{xx} = 0 \tag{3.33}$$

where

$$\tilde{\chi} = \frac{\tilde{\phi}}{\alpha} \quad , \quad \tilde{w} = \frac{\tilde{W}}{\Lambda} \tag{3.34a}$$

$$\tilde{w}_{tt} = \frac{\tilde{W}_{TT}}{\xi^2} \tag{3.34b}$$

$$\xi^2 = \frac{D}{a^2\sqrt{\mu}} \cdot \tag{3.34c}$$

3.3 Derivation of the Vibration (Buckling) Equations

The dynamic displacement, $\tilde{w}$, and stress, $\tilde{\chi}$, may be expressed by the products of the spatial and time-dependent functions given below:

$$\tilde{w} = g(x,y) \cdot h(t) \tag{3.35a}$$

$$\tilde{\chi} = f(x,y) \cdot k(t) \tag{3.35b}$$

Substituting (3.35a,b) into (3.32) and (3.33) and then separating variables by letting $h(t) = k(t)$ and by dividing through by $g(x,y) \cdot h(t)$ in (3.32) and $h(t)$ in (3.33) produces the following equations:

$$\frac{1}{g}\left\{\nabla^4 g - \chi_{yy} \cdot g_{xx} - \chi_{xx} \cdot g_{yy} - f_{yy} \cdot \theta_{xx} - f_{xx} \cdot \theta_{yy} + 2\chi_{xy} \cdot g_{xy} + 2f_{xy} \cdot \theta_{xy}\right\} = \frac{-h_{tt}}{h} \tag{3.36}$$

$$\nabla^4 f - 2g_{xy} \cdot \theta_{xy} + g_{xx} \cdot \theta_{yy} + g_{yy} \cdot \theta_{xx} = 0 \tag{3.37}$$

Since equation (3.36) must be true for any x, $0 \leq x \leq 1$, any y, $0 \leq y \leq c$, and any t, $0 \leq t \leq \infty$, both sides of the equation must be equal to some constant K. Therefore,

$$\frac{-h_{tt}}{h} = K \tag{3.38}$$

Rearranging (3.37) gives the ordinary differential equation

$$h_{tt} + K \cdot h = 0 \tag{3.39a}$$

for which the general solution is given as

$$h(t) = d_1 \cdot \cos \sqrt{K} \cdot t + d_2 \cdot \sin \sqrt{K} \cdot t \tag{3.39b}$$

Letting $K = \Omega^2$ gives the following expression for h(t):

$$h(t) = d_1 \cos \Omega t + d_2 \sin \Omega t \tag{3.40}$$

in which Ω is the non-dimensionalized frequency of the shell. Making the substitution for $K = \Omega^2$ into equation (3.36) and rewriting equation (3.37) produces the following coupled, linear, vibration equations:

$$\nabla^4 g - \chi_{yy} \cdot g_{xx} - \chi_{xx} \cdot g_{yy} - f_{yy} \cdot \theta_{xx} - f_{xx} \cdot \theta_{yy} + 2\chi_{xy} \cdot g_{xy} + 2f_{xy} \cdot \theta_{xy} - \Omega^2 \cdot g = 0 \tag{3.41}$$

$$\nabla^4 f - 2g_{xy} \cdot \theta_{xy} + g_{xx} \cdot \theta_{yy} + g_{yy} \cdot \theta_{xx} = 0 \, . \tag{3.42}$$

Equations (3.41) and (3.42), when solved simultaneously, provide the frequency, Ω, and associated displacements, g, and stresses, f, of the shell. Since at buckling the frequency of the shell equals zero, setting Ω^2 equal to zero in (3.41) results in the buckling equations.

3.4 Derivation of the Variational Principle

In order to derive a variational principle associated with the vibration of the shell, equations (3.41) and (3.42) are multiplied by g and -f, respectively. The resulting equations are integrated and added, giving

$$\int_0^1 \int_0^c g \cdot [\nabla^4 g - \chi_{yy} \cdot g_{xx} - \chi_{xx} \cdot g_{yy} - f_{yy} \cdot \theta_{xx} - f_{xx} \cdot \theta_{yy}$$

$$+ 2 \cdot \chi_{xy} \cdot g_{xy} + 2 \cdot f_{xy} \cdot \theta_{xy} - \Omega^2 \cdot g] \, dxdy$$

$$- \int_0^1 \int_0^c f \cdot [\nabla^4 f - 2 \cdot g_{xy} \cdot \theta_{xy} + g_{xx} \cdot \theta_{yy}$$

$$+ g_{yy} \cdot \theta_{xx}] \, dx \, dy = 0 \qquad (3.43)$$

where

$$0 \leq x \leq 1 \quad , \quad 0 \leq y \leq c \, .$$

Integrating by parts results in some terms evaluated at the corners, some terms evaluated along the boundaries, and a double integral. The corner terms and boundary terms will be zero due to boundary conditions (see Appendix A). The resulting double integral is given by

$$\int_0^1 \int_0^c [\chi_{yy} \cdot (g_x)^2 + \chi_{xx} \cdot (g_y)^2 - 2 \cdot \chi_{xy} \cdot g_x \cdot g_y + 2 \cdot f_x \cdot g_x \cdot \theta_{yy}$$

$$+ 2 \cdot f_y \cdot g_y \cdot \theta_{xx} - 2 \cdot f_y \cdot g_x \cdot \theta_{xy} - 2 \cdot f_x \cdot g_y \cdot \theta_{xy}$$

$$+ (\nabla^2 g)^2 - (\nabla^2 f)^2 - \Omega^2 \cdot g^2] \, dx \, dy = 0^* \qquad (3.44)$$

When f and g satisfy (3.41) and (3.42), this functional is stationary with respect to variations in f and g which satisfy the boundary conditions. (A similar variational principle for shallow shells with a circular boundary is given in [180].) This property will be utilized in the formulation of the optimization problem in Section 3.6.

---

* $\nabla^2 = \dfrac{\partial^2}{\partial x^2} + \dfrac{\partial^2}{\partial y^2}$

3.5 Derivation of the General Boundary Conditions

This section includes the derivation of the general boundary conditions on displacements and stresses. These boundary conditions must be satisfied at all times during the problem solution.

3.5.1 Displacement Boundary Conditions

The simply supported and clamped boundary conditions on the lateral displacement, w, and the in-plane displacements, u and v, are described in Figures 2.3a and 2.3b. The restrictions imposed on w in order to meet these boundary conditions are universally accepted and warrant no further discussion. However, the fact that in-plane displacements are prevented for either boundary condition differs from the often used restriction of no in-plane stresses on the boundaries. Indeed, permitting in-plane displacements to occur along the boundaries eliminates the need for deriving expressions for in-plane stresses along the boundaries and simplifies both the problem formulation and solution. However, it is anticipated that these restrictions will contribute to a more clearly defined state of buckling, and, therefore, in this study the in-plane displacements along the boundaries will be prevented.

3.5.2 Stress Boundary Conditions

The existence of the two in-plane stresses on the boundaries requires the development of two boundary stress equations. The first boundary condition is derived by applying the displacement boundary conditions to the general strain-displacement relations (3.16a,b).

The resulting relations are given as

$$\varepsilon_y = 0 \quad , \quad @\ x = 0,\ 1 \tag{3.45a}$$

and $$\varepsilon_x = 0 \quad , \quad @\ y = 0,\ c \tag{3.45b}$$

Substituting (3.5), (3.9), and (3.10) into (3.45a,b) and non-dimensionalizing results in the following expressions:

$$\chi_{xx} = \nu\, \chi_{yy} \quad , \quad @\ x = 0,\ 1 \tag{3.46a}$$

$$\chi_{yy} = \nu\, \chi_{xx} \quad , \quad @\ y = 0,\ c \tag{3.46b}$$

The second boundary condition for stress is derived by differentiating (3.7a,b,c), using the boundary conditions on u, v, and w, and observing that

$$\frac{\partial \gamma_{xy}}{\partial y} - \frac{\partial \varepsilon_y}{\partial x} = 0 \quad , \quad @\ x = 0,\ 1 \tag{3.47a}$$

$$\frac{\partial \gamma_{xy}}{\partial x} - \frac{\partial \varepsilon_x}{\partial y} = 0 \quad , \quad @\ y = 0,\ c \tag{3.47b}$$

Substituting (3.5), (3.9), and (3.10) into (3.47a,b) and non-dimensionalizing produces the following expressions:

$$\chi_{xxx} + (2+\nu)\, \chi_{xyy} = 0 \quad , \quad @\ x = 0,\ 1 \tag{3.48a}$$

$$\chi_{yyy} + (2+\nu)\, \chi_{xxy} = 0 \quad , \quad @\ y = 0,\ c \tag{3.48b}$$

Thus the necessary stress boundary conditions are provided by (3.46a) and (3.48a) along $x = 0$ and $x = 1$ and by (3.46b) and (3.48b) along $y = 0$ and $y = c$. Reference [181] offers additional discussion on the development of similar boundary conditions.

3.6 Derivation of the Governing Set of Equations

The governing set of equations consists of the previously derived equilibrium, compatibility and buckling equations and additional equations which will result from the optimization process.

3.6.1 The Lagrange Multiplier Technique

The optimization problem described in this study is one of finding the extreme value (maximum) of a function (objective function, buckling value of p) when the variables (wo, w, χ, g, f, p) are connected by some relations or constraints (previously derived equations (3.25), (3.26), (3.41), (3.42) and equations (3.52) and (3.53) to be derived). For such a problem of constrained optimization in which some of the constraints are non-linear, it is desirable to use Lagrange's Method of Undetermined Multipliers. At this time, the method will not be described in detail, but additional information on this method is provided in references [182-185].

The Lagrange multiplier technique requires the formation of an augmented objective function which consists of the original objective function plus each constraint multiplied by either a constant or a function (Lagrange multipliers). In this study, the objective function is magnitude of the load, p, and the constraints include the equations of equilibrium (3.25), compatibility (3.24), and buckling (3.41) and (3.42). Also, additional constraints must be imposed to guarantee a constant surface area (volume) and the normalization of the dynamic displacement, g(x,y).

The surface area of the shell may be expressed as the double integral of the product of the surface lengths of two perpendicular arches as follows:

$$A = \int_0^1 \int_0^c [1 + (wo_x)^2]^{\frac{1}{2}} \cdot [1 + (wo_y)^2]^{\frac{1}{2}} \, dx \, dy \tag{3.49}$$

Applying the Taylor Series expansion to (3.49) and neglecting higher order terms results in

$$A = \int_0^1 \int_0^c [1 + \frac{1}{2} \cdot (wo_x)^2] \quad [1 + \frac{1}{2} \cdot (wo_y)^2] \, dx \, dy \tag{3.50}$$

Expanding (3.50) and neglecting higher order terms yields

$$A = \int_0^1 \int_0^c dx \, dy + \frac{1}{2} \cdot \int_0^1 \int_0^c [(wo_x)^2 + (wo_y)^2] \, dx \, dy \tag{3.51}$$

in which the first integral is constant, and thus for constant surface area, the second integral is written as

$$\frac{1}{2} \int_0^1 \int_0^c [(wo_x)^2 + (wo_y)^2] \, dx \, dy = \beta^2 \tag{3.52}$$

or as

$$\frac{1}{2} \int_0^1 \int_0^c [(wo_x)^2 + (wo_y)^2] \, dx \, dy - \beta^2 = 0 \tag{3.53}$$

in which β^2 is a prescribed surface area parameter.

Normalization of the dynamic displacement, g(x,y), is performed in order to eliminate the arbitrariness of the eigenfunctions, g and f, in (3.41) and (3.42). The normalization of g(x,y) is accomplished by

$$\int_0^1 \int_0^c g^2(x,y)\ dx\ dy - 1 = 0 \tag{3.54}$$

which is convenient because the coefficient of Ω^2 in (3.44) becomes unity.

The augmented objective function, p*, to be used in the Lagrange multiplier technique is a function of (wo, χ, w, f, g, p, λ_1, λ_2, λ_3, λ_4, λ_5), with θ defined by (3.27), and is written as

$$\begin{aligned} p^* = p_0 &- \int_0^1 \int_0^c \lambda_1(x,y) \cdot [\nabla^4\chi - (w_{xy})^2 + 2 \cdot w_{xy} \cdot wo_{xy} \\ &+ w_{xx} \cdot w_{yy} - w_{xx} \cdot wo_{yy} - w_{yy} \cdot wo_{xx}]\ dx\ dy \\ &- \int_0^1 \int_0^c \lambda_2(x,y) \cdot [\nabla^4 w - p_0 \cdot R - \chi_{yy} \cdot \theta_{xx} - \chi_{xx} \cdot \theta_{yy} \\ &+ 2 \cdot \chi_{xy} \cdot \theta_{xy}]\ dx\ dy - \lambda_3 \cdot \left\{\Omega^2 + \int_0^1 \int_0^c [-\chi_{yy} \cdot (g_x)^2 \right. \\ &- \chi_{xx} \cdot (g_y)^2 + 2 \cdot \chi_{xy} \cdot g_x \cdot g_y - 2 \cdot f_x \cdot g_x \cdot \theta_{yy} \\ &- 2 \cdot f_y \cdot g_y \cdot \theta_{xx} + 2 \cdot f_y \cdot g_x \cdot \theta_{xy} + 2 \cdot f_x \cdot g_y \cdot \theta_{xy} \\ &\left. - (\nabla^2 g)^2 + (\nabla^2 f)^2]dx\ dy\right\} \\ &- \lambda_4 \cdot \left\{\frac{1}{2} \cdot \int_0^1 \int_0^c \left[(wo_x)^2 + (wo_y)^2\right]\ dx\ dy - \beta^2\right\} \\ &- \lambda_5 \cdot \left[\int_0^1 \int_0^c g^2\ dx\ dy - 1\right] \end{aligned} \tag{3.55}$$

The objective is the determination of the maximum critical value of p_0. Therefore, in equation (3.55), the load p is expressed as

$$p(x,y) = p_0 \cdot R(x,y) \tag{3.56}$$

in which

p_0 = constant magnitude (intensity) of the load

R(x,y) = spatial distribution of the load .

It should be noted that (as required in the Lagrange multiplier technique) all constraints are written in the form of being set equal to zero. Also, since equilibrium and compatibility must be satisfied at every point, (x,y), λ_1 and λ_2 must be functions of (x,y). Finally, equation (3.44) will be used instead of equations (3.41) and (3.42) to represent the buckling constraint. Thus, λ_3 is a constant. The frequency, Ω, is zero at buckling and is only included in (3.55) because the numerical solution procedure will make use of the vibration frequencies.

3.6.2 The Calculus of Variations

The governing set of equations is determined by making p* stationary with respect to each variable. However, since many of the variables upon which p* is dependent are functions themselves, p* is classified as a functional and differentiation with respect to these functions is accomplished by using the calculus of variations. Variational calculus is a well-documented area of mathematics and may be employed in one of several different formats. References [181-193] offer background information on the theory and applications of the calculus of variations.

The application of the calculus of variations to the augmented objective function is accomplished by using the "epsilon-eta" format. The variation of the functional, p*, is taken with respect to each

function using the form

$$\frac{\partial p^*}{\partial \varepsilon}\,[M + \varepsilon\eta]\Big|_{\varepsilon=0} = 0 \tag{3.57}$$

where

M = one of the functions upon which p* is dependent

ε = a constant scaling factor applied to η

η = a function which is dependent upon the same variables as M and represents the variation from M.

Substituting the eleven variables of p* into (3.57) for M will produce the eleven governing equations used to determine the optimum form of wo.

Taking the variation of p* with respect to λ_1, λ_2, λ_3, λ_4, and λ_5 simply reproduces the constraints upon which the λ's are multiplied. In other words, equations (3.25), (3.26), (3.44), (3.53) and (3.54) are reproduced, respectively.

Taking the variation of p* with respect to the functions w, χ, g, f, and wo must be accompanied by integration by parts in order to generate an integrand involving the varied function multiplied by an equation (Euler or governing equation) and the associated boundary conditions. As discussed in Appendix B, the boundary conditions vanish.

Taking the variation of p* with respect to w produces the following equation:

$$\nabla^4\lambda_2 + (\lambda_1)_{yy} \cdot \theta_{xx} + (\lambda_1)_{xx} \cdot \theta_{yy} - 2(\lambda_1)_{xy} \cdot \theta_{xy}$$
$$- (\lambda_2)_{yy} \cdot \chi_{xx} - (\lambda_2)_{xx} \cdot \chi_{yy} + 2(\lambda_2)_{xy} \cdot \chi_{xy}$$
$$+ 2\lambda_3 \cdot f_{yy} \cdot g_{xx} + 2\lambda_3 \cdot f_{xx} \cdot g_{yy} - 4\lambda_3 \cdot f_{xy} \cdot g_{xy} = 0 \quad (3.58)$$

Similarly, the variation of p* with respect to χ results in the following equation:

$$\nabla^4\lambda_1 - (\lambda_2)_{yy} \cdot \theta_{xx} - (\lambda_2)_{xx} \cdot \theta_{yy} + 2(\lambda_2)_{xy} \cdot \theta_{xy}$$
$$+ 2\lambda_3 \cdot g_{xx} \cdot g_{yy} - 2\lambda_3 \cdot (g_{xy})^2 = 0 \quad (3.59)$$

Equations (3.58) and (3.59) are the govening equations for λ_1 and λ_2 and are often referred to as the adjoint problem. Many of the boundary conditions that are generated by the integration by parts resulting in equation (3.58) vanish naturally, and the remaining terms vanish by assigning the same boundary conditions to λ_2 that exist on w. Likewise, many of the boundary terms associated with equation (3.59) vanish naturally. Those stress boundary terms that do not vanish are eliminated by assigning the same boundary conditions on λ_1 that exist on χ (see Appendix B).

Taking the variation of p* with respect to g and f reproduces the vibration equations (3.41) and (3.42) respectively. The generation of equation (3.41) is assisted by the assumptions that $\Omega = 0$ and $\lambda_5 = 0$. and the associated boundary terms cancel naturally. The boundary terms associated with equation (3.42) are discussed in Appendix B.

Taking the variation of p* with respect to wo results in the optimality equation, which is given by

$$(\lambda_1)_{yy} \cdot w_{xx} + (\lambda_1)_{xx} \cdot w_{yy} - 2(\lambda_1)_{xy} \cdot w_{xy} - (\lambda_2)_{xx} \cdot \chi_{yy}$$
$$- (\lambda_2)_{yy} \cdot \chi_{xx} + 2(\lambda_2)_{xy} \cdot \chi_{xy} + 2\lambda_3 \cdot f_{xx} \cdot g_{yy}$$
$$+ 2\lambda_3 \cdot g_{xx} \cdot f_{yy} - 4\lambda_3 \cdot g_{xy} \cdot f_{xy} + \lambda_4(wo_{xx} + wo_{yy}) = 0 \tag{3.60}$$

in which all boundary terms cancel naturally.

Finally, taking the variation of p* with respect to p results in the normalization of λ_2. In terms of p only,

$$p^*(p) = p_0 - \int_0^l \int_0^c \lambda_2(x,y) \cdot p(x,y)\, dx\, dy \,. \tag{3.61}$$

Substituting (3.56) into (3.61) yields

$$p^*(p) = p_0 - p_0 \cdot \int_0^l \int_0^c \lambda_2(x,y) \cdot R(x,y)\, dx\, dy \,. \tag{3.62}$$

Rearranging (3.62), taking the variation of p* with respect to p_o, produces the following equation:

$$1 - \int_0^l \int_0^c \lambda_2(x,y) \cdot R(x,y)\, dx\, dy = 0 \,. \tag{3.63}$$

Equation (3.63) represents the normalization of λ_2.

In summary, all of the eleven equations, (3.25), (3.26), (3.41), (3.42), (3.44), (3.53), (3.54), (3.58), (3.59), (3.60), (3.63), which have been generated by the optimality formulation, are not required for the problem solution. Equations (3.25) and (3.26) are used to evaluate equilibrium and compatibility. Equations (3.41) and (3.42) are employed for the vibration analysis, and equation (3.44) is not

required. Equation (3.53) is employed in the solution procedure by scaling the shell forms to insure that each form has the same surface area. The normalization of g, equation (3.54), is accomplished in the solution to the vibration problem. Since g and f form the eigenvectors associated with the shell frequency, Ω^2, normalization occurs within the solution to the eigenproblem. Equations (3.58) and (3.59) are used to solve the adjoint problem, and equation (3.60), the optimality condition, is used to generate a new shell form. The normalization of λ_2, equation (3.63), is accomplished within the solution process as an eigenvector in the same manner described for the normalization of g.

CHAPTER 4

SOLUTION TECHNIQUE

An iterative, numerical technique is required to solve the governing set of differential equations and boundary conditions that was developed in Chapter 3. This chapter covers the description, implementation, and verification of the solution scheme used in this study. Also discussed are the algorithms that were developed to permit the solution of the governing set of equations on the computer.

4.1 The Finite Difference Method, FDM

In this study the finite difference method, FDM, is employed as the differential equation solver. The fact that FDM is easy to understand, simple to use, and economical to run on the computer explains why FDM is often used in the solution to plate and shell problems [29,30, 32,140,141,156,162,163,172,178]. Ali [196] concludes that although both FDM and the finite element method, FEM, are powerful tools in the analysis of plate and shell problems, the simplicity of FDM is an advantage in the analysis of plate and shell vibrations. Also, Plaut, Johnson, and Parbery [137] successfully employed FDM in the form optimization of shallow shells having a circular boundary. These facts, combined with familiarity by the author with the technique, make FDM a logical choice. Additional information on the derivation and application of FDM is given in references [194,195,197-200].

4.1.1 General Description

As a differential equation solver, FDM may be applied in one of three basic forms -- backward differences, BD; central differences, CD; or forward differences, FD. Since CD is accepted as the most accurate of the three options [197,198], it is utilized in this study. FDM is applied after the continuous system upon which the equations act has been discretized into a finite number of points. Then the derivative of the continuous function at a point is represented by differences between the function values at surrounding points.

The approximation of the governing equations by the central difference equations requires the transformation of each derivative in the governing equation into an equivalent expression containing only function values. These standard CD expressions for the derivatives of the continuous function are based upon the forward and backward expansions of the Taylor series of the function [194,197] and are given below:

$$
\left.
\begin{aligned}
(A_{m,n})_x &= \frac{1}{2\cdot\Delta} \cdot (A_{m+1,n} - A_{m-1,n}) \\
(A_{m,n})_y &= \frac{1}{2\cdot\Delta} \cdot (A_{m,n+1} - A_{m,n-1}) \\
(A_{m,n})_{xx} &= \frac{1}{(\Delta)^2} \cdot (A_{m+1,n} - 2\cdot A_{m,n} + A_{m-1,n}) \\
(A_{m,n})_{xy} &= \frac{1}{4(\Delta)^2} \cdot (A_{m+1,n+1} - A_{m+1,n-1} - A_{m-1,n+1} + A_{m-1,n-1}) \\
(A_{m,n})_{yy} &= \frac{1}{(\Delta)^2} \cdot (A_{m,n+1} - 2\cdot A_{m,n} + A_{m,n-1})
\end{aligned}
\right|
$$

$$
\begin{aligned}
(A_{m,n})_{xxx} &= \frac{1}{(\Delta)^3} \cdot (A_{m+2,n} - 2 \cdot A_{m+1,n} + 2 \cdot A_{m-1,n} - A_{m-2,n}) \\
(A_{m,n})_{yyy} &= \frac{1}{(\Delta)^3} \cdot (A_{m,n+2} - 2 \cdot A_{m,n+1} + 2 \cdot A_{m,n-1} - A_{m,n-2}) \\
(A_{m,n})_{xxy} &= \frac{1}{2 \cdot (\Delta)^3} \cdot (A_{m+1,n+1} - 2 \cdot A_{m,n+1} + A_{m-1,n+1} \\
&\quad - A_{m+1,n-1} + 2 \cdot A_{m,n-1} - A_{m-1,n-1}) \\
(A_{m,n})_{xyy} &= \frac{1}{2 \cdot (\Delta)^3} \cdot (A_{m+1,n+1} - 2 \cdot A_{m+1,n} + A_{m+1,n-1} \\
&\quad - A_{m-1,n+1} + 2 \cdot A_{m-1,n} - A_{m-1,n-1}) \\
(A_{m,n})_{xxxx} &= \frac{1}{(\Delta)^4} \cdot (A_{m+2,n} - 4 \cdot A_{m+1,n} + 6 \cdot A_{m,n} \\
&\quad - 4 \cdot A_{m-1,n} + A_{m-2,n}) \\
(A_{m,n})_{yyyy} &= \frac{1}{(\Delta)^4} \cdot (A_{m,n+2} - 4 \cdot A_{m,n+1} + 6 \cdot A_{m,n} \\
&\quad - 4 \cdot A_{m,n-1} + A_{m,n-2}) \\
(A_{m,n})_{xxyy} &= \frac{1}{(\Delta)^4} \cdot [4 \cdot A_{m,n} - 2 \cdot (A_{m+1,n} + A_{m-1,n} \\
&\quad + A_{m,n+1} + A_{m,n-1}) + A_{m+1,n+1} + A_{m+1,n-1} \\
&\quad + A_{m-1,n+1} + A_{m-1,n-1}] \\
\nabla^4 \cdot (A_{m,n}) &= \frac{1}{(\Delta)^4} [20 \cdot A_{m,n} - 8 \cdot (A_{m+1,n} + A_{m-1,n} + A_{m,n+1} \\
&\quad + A_{m,n-1}) + 2 \cdot (A_{m+1,n+1} + A_{m-1,n+1} + A_{m+1,n-1} \\
&\quad + A_{m-1,n-1}) + A_{m+2,n} + A_{m-2,n} + A_{m,n+2} + A_{m,n-2}]
\end{aligned}
\qquad (4.1)
$$

where Δ = mesh interval size as shown in Figure 4.1.

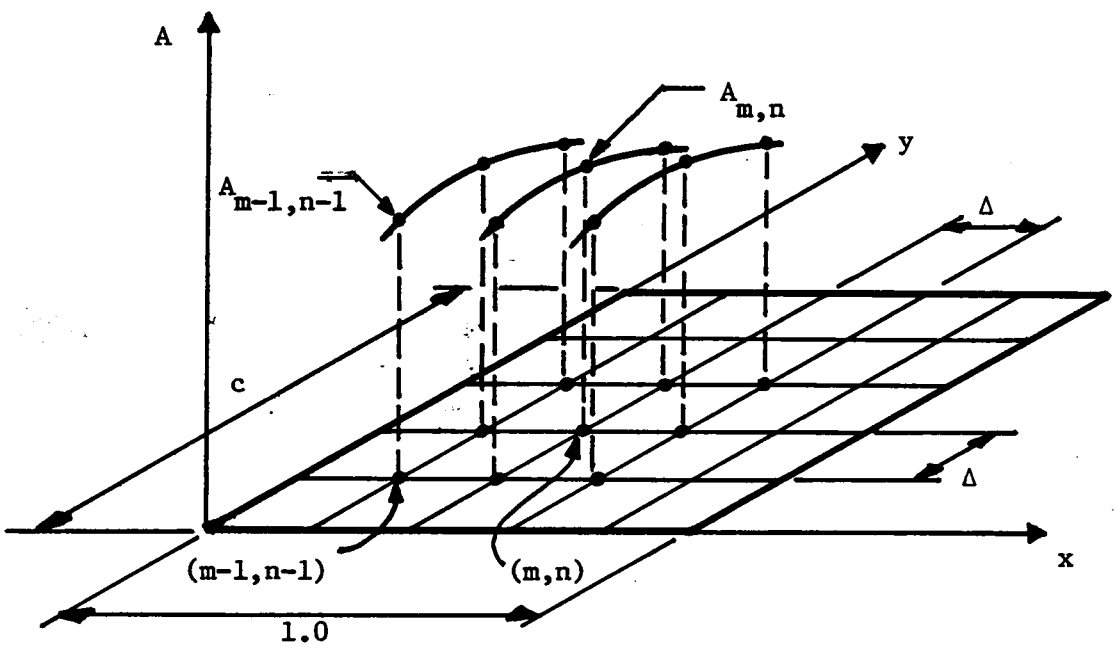

Figure 4.1: Application of Finite Differences in a Rectangular Cartesian Coordinate System

In the expressions given above, $A_{m,n}$ represents the function value at mesh point (m,n), where $A_{m,n}$ and (m,n) are shown in Figure 4.1. The CD expressions given in (4.1) represent all of the derivatives encountered in the governing equations in this study.

4.1.2 Implementation

The CD expressions given in (4.1) are substituted into the governing equations, and the resulting expressions are dependent upon function values only, since all derivative terms have been eliminated. The CD form of the compatibility equation (3.26) is given by the following equation:

$$
\begin{aligned}
&- \frac{1}{2} \cdot \Delta^2 \cdot (wo_{xy})_{m,n} \cdot w_{m-1,n+1} - \Delta^2 \cdot (wo_{xx})_{m,n} \cdot w_{m,n+1} \\
&+ \frac{1}{2} \cdot \Delta^2 \cdot (wo_{xy})_{m,n} \cdot w_{m+1,n+1} - \Delta^2 \cdot (wo_{yy})_{m,n} \cdot w_{m-1,n} \\
&+ 2 \cdot \Delta^2 \cdot (wo_{yy} + wo_{xx})_{m,n} \cdot w_{m,n} - \Delta^2 \cdot (wo_{yy})_{m,n} \cdot w_{m+1,n} \\
&+ \frac{1}{2} \cdot \Delta^2 \cdot (wo_{xy})_{m,n} \cdot w_{m-1,n-1} - \Delta^2 \cdot (wo_{xx})_{m,n} \cdot w_{m,n-1} \\
&- \frac{1}{2} \cdot \Delta^2 \cdot (wo_{xy})_{m,n} \cdot w_{m+1,n-1} - \frac{1}{16} \cdot (w_{m+1,n+1})^2 + \frac{1}{8} \cdot w_{m+1,n+1} \\
&\cdot w_{m+1,n-1} + \frac{1}{8} \cdot w_{m+1,n+1} \cdot w_{m-1,n+1} - \frac{1}{8} \cdot w_{m+1,n+1} \cdot w_{m-1,n-1} \\
&- \frac{1}{16} \cdot (w_{m+1,n-1})^2 - \frac{1}{8} \cdot w_{m+1,n-1} \cdot w_{m-1,n+1} + \frac{1}{8} \cdot w_{m+1,n-1} \\
&\cdot w_{m-1,n-1} - \frac{1}{16} \cdot (w_{m-1,n+1})^2 + \frac{1}{8} \cdot w_{m-1,n+1} \cdot w_{m-1,n-1} \\
&- \frac{1}{16} \cdot (w_{m-1,n-1})^2 + w_{m+1,n} \cdot w_{m,n+1} - 2 \cdot w_{m+1,n} \cdot w_{m,n} \\
&+ w_{m+1,n} \cdot w_{m,n-1} - 2 \cdot w_{m,n} \cdot w_{m,n+1} + 4 \cdot (w_{m,n})^2 - 2 \cdot w_{m,n} \\
&\cdot w_{m,n-1} + w_{m-1,n} \cdot w_{m,n+1} - 2 \cdot w_{m-1,n} \cdot w_{m,n} + w_{m-1,n} \cdot w_{m,n-1} \\
&+ \chi_{m,n+2} + 2 \cdot \chi_{m-1,n+1} - 8 \cdot \chi_{m,n+1} + 2 \cdot \chi_{m+1,n+1}
\end{aligned}
$$

$$+ \chi_{m-2,n} - 8 \cdot \chi_{m-1,n} + 20 \cdot \chi_{m,n} - 8 \cdot \chi_{m+1,n} + \chi_{m+2,n}$$

$$+ 2 \cdot \chi_{m-1,n-1} - 8 \cdot \chi_{m,n-1} + 2 \cdot \chi_{m+1,n-1} + \chi_{m,n-2} = 0 \qquad (4.2)$$

The CD form of the equilibrium equation (3.25) is given as

$$w_{m,n+2} + 2 \cdot w_{m-1,n+1} - 8 \cdot w_{m,n+1} + 2 \cdot w_{m+1,n+1} + w_{m-2,n}$$

$$- 8 \cdot w_{m-1,n} + 20 \cdot w_{m,n} - 8 \cdot w_{m+1,n} + w_{m+2,n} + 2 \cdot w_{m-1,n-1}$$

$$- 8 \cdot w_{m,n-1} + 2 \cdot w_{m+1,n-1} + w_{m,n-2} - \chi_{m,n+1} \cdot w_{m+1,n}$$

$$+ 2 \cdot \chi_{m,n+1} \cdot w_{m,n} - \chi_{m,n+1} \cdot w_{m-1,n} + 2 \cdot \chi_{m,n} \cdot w_{m+1,n}$$

$$- 8 \cdot \chi_{m,n} \cdot w_{m,n} + 2 \cdot \chi_{m,n} \cdot w_{m-1,n} - \chi_{m,n-1} \cdot w_{m+1,n}$$

$$+ 2 \cdot \chi_{m,n-1} \cdot w_{m,n} - \chi_{m,n-1} \cdot w_{m-1,n} - \chi_{m+1,n} \cdot w_{m,n+1}$$

$$+ 2 \cdot \chi_{m+1,n} \cdot w_{m,n} - \chi_{m+1,n} \cdot w_{m,n-1} + 2 \cdot \chi_{m,n} \cdot w_{m,n+1}$$

$$+ 2 \cdot \chi_{m,n} \cdot w_{m,n-1} - \chi_{m-1,n} \cdot w_{m,n+1} + 2 \cdot \chi_{m-1,n} \cdot w_{m,n}$$

$$- \chi_{m-1,n} \cdot w_{m,n-1} + \frac{1}{8} \cdot \chi_{m+1,n+1} \cdot w_{m+1,n+1} - \frac{1}{8} \cdot \chi_{m+1,n+1}$$

$$\cdot w_{m+1,n-1} - \frac{1}{8} \cdot \chi_{m+1,n+1} \cdot w_{m-1,n+1} + \frac{1}{8} \cdot \chi_{m+1,n+1} \cdot w_{m-1,n-1}$$

$$- \frac{1}{8} \cdot \chi_{m+1,n-1} \cdot w_{m+1,n+1} + \frac{1}{8} \cdot \chi_{m+1,n-1} \cdot w_{m+1,n-1}$$

$$+ \frac{1}{8} \cdot \chi_{m+1,n-1} \cdot w_{m-1,n+1} - \frac{1}{8} \cdot \chi_{m+1,n-1} \cdot w_{m-1,n-1}$$

$$- \frac{1}{8} \cdot \chi_{m-1,n+1} \cdot w_{m+1,n+1} + \frac{1}{8} \cdot \chi_{m-1,n+1} \cdot w_{m+1,n-1} + \frac{1}{8} \cdot \chi_{m-1,n+1}$$

$$\cdot w_{m-1,n+1} - \frac{1}{8} \cdot \chi_{m-1,n+1} \cdot w_{m-1,n-1} + \frac{1}{8} \cdot \chi_{m-1,n-1} \cdot w_{m+1,n+1}$$

$$- \frac{1}{8} \cdot \chi_{m-1,n-1} \cdot w_{m+1,n-1} - \frac{1}{8} \cdot \chi_{m-1,n-1} \cdot w_{m-1,n+1} + \frac{1}{8} \cdot \chi_{m-1,n-1}$$

$$\cdot w_{m-1,n-1} + \left(\frac{1}{2}\right) \cdot \Delta^2 \cdot (wo_{xy})_{m,n} \cdot \chi_{m-1,n+1} + \Delta^2 \cdot (wo_{xx})_{m,n} \cdot \chi_{m,n+1}$$

$$- \left(\frac{1}{2}\right) \cdot \Delta^2 \cdot (\quad_{xy})_{m,n} \cdot \chi_{m+1,n+1} + \Delta^2 \cdot (\quad_{yy})_{m,n} \cdot \chi_{m-1,n}$$

$$- 2 \cdot \Delta^2 \cdot (wo_{xx} + wo_{yy})_{m,n} \cdot \psi_{m,n} + \Delta^2 \cdot (wo_{yy})_{m,n} \cdot \chi_{m+1,n}$$
$$- \left(\frac{1}{2}\right) \cdot \Delta^2 \cdot (wo_{xy})_{m,n} \cdot \chi_{m-1,n-1} + \Delta^2 \cdot (wo_{xx})_{m,n} \cdot \chi_{m,n-1}$$
$$+ \left(\frac{1}{2}\right) \cdot \Delta^2 \cdot (wo_{xy})_{m,n} \cdot \chi_{m+1,n-1} - p \cdot \Delta^4 = 0 \qquad (4.3)$$

It should be noted that modifications are made to equations (4.2) and (4.3) when evaluated at points adjacent to the boundaries. Modifications to equation (4.2) at the y = c and x = 0 boundaries are performed as given later by equations (4.27) and (4.30), respectively. Modifications to equation (4.3) at the y = c and x = 0 boundaries are performed as given later by equations (4.13) and (4.17) and equations (4.22) and (4.23), respectively. Equations at points adjacent to the y = 0 and x = 1 boundaries are modified as permitted by symmetry in w and χ across the shell center lines. At points near the corners, the equations are modified by a combination of the changes mentioned above. The final set of equations includes 35 different pairs of equilibrium and compatibility equations.

The CD form of the vibration equations (3.41) and (3.42) is given by equations (4.4) and (4.5), respectively, as shown below:

$$g_{m,n+2} + (2 - \chi_{xy} \cdot \frac{\Delta^2}{2}) \cdot g_{m-1,n+1} - (8 + \chi_{xx} \cdot \Delta^2) \cdot g_{m,n+1}$$
$$+ (2 + \chi_{xy} \cdot \frac{\Delta^2}{2}) \cdot g_{m+1,n+1} + g_{m-2,n} - (8 + \chi_{yy} \cdot \Delta^2) \cdot g_{m-1,n}$$
$$+ [20 + 2\Delta^2 (\chi_{xx} + \chi_{yy}) - \Omega^2 \Delta^4] \cdot g_{m,n} - (8 + \chi_{yy} \cdot \Delta^2)$$
$$\cdot g_{m+1,n} + g_{m+2,n} + (2 + \chi_{xy} \cdot \frac{\Delta^2}{2}) \cdot g_{m-1,n-1} - (8 + \chi_{xx} \cdot \Delta^2)$$
$$\cdot g_{m+1,n-1} + g_{m,n-2} - (\theta_{xy} \cdot \frac{\Delta^2}{2}) \cdot f_{m-1,n+1}$$

$$
\begin{aligned}
&- (\theta_{xx} \cdot \Delta^2) \cdot f_{m,n+1} + (\theta_{xy} \cdot \frac{\Delta^2}{2}) \cdot f_{m+1,n+1} - (\theta_{yy} \cdot \Delta^2) \cdot f_{m-1,n} \\
&+ 2 \cdot \Delta^2 (\theta_{yy} + \theta_{xx}) \cdot f_{m,n} - (\theta_{yy} \cdot \Delta^2) \cdot f_{m+1,n} \\
&+ (\theta_{xy} \cdot \frac{\Delta^2}{2}) \cdot f_{m-1,n-1} - (\theta_{xx} \cdot \Delta^2) \cdot f_{m,n-1} \\
&- (\theta_{xy} \cdot \frac{\Delta^2}{2}) \cdot f_{m+1,n-1} = 0
\end{aligned} \tag{4.4}
$$

$$
\begin{aligned}
&- f_{m,n+2} - 2 \cdot f_{m-1,n+1} + 8 \cdot f_{m,n+1} - 2 \cdot f_{m+1,n+1} - f_{m-2,n} \\
&+ 8 \cdot f_{m-1,n} - 20 \cdot f_{m,n} + 8 \cdot f_{m+1,n} - f_{m+2,n} - 2 \cdot f_{m-1,n-1} \\
&+ 8 \cdot f_{m,n-1} - 2 \cdot f_{m+1,n-1} - f_{m,n-2} - (\theta_{xy} \cdot \frac{\Delta^2}{2}) \cdot g_{m-1,n+1} \\
&- (\theta_{xx} \cdot \Delta^2) \cdot g_{m,n+1} + (\theta_{xy} \cdot \frac{\Delta^2}{2}) \cdot g_{m+1,n+1} - (\theta_{yy} \cdot \Delta^2) \cdot g_{m-1,n} \\
&+ 2 \cdot \Delta^2 \cdot (\theta_{xx} + \theta_{yy}) \cdot g_{m,n} - (\theta_{yy} \cdot \Delta^2) \cdot g_{m+1,n} \\
&+ (\theta_{xy} \cdot \frac{\Delta^2}{2}) \cdot g_{m-1,n-1} - (\theta_{xx} \cdot \Delta^2) \cdot g_{m,n-1} \\
&- (\theta_{xy} \cdot \frac{\Delta^2}{2}) \cdot g_{m+1,n-1} = 0
\end{aligned} \tag{4.5}
$$

The modifications to equations (4.4) and (4.5) which are required when the equations are evaluated at points adjacent to the boundaries are described by (4.13), (4.17) - (4.23) for equation (4.4) and (4.27) - (4.30) for equation (4.5). In these equations, "g" and "f" are substituted for "w" and "χ", respectively. At points near the corners, the equations are modified by a combination of these changes. The final set of finite difference equations includes 45 different pairs of vibration equations.

The CD form of the adjoint problem equations (3.58) and (3.59)

is given by equations (4.6) and (4.7), respectively, as shown below:

$$\lambda 2_{m+2,n} - 4 \cdot \lambda 2_{m+1,n} + 6 \cdot \lambda 2_{m,n} - 4 \cdot \lambda 2_{m-1,n} + \lambda 2_{m-2,n}$$
$$+ 2 \cdot (4 \cdot \lambda 2_{m,n} - 2 \cdot \lambda 2_{m+1,n} - 2 \cdot \lambda 2_{m-1,n} - 2 \cdot \lambda 2_{m,n+1}$$
$$- 2 \cdot \lambda 2_{m,n-1} + \lambda 2_{m+1,n+1} + \lambda 2_{m+1,n-1} + \lambda 2_{m-1,n+1} + \lambda 2_{m-1,n-1})$$
$$+ \lambda 2_{m,n+2} - 4 \cdot \lambda 2_{m,n+1} + 6 \cdot \lambda 2_{m,n} - 4 \cdot \lambda 2_{m,n-1} + \lambda 2_{m,n-2}$$
$$+ \Delta^2 \cdot \theta_{xx} \cdot (\lambda 1_{m,n+1} - 2 \cdot \lambda 1_{m,n} + \lambda 1_{m,n-1})$$
$$+ \Delta^2 \cdot \theta_{yy} \cdot (\lambda 1_{m+1,n} - 2 \cdot \lambda 1_{m,n} + \lambda 1_{m-1,n})$$
$$- \frac{1}{2} \cdot \Delta^2 \cdot \theta_{xy} \cdot (\lambda 1_{m+1,n+1} - \lambda 1_{m+1,n-1} - \lambda 1_{m-1,n+1} + \lambda 1_{m-1,n-1})$$
$$- \Delta^2 \cdot \chi_{xx} \cdot (\lambda 2_{m,n+1} - 2 \cdot \lambda 2_{m,n} + \lambda 2_{m,n-1})$$
$$- \Delta^2 \cdot \chi_{yy} \cdot (\lambda 2_{m+1,n} - 2 \cdot \lambda 2_{m,n} + \lambda 2_{m-1,n})$$
$$+ \frac{1}{2} \cdot \Delta^2 \cdot \chi_{xy} \cdot (\lambda 2_{m+1,n+1} - \lambda 2_{m+1,n-1} - \lambda 2_{m-1,n+1} + \lambda 2_{m-1,n-1})$$
$$= - 2 \cdot \Delta^4 \cdot \lambda_3 \cdot (f_{yy} \cdot g_{xx} + f_{xx} \cdot g_{yy} - 2 \cdot f_{xy} \cdot g_{xy}) \qquad (4.6)$$

$$\lambda 1_{m+2,n} - 4 \cdot \lambda 1_{m+1,n} + 6 \cdot \lambda 1_{m,n} - 4 \cdot \lambda 1_{m-1,n} + \lambda 1_{m-2,n}$$
$$+ 2 \cdot (4 \cdot \lambda 1_{m,n} - 2 \cdot \lambda 1_{m+1,n} - 2 \cdot \lambda 1_{m-1,n} - 2 \cdot \lambda 1_{m,n+1}$$
$$- 2 \cdot \lambda 1_{m,n-1} + \lambda 1_{m+1,n+1} + \lambda 1_{m+1,n-1} + \lambda 1_{m-1,n+1} + \lambda 1_{m-1,n-1})$$
$$+ \lambda 1_{m,n+2} - 4 \cdot \lambda 1_{m,n+1} + 6 \cdot \lambda 1_{m,n} - 4 \cdot \lambda 1_{m,n-1} + \lambda 1_{m,n-2}$$
$$- \Delta^2 \cdot \theta_{xx} \cdot (\lambda 2_{m,n+1} - 2 \cdot \lambda 2_{m,n} + \lambda 2_{m,n-1})$$
$$- \Delta^2 \cdot \theta_{yy} \cdot (\lambda 2_{m+1,n} - 2 \cdot \lambda 2_{m,n} + \lambda 2_{m-1,n})$$
$$+ \frac{1}{2} \cdot \Delta^2 \cdot \theta_{xy} \cdot (\lambda 2_{m+1,n+1} - \lambda 2_{m+1,n-1} - \lambda 2_{m-1,n+1} + \lambda 2_{m-1,n-1})$$
$$= 2 \cdot \Delta^4 \cdot \lambda_3 \cdot [(g_{xy})^2 - g_{xx} \cdot g_{yy}] \qquad (4.7)$$

The description of the modifications to equations (4.6) and (4.7) is identical to that given previously for equations (4.4) and (4.5).

The CD form of the optimality equation (3.60) is given as

$$wo_{m+1,n} - 2 \cdot wo_{m,n} + wo_{m-1,n} + wo_{m,n+1} - 2 \cdot wo_{m,n} + wo_{m,n-1} = \Delta^2 \cdot (-\lambda 1_{yy} \cdot w_{xx} - \lambda 1_{xx} \cdot w_{yy} + 2 \cdot \lambda 1_{xy} \cdot w_{xy} + \lambda 2_{xx} \cdot \chi_{yy} + \lambda 2_{yy} \cdot \chi_{xx} - 2 \cdot \lambda 2_{xy} \cdot \chi_{xy} - 2 \cdot f_{xx} \cdot g_{yy} - 2 \cdot f_{yy} \cdot g_{xx} + 4 \cdot f_{xy} \cdot g_{xy}) \quad (4.8)$$

No modifications are required to (4.8) since it is evaluated at interior points only, and no fictitious points are generated.

The CD form of the surface area equation (3.53) is given as

$$\beta^2 = \left(\frac{1}{8 \cdot \Delta^2}\right) \cdot \int_0^1 \int_0^c [(wo_{m+1,n} - wo_{m-1,n})^2 + (wo_{m,n+1} - wo_{m,n-1})^2] \, dx \, dy \quad (4.9)$$

Equation (4.9) is modified to eliminate fictitious points by applying BD at points along the x = 1 and y = c boundaries and by applying FD at points along the x = 0 and y = 0 boundaries.

Instead of requiring just the determination of a derivative at one point, the equation solution is now dependent upon the determination of the function values at several points. This poses no problem if, as shown in Figure 4.2a, the points involved are contained within the boundaries. A problem arises, however, when an equation is evaluated at a point which, through the CD expressions, requires the solution of the function at points outside of the boundaries. These "fictitious"

points are shown in Figure 4.2b.

Although the function values could be determined at the fictitious points described above, such a solution has two disadvantages. First, the inclusion of these points increases the number of unknowns, and thus increases the amount of computational effort required. Secondly, to solve for these additional unknowns, a corresponding number of additional equations must be developed since the governing equations do not apply at the fictitious points. Therefore, these fictitious points will be eliminated from the CD expressions, and equations (4.1) cannot be applied to points near the boundaries without some modifications. The modifications that must be performed on (4.1) in order to eliminate any fictitious points are discussed in the next two sections.

4.1.2.1 Governing Equations

The governing equations apply to interior points only. That is, the points on the boundaries are governed by the displacement and stress boundary conditions. The pattern of points generated by the CD representation of each derivative reveals that the biharmonic operator, ∇^4, will generate one fictitious point when applied at a point adjacent to the boundary (see Figure 4.2b). This fictitious point must be expressed in terms of the points within the boundaries, and these expressions will differ for $\nabla^4 w$ and $\nabla^4 \chi$.

In the case of $\nabla^4 w$ adjacent to the y = c boundary, the fictitious point shown in Figure 4.2b is eliminated by utilizing the boundary conditions for w as shown in Figure 2.4b. For clamped conditions

$$(w_{m,n+1})_y = 0 \tag{4.10}$$

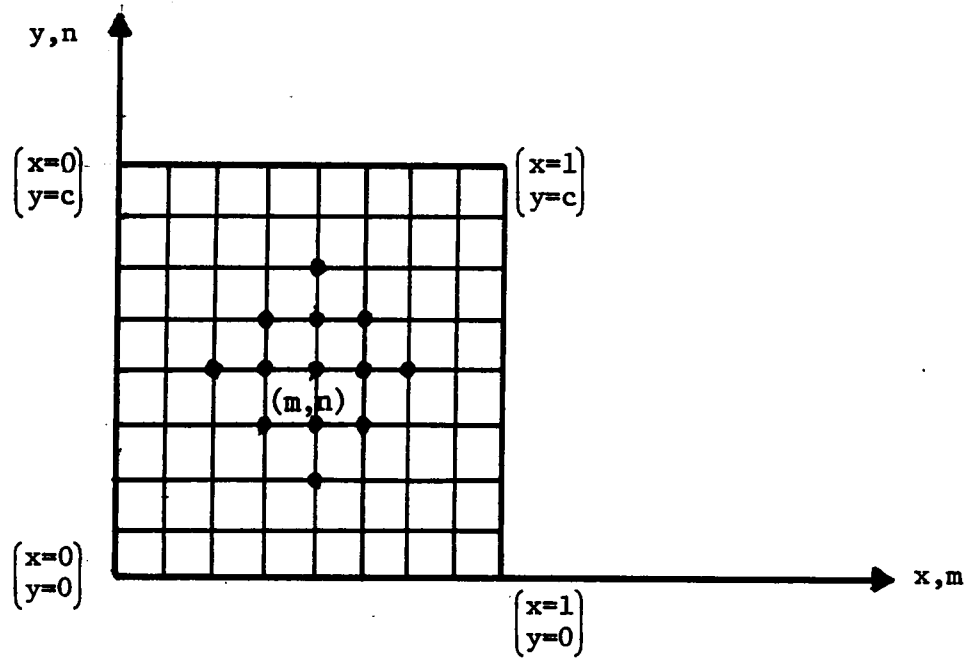

(a) Interior Point

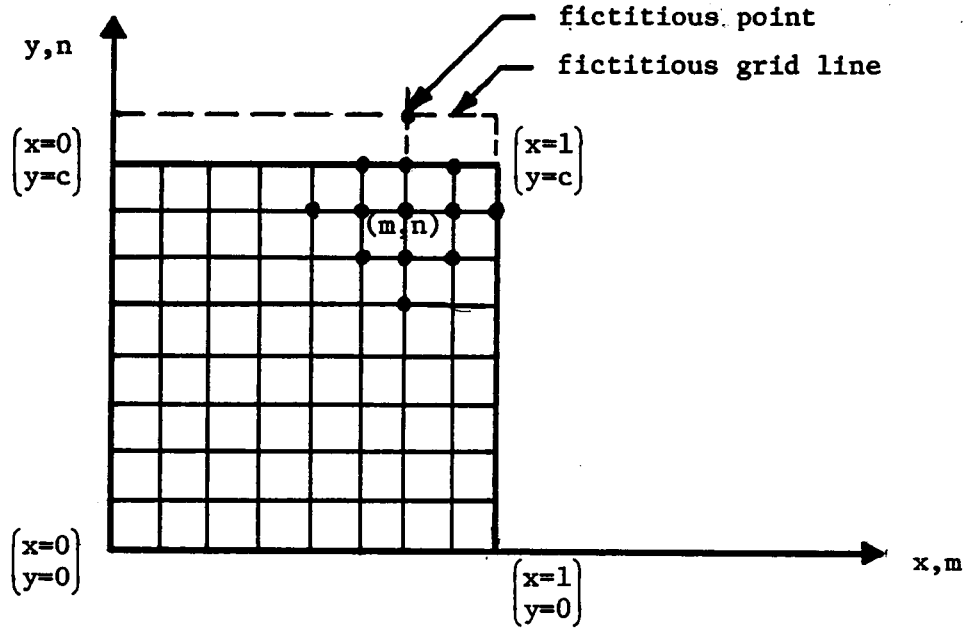

(b) Point Near the Boundary

Figure 4.2: Finite Difference Pattern of Points in the CD Representation of $\nabla^4 \cdot (A_{m,n})$

which by (4.1) can be expressed as

$$\left(\frac{1}{2\cdot\Delta}\right) \cdot (w_{m,n+2} - w_{m,n}) = 0 \ . \tag{4.11}$$

Rearranging (4.11) produces

$$w_{m,n+2} = w_{m,n} \tag{4.12}$$

and substituting (4.12) into (4.1) for $\nabla^4 w$ results in

$$\begin{aligned}\nabla^4 w_{m,n} = \frac{1}{\Delta^4} [21 \cdot w_{m,n} - 8(w_{m+1,n} + w_{m-1,n} + w_{m,n+1} + w_{m,n-1}) \\ + 2 \cdot (w_{m+1,n+1} + w_{m-1,n+1} + w_{m+1,n-1} + w_{m-1,n-1}) \\ + w_{m+2,n} + w_{m-2,n} + w_{m,n-2}]\end{aligned} \tag{4.13}$$

in which the fictitious point, $w_{m,n+2}$, has been eliminated. For simply supported conditions

$$(w_{m,n+1})_{yy} = 0 \tag{4.14}$$

which by (4.1) can be expressed as

$$\frac{1}{\Delta^2} \cdot (w_{m,n+2} - 2 \cdot w_{m,n+1} + w_{m,n}) = 0 \tag{4.15}$$

Rearranging (4.15) and recognizing that $w_{m,n+1} = 0$ yields

$$w_{m,n+2} = - w_{m,n} \tag{4.16}$$

Substituting (4.16) into (4.1) for $\nabla^4 w$ results in

$$\nabla^4 w_{m,n} = \frac{1}{\Delta^4} [19 \cdot w_{m,n} - 8 \cdot (.....)] \tag{4.17}$$

in which the remainder of (4.17) is identical to (4.13) and in which $w_{m,n+2}$ has been eliminated. Expressions for $\nabla^4 w$ are obtained for points

adjacent to the other three boundaries in a similar manner, and they are given as follows:

At y = 0: (clamped)
$$\nabla^4 w_{m,n} = \left(\frac{1}{\Delta^4}\right) \cdot [21 \cdot w_{m,n} - 8 \cdot (\text{same as (4.5)}) + 2 \cdot (\text{same as (4.5)}) + w_{m+2,n} + w_{m-2,n} + w_{m,n+2}] \quad (4.18)$$

At y = 0: (simply supported)
$$\nabla^4 w_{m,n} = \left(\frac{1}{\Delta^4}\right) \cdot [19 \cdot w_{m,n} + \ldots (\text{same as (4.18)})] \quad (4.19)$$

At x = 1: (clamped)
$$\nabla^4 w_{m,n} = \left(\frac{1}{\Delta^4}\right) \cdot [21 \cdot w_{m,n} - 8 \cdot (\text{same as (4.5)}) + 2 \cdot (\text{same as (4.5)}) + w_{m-2,n} + w_{m,n-2} + w_{m,n+2}] \quad (4.20)$$

At x = 1: (simply supported)
$$\nabla^4 w_{m,n} = \left(\frac{1}{\Delta^4}\right) \cdot [19 \ w_{m,n} + \ldots \text{same as (4.20)}] \quad (4.21)$$

At x = 0: (clamped)
$$\nabla^4 w_{m,n} = \left(\frac{1}{\Delta^4}\right) \cdot [21 \cdot w_{m,n} + 8 \cdot (\text{same as (4.5)}) + 2 \cdot (\text{same as (4.5)}) + w_{m+2,n} + w_{m,n-2} + w_{m,n+2}] \quad (4.22)$$

At x = 0: (simply supported)
$$\nabla^4 w_{m,n} = \left(\frac{1}{\Delta^4}\right) \cdot [19 \cdot w_{m,n} + \ldots \text{same as (4.22)}] \quad (4.23)$$

In the case of $\nabla^4 \chi$ adjacent to the y = c boundary, the fictitious point shown in Figure 4.2b, for example, is eliminated by using the boundary condition for χ expressed in equation (3.46b). For clamped

and simply supported conditions, (3.46b) is expressed in CD form as

$$\frac{1}{\Delta^2} \cdot (\chi_{m,n+1} - 2 \cdot \chi_{m,n} + \chi_{m,n-1}) - \frac{\nu}{\Delta^2} \cdot (\chi_{m+1,n} - 2 \cdot \chi_{m,n} + \chi_{m-1,n}) = 0 \tag{4.24}$$

in which point (m,n) is on the boundary. Rearranging (4.24) produces

$$\chi_{m,n+1} = 2(1-\nu) \cdot \chi_{m,n} - \chi_{m,n-1} + \nu \cdot \chi_{m+1,n} + \nu \cdot \chi_{m-1,n} \tag{4.25}$$

Rewriting (4.25) to agree with the point pattern shown in Figure 4.2b yields

$$\chi_{m,n+2} = 2(1-\nu) \cdot \chi_{m,n+1} - \chi_{m,n} + \nu \cdot \chi_{m+1,n+1} + \nu \cdot \chi_{m-1,n+1} \tag{4.26}$$

Substituting (4.26) into (4.1) for $\nabla^4\chi$ results in

$$\begin{aligned}\nabla^4\chi_{m,n} = \frac{1}{\Delta^4} \cdot [&19 \cdot \chi_{m,n} - 8 \cdot (\chi_{m+1,n} + \chi_{m-1,n} + \chi_{m,n-1}) \\ &- [8 + 2 \cdot (1+\nu)] \cdot \chi_{m,n+1} + 2(\chi_{m-1,n-1} + \chi_{m+1,n-1}) \\ &+ (2+\nu) \cdot (\chi_{m-1,n+1} + \chi_{m+1,n+1}) + \chi_{m-2,n} + \chi_{m+2,n} \\ &+ \chi_{m,n-2}]\end{aligned} \tag{4.27}$$

in which the fictitious point, $w_{m,n+2}$, has been eliminated. Expressions for $\nabla^4\chi$ are obtained for points adjacent to the other three boundaries in a similar manner, and they are given as follows:

At y = 0:
$$\begin{aligned}\nabla^4\chi_{m,n} = \left(\frac{-1}{\Delta^4}\right) \cdot [&19 \cdot \chi_{m,n} - 8 \cdot (\chi_{m+1,n} + \chi_{m-1,n} + \chi_{m,n+1}) \\ &- [8 + 2 \cdot (1+\nu)] \cdot \chi_{m,n-1} + 2 \cdot (\chi_{m-1,n+1} \\ &+ \chi_{m+1,n+1}) + (2+\nu) \cdot (\chi_{m-1,n-1} + \chi_{m+1,n-1}) \\ &+ \chi_{m-2,n} + \chi_{m+2,n} + \chi_{m,n+2}]\end{aligned} \tag{4.28a}$$

$$\text{At } x = 1: \quad \nabla^4\chi_{m,n} = \left(\frac{1}{\Delta^4}\right) \cdot [19 \cdot \chi_{m,n} - 8 \cdot (\chi_{m,n+1} + \chi_{m,n-1} + \chi_{m+1,n})$$
$$- [8 + 2 \cdot (1+\nu)] \cdot \chi_{m-1,n} + 2 \cdot (\chi_{m+1,n-1} + \chi_{m+1,n+1})$$
$$+ (2+\nu) \cdot (\chi_{m-1,n-1} + \chi_{m-1,n+1}) + \chi_{m,n-2} + \chi_{m,n+2}$$
$$+ \chi_{m+2,n}] \qquad (4.28b)$$

$$\text{At } x = 0: \quad \nabla^4\chi_{m,n} = \left(\frac{-1}{\Delta^4}\right) \cdot [19 \cdot \chi_{m,n} - 8 \cdot (\chi_{m,n+1} + \chi_{m,n-1} + \chi_{m-1,n})$$
$$- [8 + 2 \cdot (1+\nu)] \cdot \chi_{m+1,n} + 2 \cdot (\chi_{m-1,n-1} + \chi_{m-1,n+1})$$
$$+ (2+\nu) \cdot (\chi_{m+1,n-1} + \chi_{m+1,n+1}) + \chi_{m,n-2} + \chi_{m,n+2}$$
$$+ \chi_{m-2,n}] \qquad (4.28c)$$

4.1.2.2 Boundary Equations

No equations for w are required, since w = 0 on the boundaries. However, $\chi \neq 0$ on the boundaries, and χ is governed by equations (3.46a,b) and (3.48a,b). In the case of a point on the boundary, y = c, for example, the pattern of points involved in equations (3.46b) and (3.48b) are shown in Figures 4.3a and 4.3b, respectively. There are one and four fictitious points that must be eliminated from equations (3.46b) and (3.48b), respectively.

The point (m,n+2) is eliminated by modifying the form of χ_{yyy} given in (4.1). Instead of expressing all three derivatives of χ by the CD form, two derivatives are performed according to CD resulting in

$$\chi_{yyy} = \frac{1}{\Delta^2} \cdot [\chi_{m,n+1} - 2\chi_{m,n} + \chi_{m,n-1}]_y \qquad (4.29)$$

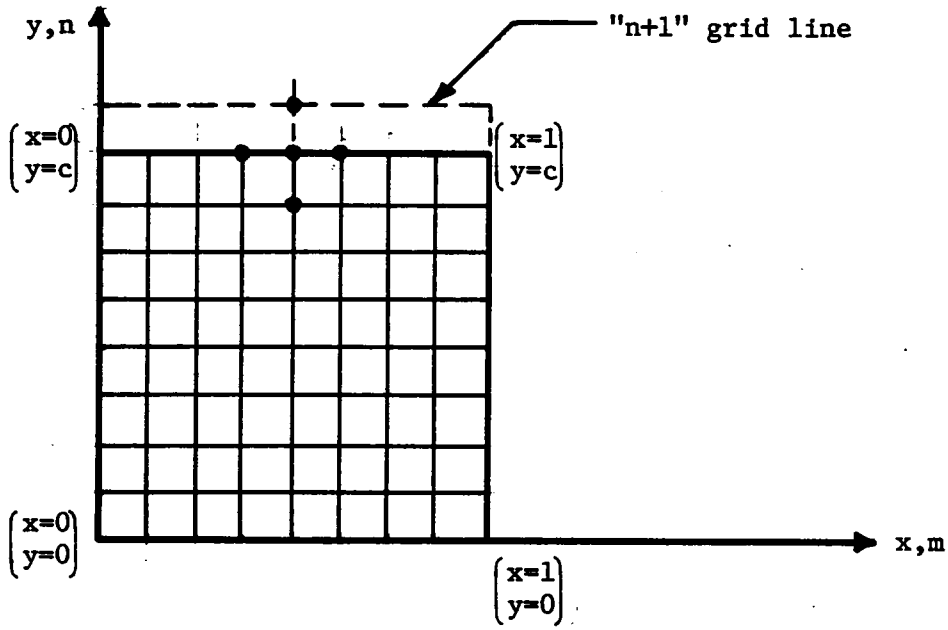

(a) Equation 3.46b

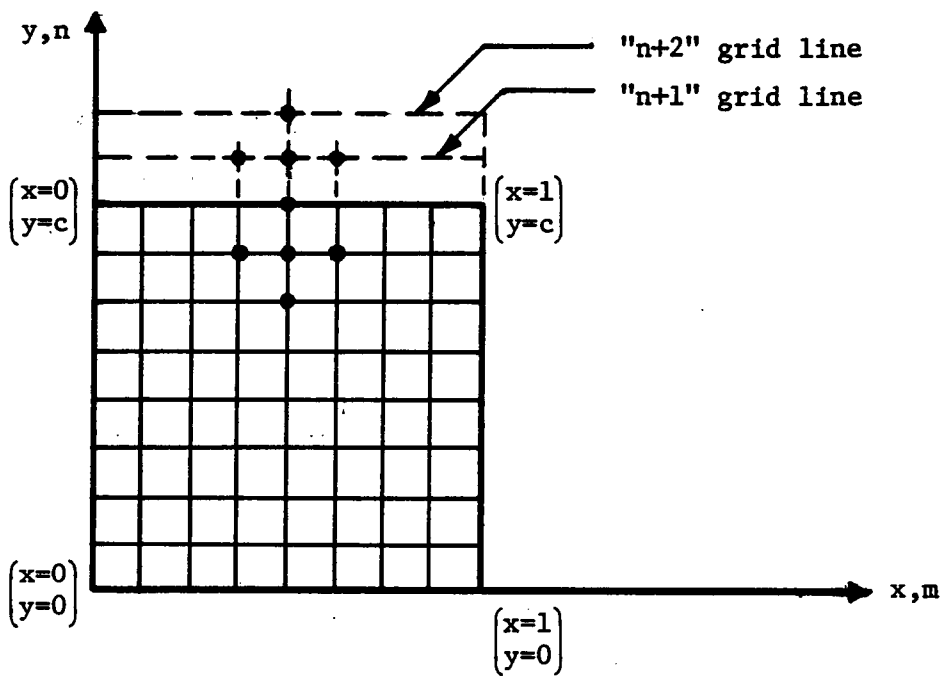

(b) Equation 3.48b

Figure 4.3: Finite Difference Pattern of Points

The third derivative is then performed according to BD, and the resulting expression is

$$\chi_{yyy} = \frac{1}{\Delta^3} \cdot [\chi_{m,n+1} - 3 \cdot \chi_{m,n} + 3 \cdot \chi_{m,n-1} - \chi_{m,n-2}] \qquad (4.30)$$

In (4.30) the fictitious point (m,n+2) has been eliminated, but the fictitious point (m,n+1) remains.

In Figures 4.3a and 4.3b the points on the "n+1" line are eliminated by substituting equation (4.25) for each "n+1" point in the expression for χ_{xxy} in (4.1) and in the expression for χ_{yyy} in (4.30). Making these substitutions and combining terms, equation (3.48b) may be rewritten in finite difference form as

$$\begin{aligned} &2 \cdot (1+\nu) \cdot (\chi_{m-1,n} + \chi_{m+1,n}) - (5+4\nu) \cdot \chi_{m,n} \\ &- (2+\nu) \cdot (\chi_{m-1,n-1} + \chi_{m+1,n-1}) + 2 \cdot (3+\nu) \cdot \chi_{m,n-1} \\ &- \chi_{m,n-2} = 0 \end{aligned} \qquad (4.31)$$

Equation (4.31) is an equivalent expression for equations (3.46b) and (3.48b) at y = c in which the fictitious points on the "n+1" and "n+2" lines have been eliminated. Expressions for the stress boundary conditions on the three other boundaries can be derived in a similar manner, and they are given as follows:

At y = 0:
$$\begin{aligned} &2 \cdot (1+\nu) \cdot (\chi_{m-1,n} + \chi_{m+1,n}) - (5+4\nu) \cdot \chi_{m,n} \\ &- (2+\nu) \cdot (\chi_{m-1,n+1} + \chi_{m+1,n+1}) + 2 \cdot (3+\nu) \cdot \chi_{m,n+1} \\ &- \chi_{m,n+2} = 0 \end{aligned} \qquad (4.32a)$$

$$\text{At } x = 1: \quad 2(1+\nu) \cdot (\chi_{m,n-1} + \chi_{m,n+1}) - (5+4\nu) \cdot \chi_{m,n}$$
$$- (2+\nu) \cdot (\chi_{m-1,n-1} + \chi_{m-1,n+1}) + 2 \cdot (3+\nu) \cdot \chi_{m-1,n}$$
$$- \chi_{m-2,n} = 0 \qquad (4.32b)$$

$$\text{At } x = 0: \quad 2 \cdot (1+\nu) \cdot (\chi_{m,n-1} + \chi_{m,n+1}) - (5+4\nu) \cdot \chi_{m,n}$$
$$- (2+\nu) \cdot (\chi_{m+1,n-1} + \chi_{m+1,n+1}) + 2 \cdot (3+\nu) \cdot \chi_{m+1,n}$$
$$- \chi_{m+2,n} = 0 \qquad (4.32c)$$

4.1.2.3 Mesh Size

In order to determine the most efficient mesh size for the finite difference discretization, an investigation is performed on selected test cases in order to monitor accuracy and computer time. (A discussion of the computer algorithms is given in later sections.) Only the results of equilibrium and vibration solutions are used in evaluating the various mesh sizes since no results exist for comparison to the solutions of the adjoint problem and the optimality equation.

The equilibrium solution is evaluated for square plates having clamped and simply supported boundaries, and the results for various mesh sizes are presented in Figures 4.4(a) and (b) and in Table 4.1. Shallow shells having a square base and no curvature along the boundaries are also evaluated for clamped and simply supported boundaries, and the results are presented in Figures 4.6(a) and (b) and in Table 4.3. Test cases for comparing mesh sizes with respect to vibration analysis include only square plates having clamped and simply supported boundaries. Results are presented in Figures 4.5(a)

and (b) and in Table 4.2. Studies have been conducted on the vibration of shells having a rectangular base [201-203] and no curvature along the boundaries [204,205], but because of specific differences (boundary conditions, for example), comparisons to this study cannot be made. No mesh sizes smaller than 9 x 9 are investigated, since the 9 x 9 mesh is the smallest size that will accommodate the point pattern for ∇^4 in one quadrant only. As discussed in a later section, equilibrium and compatibility are evaluated using one quadrant only in order to reduce the number of unknowns through symmetry. Also, the results given for computer time are averages compiled over many computer runs and are used to indicate trends only.

As indicated by the results, either the 11 x 11 or 13 x 13 square mesh or the 9 x 13 or 11 x 17 rectangular mesh provide good results with relatively small increases in computer time. The solution to the overall optimization problem is relative where each improvement in form is based upon the previous form. Thus, small inaccuracies in the solution of the initial form when compared to analytical results are carried through the entire solution with no significant effect on the final output. Therefore emphasis is placed on minimizing the computer effort, and the 11 x 11 and 9 x 13 meshes are used in this study for solving square and rectangular problems, respectively.

4.2 Solution Algorithm

The finite difference form of the governing equations and boundary equations are coded in the FORTRAN-77 language. However, before a solution is generated, a step-by-step solution scheme (algorithm) is

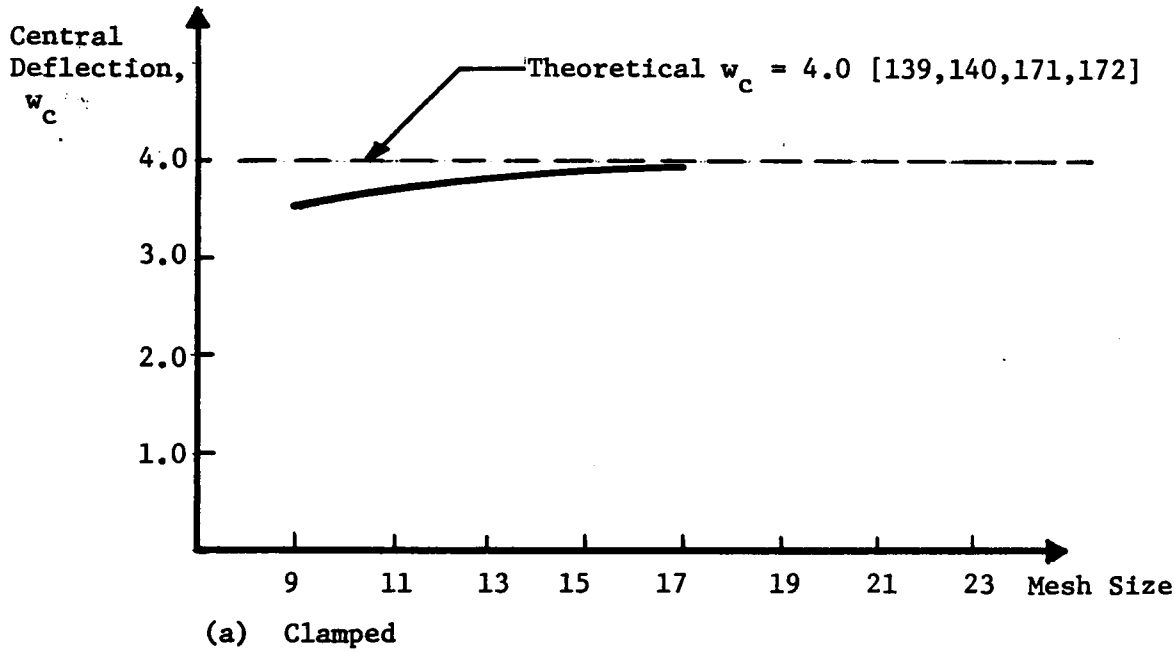

(a) Clamped

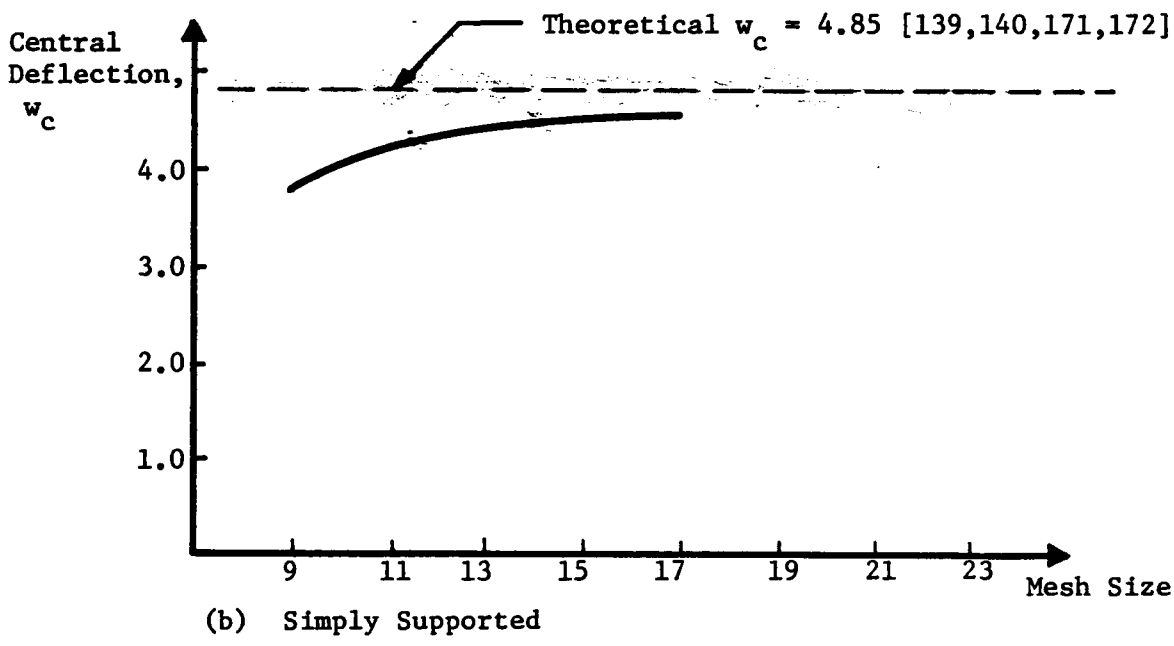

(b) Simply Supported

Figure 4.4: Comparison of Mesh Sizes for the Deflection of a Square Plate (non-dimensionalized load = 5280)

Table 4.1

Test Cases for Equilibrium Analysis of Square Plate

	Boundary Condition	Base	Mesh Size	CPU Increase	P/Δ Curve
Plate	C	Sq.	9x9	--	Figure 4.4a
"	"	"	11x11	2.7	"
"	"	"	13x13	5.8	"
"	"	"	15x15	12.3	"
"	"	"	17x17	33.5	"
"	"	"	19x19	*	"
"	"	"	21x21	68.8	"
Plate	SS	Sq.	9x9	—	Figure 4.4b
"	"	"	11x11	2.8	"
"	"	"	13x13	6.0	"
"	"	"	15x15	12.7	"
"	"	"	17x17	34.6	"
"	"	"	19x19	*	"
"	"	"	21x21	*	"

Note: "CPU Increase" = (Actual CPU)/(CPU for 9x9)

* - Not run

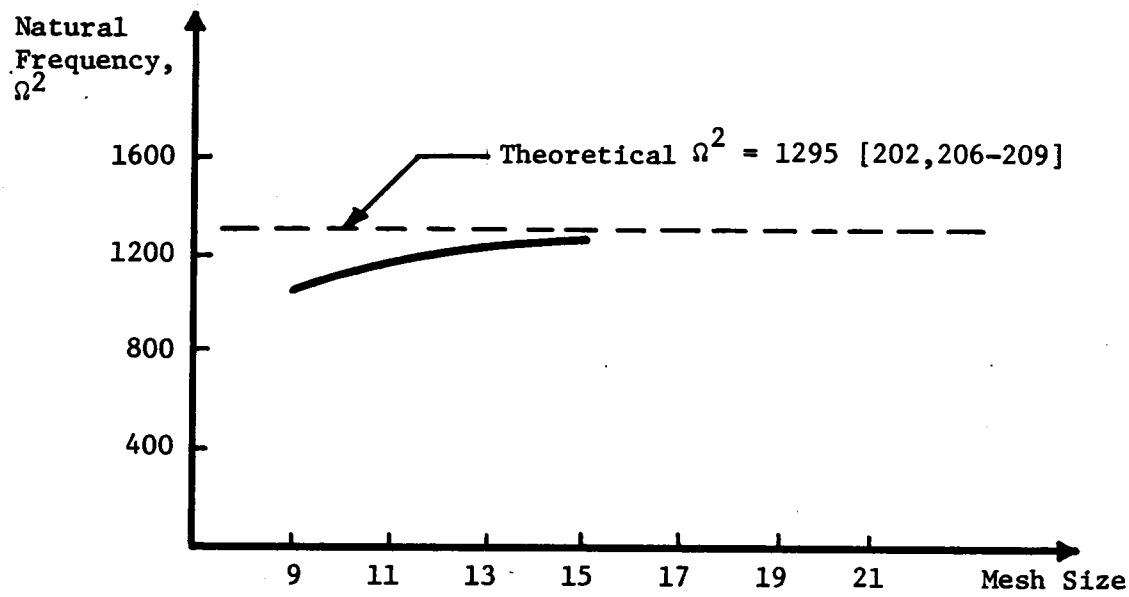

(a) Clamped

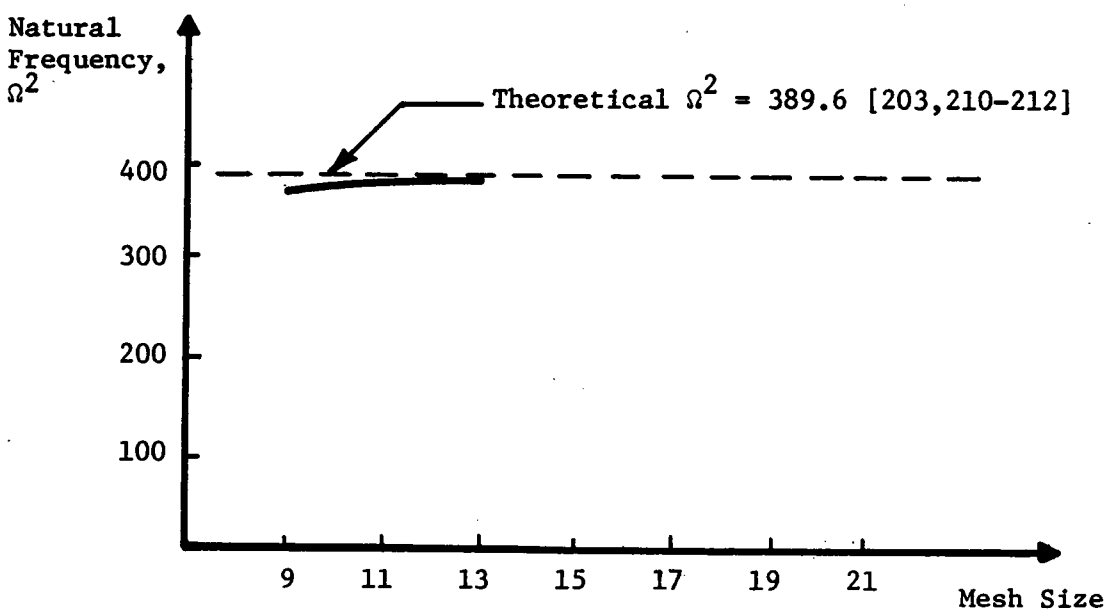

(b) Simply Supported

Figure 4.5: Comparison of Mesh Sizes for Free Vibration of a Square Plate

Table 4.2

Test Cases for Vibration Analysis of a Square Plate

	Boundary Condition	Base	Mesh Size	CPU Increase	P/Δ Curve
Plate	C	Sq.	9x9	--	Figure 4.5a
"	"	"	11x11	6.2	"
"	"	"	13x13	11.4	"
"	"	"	15x15	20.6	"
"	"	"	17x17	*	"
"	"	"	19x19	*	"
"	"	"	21x21	**	"
Plate	SS	Sq.	9x9	--	Figure 4.5b
"	"	"	11x11	6.6	"
"	"	"	13x13	12.2	"
"	"	"	15x15	22.1	"
"	"	"	17x17	*	"
"	"	"	19x19	101.5	"
"	"	"	21x21	**	"

Note: "CPU Increase" = (Actual CPU)/(CPU for 9x9)

* - Not run

** - Not enough computer memory

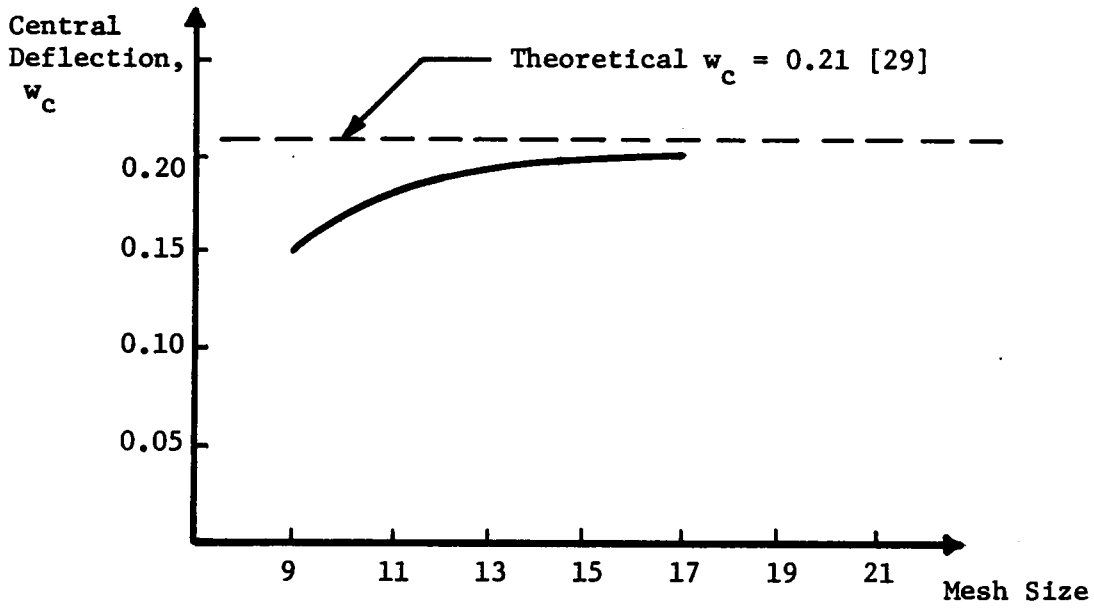

(a) Clamped

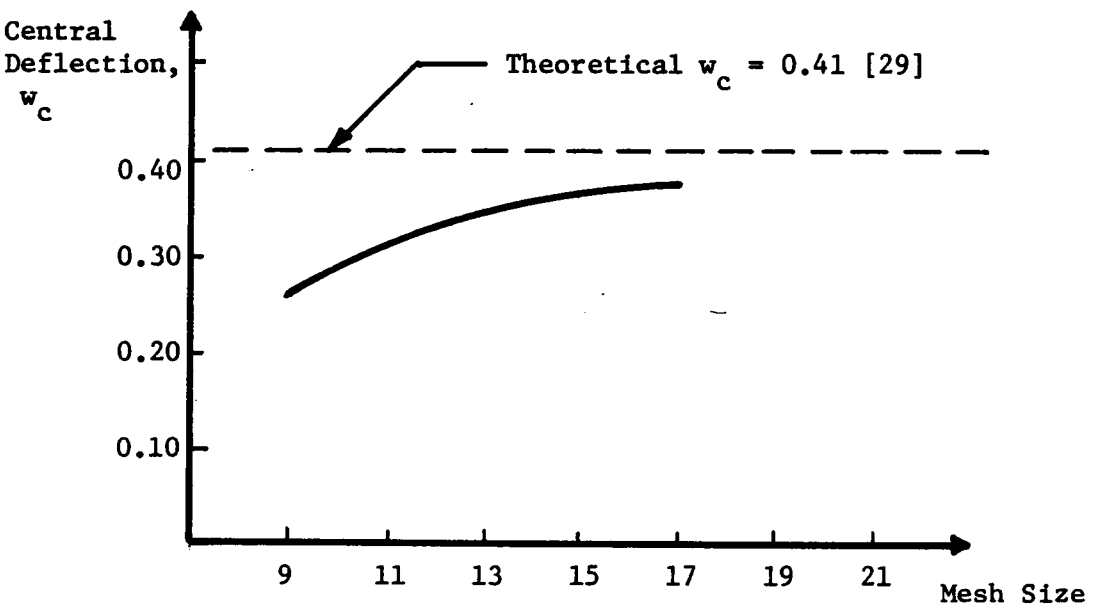

(b) Simply Supported

Figure 4.6: Comparison of Mesh Sizes for Deflection of Shell Having a Square Boundary
(Non-dimensionalized load = 330)
(Non-dimensionalized form = 3.3 (sin π x)(sin π y)

Table 4.3

Test Cases for Equilibrium Analysis of a Shell Having a Square Base

	Boundary Condition	Base	Mesh Size	CPU Increase	P/Δ Curve
Shell	C	Sq.	9x9	--	Figure 4.6a
"	"	"	11x11	3.1	"
"	"	"	13x13	6.7	"
"	"	"	15x15	14.2	"
"	"	"	17x17	38.5	"
"	"	"	19x19	55.2	"
"	"	"	21x21	*	"
Shell	SS	Sq.	9x9	--	Figure 4.6b
"	"	"	11x11	3.2	"
"	"	"	13x13	6.9	"
"	"	"	15x15	*	"
"	"	"	17x17	39.7	"
"	"	"	19x19	*	"
"	"	"	21x21	*	"

Note: "CPU Increase" = (Actual CPU)/(CPU for 9x9)

* = Not run

developed. The scheme places the independent finite difference equations in a specific order and form so that the solutions to the individual equations lead to the total problem solution. The algorithm is discussed in detail in the sections that follow.

4.2.1 General Description

Once the mesh size and surface area coefficient, β^2, have been chosen, the solution procedure can begin:

1. Initialize wo and p_o and scale wo by equation (4.9).
2. Determine w and χ from equations (4.2) and (4.3).
3. Determine Ω^2, f, and g from equations (4.4) and (4.5).
4. Repeat steps 1-3, increasing p_o each time, until the lowest Ω^2 goes to zero. When $\Omega^2 = 0$, p_o is the buckling load, and f and g are the dynamic displacements and stresses at buckling.
5. Determine λ_1 and λ_2 from equations (4.6) and (4.7).
6. Determine a new wo from equation (4.8) and scale the new wo by equation (4.9).
7. Using the new form, wo, and the previous buckling load, p_o, repeat steps 2-6 until no new form, wo, is generated or until there is no increase in buckling load with a new form.
8. The last form generated for which there is an increase in the buckling load is the optimum form of the shell having that particular value of β^2. The values of p_o, w, χ, and g provide the buckling load, displacements and stresses at buckling, and buckling mode, respectively.

4.2.2 Accuracy

As discussed in section 4.1.2.3, the accuracy of the program was evaluated for equilibrium and for vibration analysis for those forms which have results available in the literature. Using the proper mesh size, the program produces results which are in good agreement with analytical results and with results of other studies. Although only selected test cases are shown in Figures 4.4 - 4.6, results for plates and shells having a rectangular base and either clamped and simply supported boundaries yielded similar comparisons with published results.

Additional quantitative verification of the accuracy of the program is impossible since results for comparison are not available for any of the following:

a) equilibrium and vibration of non-standard forms;

b) adjoint problem solution;

c) new form generation.

However, since certain trends in the shell behavior should be evident during the problem solution, such trends are monitored and serve as qualitative verification of the performance of the program. These trends include the following:

a) Since the geometry, load, and boundary conditions are symmetric, all results should be symmetric (except eigenvectors, f and g, which might be anti-symmetric).

b) An increase in the load, p, on a shell should produce a decrease in the frequency of vibration of that shell.

c) For a given load, an increase in the height (apex) of the shell form should produce an increase in the frequency of

vibration.

d) An increase in the height of the shell form should produce an increase in the buckling load.

All of the trends mentioned above are observed in all test problems, and thus qualitatively verify the program.

4.2.3 Equilibrium and Compatibility

The solution for w and χ in the equilibrium and compatibility equations (4.3) and (4.2), respectively, requires the use of a non-linear equation solver. Several non-linear equation solver subroutines are available through the International Mathematical and Statistical Libraries, Inc. (IMSL). Two subroutines, ZSCNT and ZSPOW, were tried in the early stages of the research, and both resulted in limited success with inconsistent accuracy, convergence problems, and expensive computer time. Therefore, another subroutine, BROYDN, was utilized and produced excellent results. BROYDN was written by Dr. Lee Johnson of the Virginia Tech Mathematics Department and uses a modified Newton's method which includes directional and step size changes. BROYDN consistently produced accurate results and quick convergence, thus minimizing computer time.

In order to minimize the computational effort further, symmetry across the center lines is employed, and only one quadrant of the shell is required for the equilibrium analysis. Thus the mesh sizes reduce to 6 x 6 and 7 x 5 (per quadrant) for square and rectangular bases, respectively (see Figure 4.7). The size of the mesh is reduced, the finite difference equations are modified to reflect symmetry across the

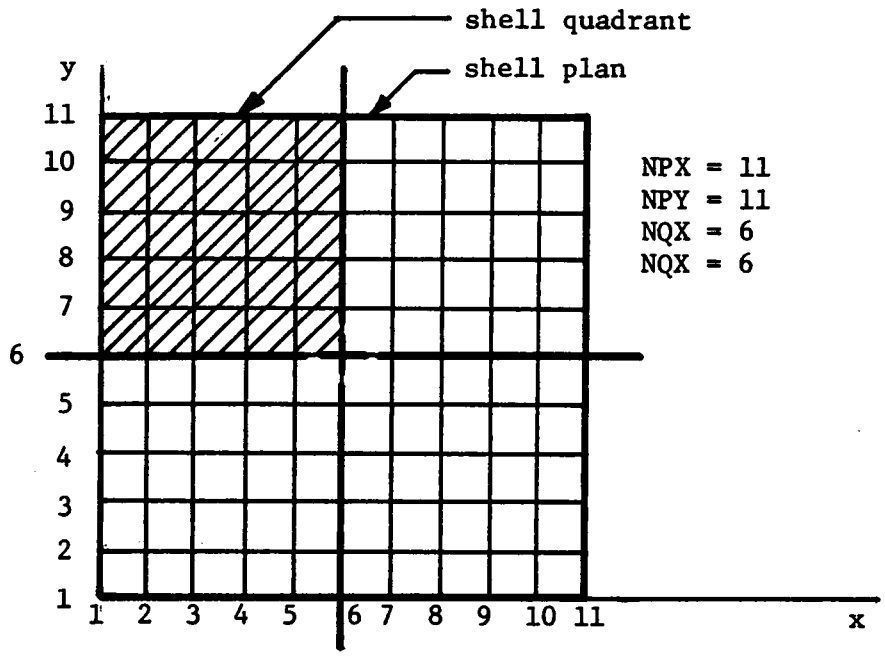

(a) Square

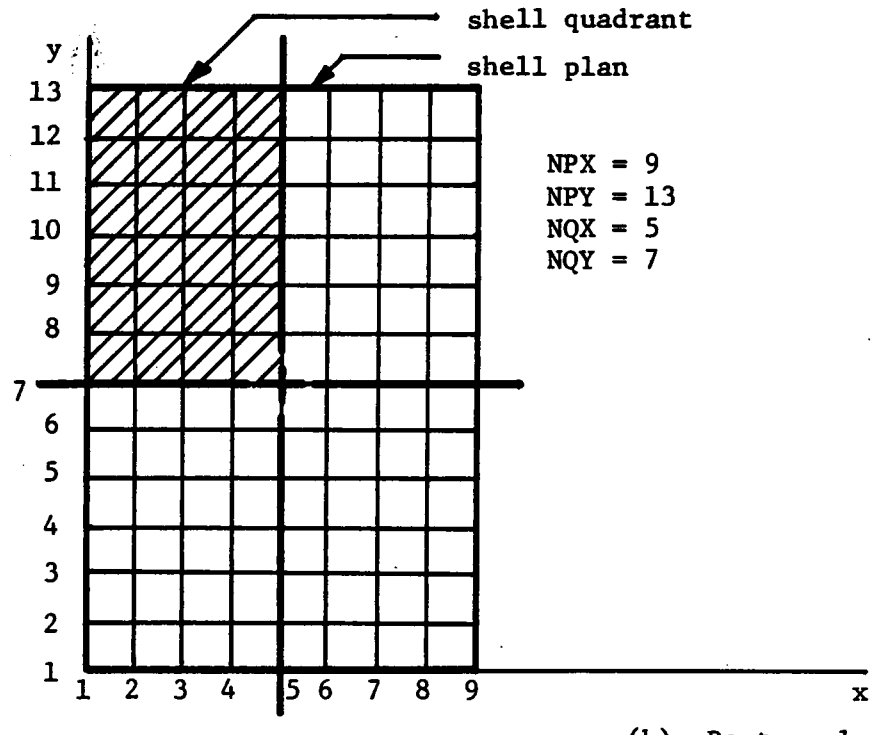

(b) Rectangular

Figure 4.7: Reduction in Mesh Size Due to Symmetry

center lines, and the number of unknowns is reduced significantly.

The solution for w and χ requires the following steps:

(1) Initialize w and χ (usually $w = \chi = 0$) and store in $\{x\}_i$ where

$\{x_i\}$ = N x 1 vector containing the "guessed" values of w and χ.

N = number of unknowns (w and χ) = (NQX • NQY) - 1 + (NQX - 1) • (NQY - 1)

NQX = number of grid lines in one quadrant in the x-direction = $\frac{NPX}{2} + 1$

NQY = number of grid lines in one quadrant in the y-direction = $\frac{NPY}{2} + 1$

NPX = total number of grid lines in the x-direction

NPY = total number of grid lines in the y-direction

(2) Evaluate equations (4.2) and (4.3) at each interior point and evaluate equation (4.30) at each boundary point (except the corner).

(3) Utilize BROYDN to compute new values of w and χ, and store them in $\{x\}_{i+1}$ where

$\{x\}_{i+1}$ = N x 1 vector containing computed values of w and χ.

(4) Check for convergence on $\{x\}$ by calculating the norm between $\{x\}_i$ and $\{x\}_{i+1}$ and comparing to a predetermined acceptable value.

(5) If convergence is not obtained, repeat steps (2) - (4) with the new values of w and χ, $\{x\}_{i+1}$, as the guessed values, $\{x\}_i$.

Through trial and error, a norm equal to 10^{-5} was found to yield accurate, symmetric results while requiring a minimum acount of computer time.

4.2.4 Vibration

The solution for Ω^2, f, and g in equations (4.4) and (4.5) requires the transformation of these equations into the format of an eigenproblem. In matrix form, equations (4.4) and (4.5) are expressed as

$$[C]\{f\} + [D]\{g\} - \Omega^2\{g\} = 0 \qquad (4.33a)$$

$$[A]\{f\} + [B]\{g\} = 0 \qquad (4.33b)$$

in which [A], [B], [C], [D] are coefficient matrices whose values are based upon χ, w, and wo. The sizes of the matrices and vectors are given as

$$\begin{aligned} \{f\} &= NFG \times 1 \\ \{g\} &= NG \times 1 \\ [A] &= NFG \times NFG \\ [B] &= NFG \times NG \\ [C] &= NG \times NFG \\ [D] &= NG \times NG \end{aligned} \qquad (4.34)$$

where

$$NG = (NPX - 2) \cdot (NPY - 2) \qquad (4.35a)$$

$$NFG = (NPX \cdot NPY) - 4 \qquad (4.35b)$$

The sizes of the matrices reflect the fact that the full mesh is used in the analysis. Since the eigenvectors, {f} and {g}, may be anti-symmetric, symmetry is not employed to reduce the mesh to one quadrant only. Equation (4.33) may be written as

$$\{f\} = -[A]^{-1} \cdot [B] \cdot \{g\} \tag{4.36}$$

Substituting (4.36) into (4.32) yields

$$-[C] \cdot [A]^{-1} \cdot [B] \cdot \{g\} + [D] \cdot \{g\} = \Omega^2 \cdot \{g\} \tag{4.37}$$

which may be rearranged in the form of

$$([D] - [C] \cdot [A]^{-1} \cdot [B]) \cdot \{g\} = \Omega^2 \cdot \{g\} \tag{4.38}$$

For convenience, let

$$[E] = [D] - [C] \cdot [A]^{-1} \cdot [B] \tag{4.39}$$

in which the size of [E] is NG x NG.

Substituting (4.39) into (4.38) gives

$$[E] \cdot \{g\} = \Omega^2 \cdot \{g\} \tag{4.40}$$

which may be written as

$$([E] - \Omega^2 [I]) \cdot \{g\} = 0 \tag{4.41}$$

Equation (4.41) is the eigenproblem in which Ω^2 is the shell frequency (eigenvalue), and {g} is the buckling mode (eigenvector).

Many techniques are available for the solution of eigenproblems. However, the IMSL system offers convenience through the use of "canned" subroutines, and, thus, the subroutine, EIGRF, was chosen as the eigen-problem solver, and LINV1F was used as the matrix inversion scheme. The IMSL subroutine EIGRF first balances the coefficient matrix, then

performs the Hessian transformation, and finally computes the eigenvalues and eigenvector and back transforms the eigenvector. The IMSL subroutine LINV1F computes the inverse of an N x N matrix, [A], by calling the linear equation solver, LEQT1F, to solve the system

$$[A]\ \{x\}_j = \{e\}_j \quad , \quad \text{for } j = 1,\ldots,N \tag{4.42}$$

in which

$\{x\}_j$ = jth column of $[A]^{-1}$

$\{e\}_j$ = jth column of [I]

Once {g} is determined, substitution into (4.36) permits the solution for {f} and the solution to the eigenproblem is complete.

4.2.5 Adjoint Problem

The solution for λ_1 and λ_2 requires some manipulation to equations (4.6) and (4.7) similar to that performed on equations (4.4) and (4.5) for the solution of f and g. The resulting coefficient matrices are identical to those in equations (4.32) and (4.33), and, therefore, the matrix form of equations (4.6) and (4.7) is given by

$$[C]\ \{-\lambda_1\} + [D]\ \{\lambda_2\} = \lambda_3 \cdot \{c_1\} \tag{4.43}$$

$$[A]\ \{-\lambda_1\} + [B]\ \{\lambda_2\} = \lambda_3 \cdot \{c_2\} \tag{4.44}$$

in which $\{c_1\}$ and $\{c_2\}$ are constant vectors whose values are determined by {f} and {g}. The sizes of [A], [B], [C], and [D] are given in (4.34), and the sizes of $\{\lambda_1\}$, $\{\lambda_2\}$, $\{c_1\}$, and $\{c_2\}$ are

$$\{\lambda_1\} = NFG \times NFG$$
$$\{\lambda_2\} = NG \times NG$$
$$\{c_1\} = NG \times 1 \qquad (4.45)$$
$$\{c_2\} = NFG \times 1$$

Since λ_3 is a constant multiplying the right hand side of each equation, let

$$\lambda_3 = 1 \qquad (4.46)$$

Also, for convenience let

$$\lambda_{11} = -\lambda_1 \qquad (4.47)$$

and equations (4.43) and (4.44) may be rewritten as

$$[C] \cdot \{\lambda_{11}\} + [D] \cdot \{\lambda_2\} = \{c_1\} \qquad (4.48)$$

$$[A] \cdot \{\lambda_{11}\} + [B] \cdot \{\lambda_2\} = \{c_2\} \qquad (4.49)$$

Solving for $\{\lambda_{11}\}$ in equation (4.49) yields

$$\{\lambda_{11}\} = [A]^{-1} \cdot [\{c_2\} - [B] \cdot \{\lambda_2\}] \qquad (4.50)$$

and substituting (4.50) into (4.48) produces

$$[C] \cdot [A]^{-1} \cdot [\{c_2\} - [B] \cdot \{\lambda_2\}] + [D] \cdot \{\lambda_2\} = \{c_1\} \qquad (4.51)$$

Rearranging (4.51) gives

$$[[D] - [C] \cdot [A]^{-1} \cdot [B]] \cdot \{\lambda_2\} = \{c_1\} - [C] \cdot [A]^{-1} \cdot \{c_2\} \qquad (4.52)$$

Substituting (4.39) and the following equation

$$\{p_1\} = \{c_1\} - [C] \cdot [A]^{-1} \cdot \{c_2\} \qquad (4.53)$$

into equation (4.52) results in

$$[E] \cdot \{\lambda_2\} = \{p_1\} \tag{4.54}$$

in which the size of $\{p_1\}$ is NG x 1 and [E] is defined in (4.39).

The solution of (4.54) requires a linear equation solver, and LEQT1F of the IMSL package is used. This particular subroutine employs the Gaussian elimination scheme according to the Crout algorithm and uses equilibration and partial pivoting. Once the values of $\{\lambda_2\}$ have been determined, $\{\lambda_{11}\}$ is obtained by solving equation (4.50). Subsequently, $\{\lambda_1\}$ is found by using equation (4.47), and the solution to the adjoint problem is complete.

4.2.6 Optimality Condition

Expressing equation (4.8) in matrix form yields

$$\lambda_4 \cdot [Q] \cdot \{wo\} = \{c_3\} \tag{4.55}$$

in which $\{c_3\}$ is a vector of constants whose values are dependent upon w, χ, f, g, λ_1, and λ_2, and [Q] is a coefficient matrix whose entries are determined by the finite difference scheme. Realizing that the constant, λ_4, only scales the solution, let

$$\lambda_4 = 1 \tag{4.56}$$

and equation (4.55) is rewritten as

$$[Q] \cdot \{wo\} = \{c_3\} \tag{4.57}$$

in which the matrix and vector sizes are given by

$$\begin{aligned} [Q] &= NG \times NG \\ \{wo\} &= NG \times 1 \\ \{c_3\} &= NG \times 1 \end{aligned} \tag{4.58}$$

The solution to equation (4.57) is a new shell form, {wo}, and is generated by using the IMSL linear equation solving subroutine, LEQT1F, which is described in a previous section.

Before the new form can be evaluated for improvement in buckling load, the surface area must be scaled so as to equal the prescribed surface area coefficient, β^2. The surface area of the new form is determined by equation (4.9) in which the double integration is performed numerically using Simpson's Product Rule [195]. For this case, the integration takes the form

$$SA = \sum_{i=0}^{NPY} \sum_{j=0}^{NPX} A_i \cdot B_j \cdot F_{ij} \tag{4.59}$$

in which

$$\left.\begin{aligned} &SA = \text{actual surface area of new form, wo} \\ &A_i = \frac{\Delta}{3} \text{ for } i = 1 \text{ or NPY} \\ &A_i = \frac{4 \cdot \Delta}{3} \text{ for } i = 2,4,6, \ldots \text{ NPY-1} \\ &A_i = \frac{2 \cdot \Delta}{3} \text{ for } i = 3,5,7, \ldots \text{ NPY-2} \\ &B_j = \text{same pattern as } A_i \end{aligned}\right\} \tag{4.60}$$

$$F_{i,j} = [(wo(i,j))_x]^2 + [(wo(i,j))_y]^2 \tag{4.61}$$

The scaling is then performed by multiplying the magnitude of wo at each mesh point by the following scaling factor, SF:

$$SF = \frac{\beta^2}{SA} \tag{4.62}$$

The result is a new shell form which has the prescribed surface area parameter, β^2.

Chapter 5

RESULTS

Numerical results are presented for several cases in which the parameters given in (2.1) are assigned. The magnitude of the applied load, p_o, the shell form, wo, the equilibrium form (wo - w), and the buckling mode, g, are defined in Chapter 3 and are non-dimensionalized according to (3.22) through (3.24). The boundary conditions are either clamped or simply supported and are described in Chapter 3. In all examples, the rectangular shells have an aspect ratio, b/a, of 1.5. As shown in Figure 2, the uniform, lateral load is applied over either the full shell area ("full") or a central region ("partial") of approximately one-half the total area. For shells having square boundaries, 40% of the shell area is loaded, whereas, for shells having rectangular boundaries 50% of the shell area is loaded (see Figure 2.3).

Results are presented in Tables 5.1 - 5.12 for the following examples:

square, clamped shells having full uniform load

square, clamped shells having partial uniform load

rectangular, clamped shells having full uniform load

rectangular, clamped shells having partial uniform load

square, simply supported shells having full uniform load

square, simply supported shells having partial uniform load

rectangular, simply supported shells having full uniform load

rectangular, simply supported shells having partial uniform load

In each example, results are given for the reference form and the optimal form with each having surface area coefficient, β^2, values of 50, 100, and 150, and with each reference form being given by a double-sine shape. For each test case, the shell form, the equilibrium form prior to buckling, and the buckling mode are presented in tabular form where the points at which values are given represent the finite difference mesh points. Note that beyond the midpoint, the results are denoted as either symmetric (S) or anti-symmetric (A).

Cross sections of the shell forms, equilibrium forms, and buckling modes are presented in Figures 5.1 - 5.12. For square shells, results along $x = 0.5$ are plotted and results along $y = 0.5$ are identical, whereas for rectangular shells, results along $x = 0.5$ and $y = 0.75$ are plotted. Several rectangular cases resulted in forms that were similar in appearance to square cases, and thus the rectangular forms are not redrawn. Magnitudes can be obtained from Tables 5.1 - 5.12.

Results are summarized in Tables 5.13 - 5.16. In Table 5.13 the ratio of optimal form buckling load to the reference form buckling load is given for the various examples. In Table 5.14 the symmetry or anti-symmetry of the buckling modes is summarized for the different cases. The notation used in Table 5.14 denotes symmetric or anti-symmetric buckling along the x and y-axes. For example, "SS" indicates symmetry along both axes, whereas "AS" indicates anti-symmetric buckling along the x-axis and symmetric buckling along the y-axis. A comparison between reference forms and optimal forms is presented in Table 5.15 for each test case. For a given reference form and associated optimal forms, all values have been scaled such that the value at the apex of

the reference form is unity.

5.1 Clamped, Square Shells

Results for shells having square boundaries and clamped boundary conditions are presented in Table 5.1 for full uniform load and Table 5.2 for partial uniform load. Cross sections of the various forms are shown for the reference and optimal forms under full uniform load in Figures 5.1 and 5.2, respectively, and for the reference and optimal forms under partial uniform load in Figures 5.3 and 5.4, respectively.

The shell forms and equilibrium forms are shown in Figures 5.1a - 5.4a and in each case are plotted for $\beta^2 = 100$ only. The forms for $\beta^2 = 50$ and $\beta^2 = 150$ are similar in shape, and, of course, the apex of the reference form increases as β^2 increases. The buckling modes are presented in Figures 5.1b - 5.4b, and in each case the buckling modes for $\beta^2 = 50$ and $\beta^2 = 100$ are doubly symmetric. However, for $\beta^2 = 150$ only the reference form under partial uniform loading is doubly symmetric as the remaining three cases are symmetric-antisymmetric.

The behavior of the square, clamped shells may be described as follows:

(1) For a given β^2, the optimal form has a higher apex than the reference form and has zero slope at the boundaries.

(2) For a given β^2, the optimal form for partial loading has a higher apex and is lower near the boundaries than the optimal form for full loading.

(3) The ratio of the height of the apex of the optimal form to the height of the apex of the reference form follows no

specific pattern as β^2 increases, except that this ratio for $\beta^2 = 150$ is always less than the ratio for $\beta^2 = 50$.

(4) The displacement, w, of the reference form prior to buckling decreases with β^2, whereas the displacement, w, of the optimal form prior to buckling increases with β^2.

(5) For a given β^2, the optimal form undergoes more displacement, w, prior to buckling than the reference form.

(6) For a given β^2, the optimal form for partial loading undergoes less displacement, w, prior to buckling than the optimal form for full loading.

(7) With respect to the reference form, for a given β^2 the equilibrium form prior to buckling resulting from partial loading is "flatter" than the corresponding equilibrium form resulting from full loading.

(8) With respect to the reference form, the equilibrium form prior to buckling becomes more curved as β^2 increases.

(9) The optimal forms under full uniform load show an increase in buckling load of between 26 and 50 percent over those of the reference forms.

(10) The optimal forms under partial uniform load show an increase in buckling load of between 43 and 72 percent over those of the reference forms.

The determination of the optimal forms required between 4 and 9 iterations, depending upon the particular example. The numerical computations were lengthy and complicated partly because of the inner loop in the solution algorithm in which the buckling load is obtained

incrementally by making the lowest frequency of vibration go to zero. In the case of $\beta^2 = 50$, few problems were encountered, and the new shape that resulted from one iteration could be input into the next iteration without first being modified. Thus the number of iterations was reduced. In the cases of $\beta^2 = 100$ and $\beta^2 = 150$, problems arose during the process of incrementally increasing the load. At certain stages, the determination of the equilibrium path was hindered by the existence of other equilibrium states nearby. In some cases convergence to an adjacent equilibrium state was avoided by altering the load increment; however, in other cases, the shell form had to be modified and the solution procedure restarted. Thus, more iterations were required.

Additional problems were encountered in the cases of $\beta^2 = 150$ particularly when subjected to full uniform load. The vibration analysis of the reference form resulted in a double eigenvalue at the lowest frequency, and therefore an alternate initial form had to be chosen. The double eigenvalue is no surprise since at the higher values of β^2, a number of bifurcation points are close together on the equilibrium path. A new initial form was chosen, and by taking only a small percentage of each new shape and modifying it as required, several iterations were completed and a more efficient form was obtained. In the case of $\beta^2 = 150$ under partial load, the reference shape did not generate double eigenvalues. However, certain iterated shapes did possess the double eigenvalue. Therefore, the same amount of care and effort had to be extended in this case.

Table 5.1: Results at x = 0.5 for Square, Clamped Shells Under Full Uniform Load

y	Shell Form			Equilibrium Form			Buckling Mode		
	$\beta^2 = 50$	$\beta^2 = 100$	$\beta^2 = 150$	$\beta^2 = 50$	$\beta^2 = 100$	$\beta^2 = 150$	$\beta^2 = 50$	$\beta^2 = 100$	$\beta^2 = 150$
Reference Form									
0.0	0.00	0.00	0.00	0.00	0.00	0.00	0.00	0.00	0.00
0.1	1.41	2.00	2.45	0.99	1.46	1.73	0.21	0.14	0.61
0.2	2.70	3.80	4.65	1.38	2.33	2.93	0.86	0.66	1.92
0.3	3.70	5.23	6.40	1.54	3.00	4.27	1.74	1.72	2.45
0.4	4.35	6.15	7.54	1.59	3.52	5.51	2.49	2.70	1.63
0.5	4.57	6.47	7.93	1.59	3.74	6.02	2.78	3.09	0.00
	S	S	S	S	S	S	S	S	A
Optimal Form									
0.0	0.00	0.00	0.00	0.00	0.00	0.00	0.00	0.00	0.00
0.1	0.24	0.27	0.32	-1.00	-1.89	-2.25	0.24	0.19	0.63
0.2	1.54	1.85	2.38	-2.10	-3.88	-4.43	0.85	0.66	1.96
0.3	3.36	4.52	5.66	-2.20	-4.42	-4.84	1.73	1.55	2.58
0.4	5.11	7.16	8.47	-1.47	-3.44	-3.35	2.55	2.91	1.69
0.5	5.79	8.15	9.52	-1.04	-2.91	-2.42	2.87	3.67	0.00
	S	S	S	S	S	S	S	S	A

Table 5.2: Results at x = 0.5 for Square, Clamped Shells Under Partial Uniform Load

y	Shell Form			Equilibrium Form			Buckling Mode		
	$\beta^2 = 50$	$\beta^2 = 100$	$\beta^2 = 150$	$\beta^2 = 50$	$\beta^2 = 100$	$\beta^2 = 150$	$\beta^2 = 50$	$\beta^2 = 100$	$\beta^2 = 150$
Reference Form									
0.0	0.00	0.00	0.00	0.00	0.00	0.00	0.00	0.00	0.00
0.1	1.41	2.00	2.45	1.05	1.86	2.39	0.28	0.12	0.04
0.2	2.70	3.80	4.66	1.31	3.02	4.01	0.96	0.70	0.56
0.3	3.70	5.24	6.42	0.97	3.37	4.62	1.75	1.71	1.66
0.4	4.35	6.16	7.54	0.55	3.39	4.77	2.35	2.70	2.85
0.5	4.57	6.47	7.93	0.37	3.37	4.79	2.57	3.12	3.39
	S	S	S	S	S	S	S	S	S
Optimal Form									
0.0	0.00	0.00	0.00	0.00	0.00	0.00	0.00	0.00	0.00
0.1	0.14	0.14	0.20	-0.78	-1.50	-1.62	0.29	0.22	0.68
0.2	1.33	1.36	1.92	-1.23	-3.56	-3.81	0.97	0.76	2.05
0.3	3.14	3.99	5.15	-0.75	-4.59	-4.77	1.77	1.64	2.52
0.4	5.14	7.17	8.56	0.37	-3.37	-2.96	2.33	2.67	1.79
0.5	5.87	8.42	9.73	1.04	-2.49	-1.83	2.50	3.09	0.00
	S	S	S	S	S	S	S	S	A

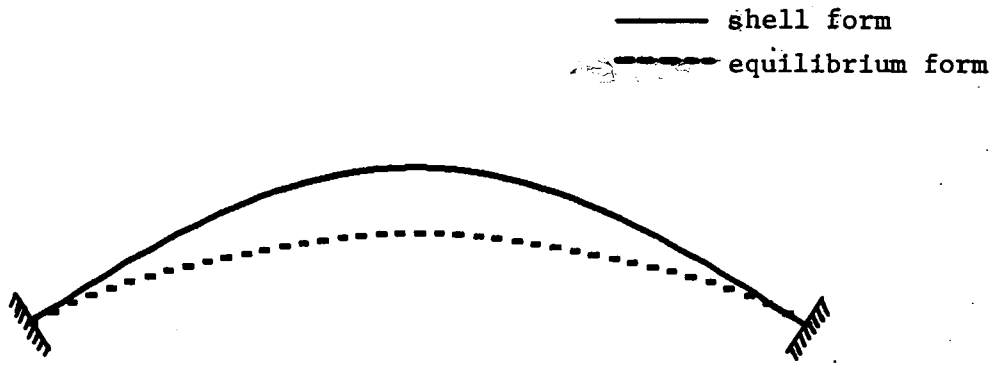

(a) Shell Form and Equilibrium Form Prior to Buckling

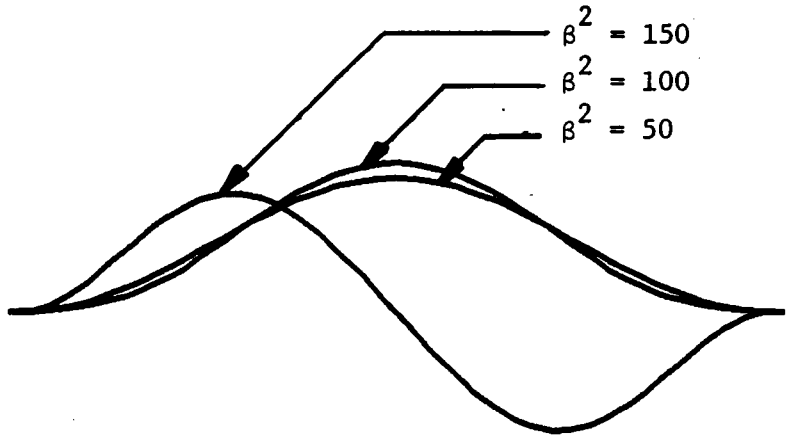

(b) Buckling Modes

Figure 5.1: Results at x = 0.5 for the Reference Form of a Square, Clamped Shell Under Full Uniform Load

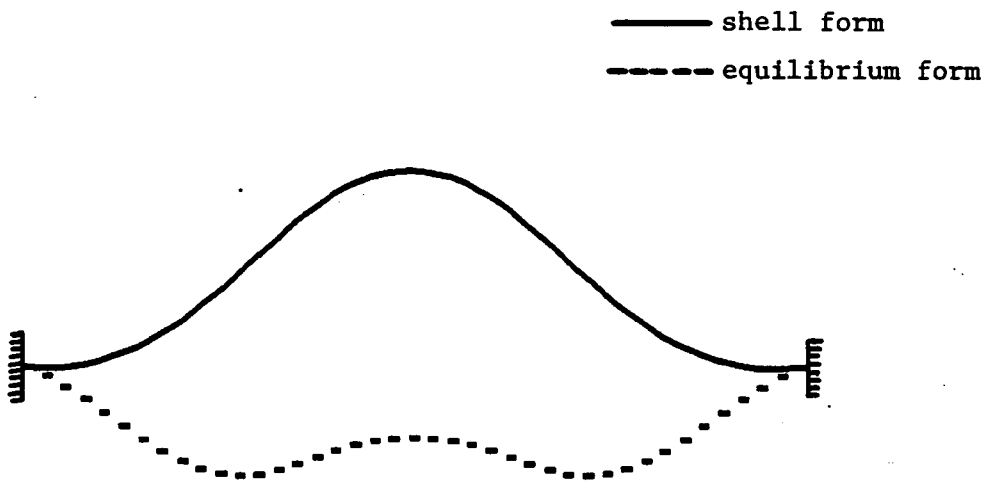

(a) Shell Form and Equilibrium Form Prior to Buckling

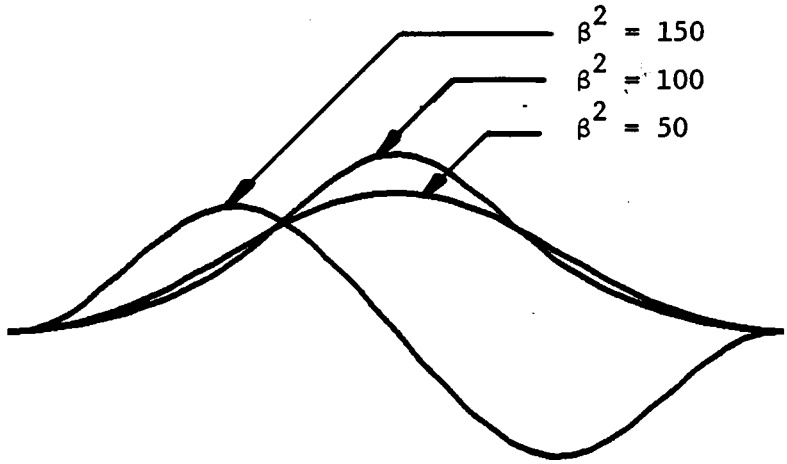

(b) Buckling Modes

Figure 5.2: Results at x = 0.5 for the Optimal Form of a Square, Clamped Shell Under Full Uniform Load

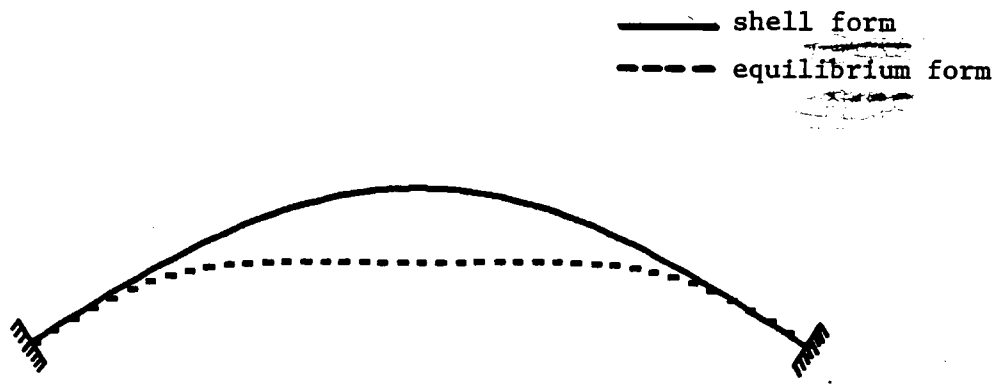

(a) Shell Form and Equilibrium Form Prior to Buckling

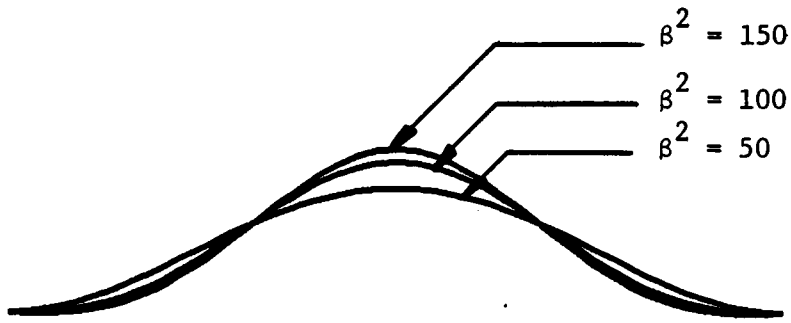

(b) Buckling Modes

Figure 5.3: Results at x = 0.5 for the Reference Form of a Rectangular, Clamped Shell Under Partial Uniform Load

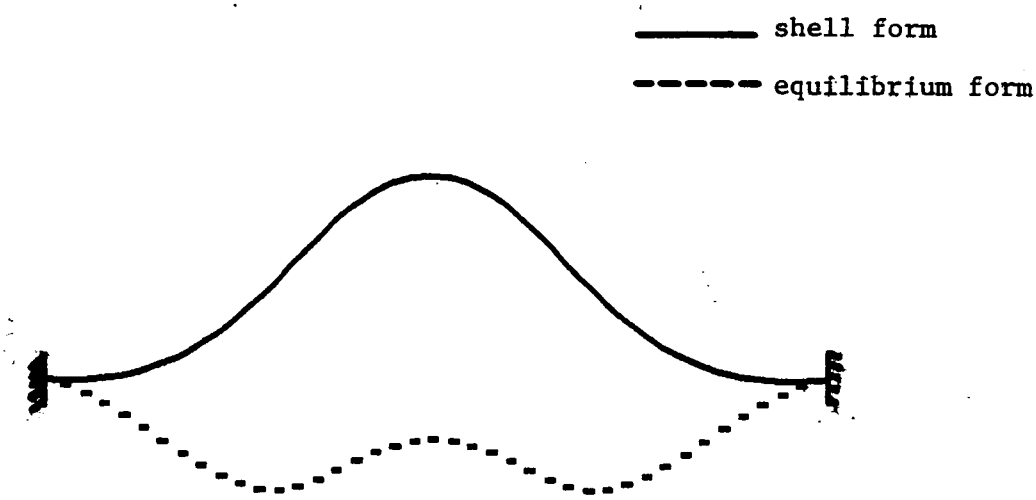

(a) Shell Form and Equilibrium Form Prior to Buckling

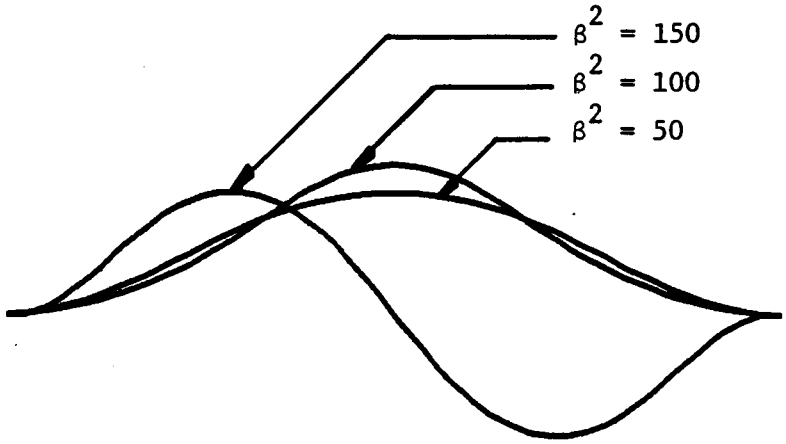

(b) Buckling Modes

Figure 5.4: Results at x = 0.5 for the Optimal Form of a Square, Clamped Shell Under Partial Uniform Load

5.2 Clamped, Rectangular Shells

Results for shells having rectangular boundaries and clamped boundary conditions are presented for full uniform load in Table 5.3 (at $x = 0.5$) and in Table 5.4 (at $y = 0.75$). Results for partial uniform load are presented in Table 5.5 (at $x = 0.5$) and Table 5.6 (at $y = 0.75$). Results for the reference form under full uniform load are given in Figure 5.5 (at $x = 0.5$) and in Figure 5.6 (at $y = 0.75$). Cross sections in each direction of the optimal form under full uniform load, of the reference form under partial load, and of the optimal form under partial load are similar to those given in Figure 5.2, Figure 5.3, and Figure 5.4, respectively, for square shells.

As discussed in Section 5.1 for square shells, optimal forms and corresponding equilibrium forms are plotted in Figures 5.2a - 5.6a for $\beta^2 = 100$ only. The buckling modes are presented in Figures 5.2b - 5.6b, and in each case the buckling modes for $\beta^2 = 50$ and $\beta^2 = 100$ are doubly symmetric. However, for $\beta^2 = 150$, both reference forms have doubly symmetric buckling modes, and the buckling modes for the optimal forms are symmetric in the y-direction and anti-symmetric in the x-direction.

The behavior of the rectangular, clamped shells is characterized by the first 8 items listed for square shells in Section 5.1. Additional points include the following:

(1) The optimal forms under full uniform load show an increase in buckling load of between 38 and 68 percent over those of the reference form.

(2) The optimal forms under partial uniform load show an increase in buckling load of between 47 and 63 percent over those of the reference form.

The determination of the optimal form required between 4 and 9 iterations. The same problems with adjacent equilibrium paths and multiple eigenvalues were encountered as were encountered with square plates and discussed in Section 5.1. However it should be noted that these problems occurred more frequently with the rectangular shells. Although they were more prevalent in the shells with $\beta^2 = 150$, there was less difference between the full and partially loaded cases, and even the cases with $\beta^2 = 50$ exhibited some of these same obstructions to convergence.

5.3 Simply Supported, Square Shells

Results for shells having square boundaries and simply supported boundary conditions are presented in Table 5.7 for full uniform load and in Table 5.8 for partial uniform load. Cross sections of the various forms are shown for the reference and optimal forms under full uniform load in Figures 5.7 and 5.8, respectively, and for the reference and optimal forms under partial uniform load in Figures 5.9 and 5.10, respectively.

The shell forms and equilibrium forms are shown in Figures 5.7a - 5.10a, and in each case only the results for $\beta^2 = 100$ are plotted. The buckling modes are presented in Figures 5.7b - 5.10b, and they exhibit a higher occurrence of anti-symmetric buckling than the corresponding clamped cases. All cases of $\beta^2 = 50$ have doubly symmetric buckling

Table 5.3: Results at x = 0.5 for Rectangular, Clamped Shells Under Full Uniform Load

y	Shell Form			Equilibrium Form			Buckling Mode		
	$\beta^2 = 50$	$\beta^2 = 100$	$\beta^2 = 150$	$\beta^2 = 50$	$\beta^2 = 100$	$\beta^2 = 150$	$\beta^2 = 50$	$\beta^2 = 100$	$\beta^2 = 150$
Reference Form									
0.000	0.00	0.00	0.00	0.00	0.00	0.00	0.00	0.00	0.00
0.125	1.07	1.52	1.86	0.59	0.75	0.84	0.17	0.29	0.49
0.250	2.08	2.94	3.60	0.86	1.07	1.23	0.62	1.01	1.48
0.375	2.94	4.16	5.09	1.10	1.61	2.12	1.20	1.79	2.25
0.500	3.60	5.09	6.24	1.38	2.42	3.49	1.75	2.31	2.37
0.625	4.02	5.68	6.96	1.62	3.17	4.75	2.16	2.51	2.02
0.750	4.16	5.88	7.21	1.72	3.48	5.24	2.75	2.54	1.80
	S	S	S	S	S	S	S	S	S
Optimal Form									
0.000	0.00	0.00	0.00	0.00	0.00	0.00	0.00	0.00	0.00
0.125	0.37	0.51	0.82	-0.82	-1.07	-1.09	0.15	0.13	0.00
0.250	1.15	1.66	2.35	-1.92	-2.73	-2.98	0.51	0.48	0.00
0.375	2.31	3.60	4.62	-2.56	-4.26	-4.87	1.11	1.07	0.00
0.500	3.78	6.10	7.28	-2.35	-5.41	-5.73	1.93	2.16	0.00
0.625	5.16	7.72	8.65	-1.54	-4.81	-5.15	2.70	2.81	0.00
0.750	5.71	8.20	9.45	-1.11	-4.29	-4.66	3.00	3.24	0.00
	S	S	S	S	S	S	S	S	S

Table 5.4: Results at y = 0.75 for Rectangular, Clamped Shells Under Full, Uniform Load

x	Shell Form			Equilibrium Form			Buckling Mode		
	$\beta^2 = 50$	$\beta^2 = 100$	$\beta^2 = 150$	$\beta^2 = 50$	$\beta^2 = 100$	$\beta^2 = 150$	$\beta^2 = 50$	$\beta^2 = 100$	$\beta^2 = 150$
Reference Form									
0.000	0.00	0.00	0.00	0.00	0.00	0.00	0.00	0.00	0.00
0.125	1.59	2.25	2.76	1.14	1.86	2.42	0.33	0.08	0.07
0.250	2.94	4.16	5.09	1.60	2.90	4.04	1.28	0.91	0.58
0.375	3.84	5.43	6.66	1.71	3.36	4.95	2.31	2.02	1.42
0.500	4.16	5.38	7.21	1.72	3.48	5.24	2.75	2.54	1.80
	S	S	S	S	S	S	S	S	S
Optimal Form									
0.000	0.00	0.00	0.00	0.00	0.00	0.00	0.00	0.00	0.00
0.125	0.47	0.90	1.22	-1.42	-2.57	-2.92	0.42	0.38	1.15
0.250	2.46	4.02	5.08	-2.14	-4.96	-5.34	1.45	1.36	2.08
0.375	4.74	7.14	8.44	-1.58	-4.63	-5.06	2.55	2.62	1.09
0.500	5.71	8.20	9.45	-1.11	-4.29	-4.66	3.00	3.24	0.00
	S	S	S	S	S	S	S	S	A

Table 5.5: Results at x = 0.5 for Rectangular, Clamped Shells Under Partial Uniform Load

y	Shell Form			Equilibrium Form			Buckling Mode		
	$\beta^2 = 50$	$\beta^2 = 100$	$\beta^2 = 150$	$\beta^2 = 50$	$\beta^2 = 100$	$\beta^2 = 150$	$\beta^2 = 50$	$\beta^2 = 100$	$\beta^2 = 150$
Reference Form									
0.000	0.00	0.00	0.00	0.00	0.00	0.00	0.00	0.00	0.00
0.125	1.07	1.52	1.86	0.65	1.34	1.70	0.26	0.10	0.09
0.250	2.08	2.94	3.60	1.36	2.20	2.82	0.80	0.54	0.52
0.375	2.94	4.16	5.09	1.63	2.60	3.38	1.43	1.29	1.33
0.500	3.60	5.09	6.24	1.79	2.90	3.91	1.98	2.15	2.27
0.625	4.02	5.68	6.96	1.95	3.18	4.39	2.35	2.84	2.98
0.750	4.16	5.88	7.21	1.98	3.26	4.59	2.47	3.10	3.25
	S	S	S	S	S	S	S	S	S
Optimal Form									
0.000	0.00	0.00	0.00	0.00	0.00	0.00	0.00	0.00	0.00
0.125	0.27	0.29	0.28	-0.65	-0.91	-1.02	0.15	0.12	0.00
0.250	1.03	1.13	1.25	-1.86	-2.59	-2.86	0.62	0.43	0.00
0.375	2.21	2.64	2.96	-2.75	-4.39	-5.03	1.04	0.91	0.00
0.500	4.36	6.84	6.92	-2.06	-5.27	-5.61	1.78	1.74	0.00
0.625	5.74	7.85	8.87	-1.28	-4.58	-4.83	2.64	2.93	0.00
0.750	6.18	8.38	9.66	-0.56	-3.93	-4.32	2.77	3.52	0.00
	S	S	S	S	S	S	S	S	S

Table 5.6: Results at y = 0.75 for Rectangular, Clamped Shells Under Partial Uniform Load

x	Shell Form			Equilibrium Form			Buckling Mode		
	$\beta^2 = 50$	$\beta^2 = 100$	$\beta^2 = 150$	$\beta^2 = 50$	$\beta^2 = 100$	$\beta^2 = 150$	$\beta^2 = 50$	$\beta^2 = 100$	$\beta^2 = 150$
Reference Form									
0.000	0.00	0.00	0.00	0.00	0.00	0.00	0.00	0.00	0.00
0.125	1.59	2.25	2.76	1.37	2.00	2.63	0.51	0.14	-0.04
0.250	2.94	4.16	5.09	1.79	2.94	3.98	1.42	1.15	0.93
0.375	3.84	5.43	6.66	1.95	3.22	4.49	2.19	2.48	2.47
0.500	4.16	5.88	7.21	1.98	3.26	4.59	2.47	3.10	3.25
	S	S	S	S	S	S	S	S	S
Optimal Form									
0.000	0.00	0.00	0.00	0.00	0.00	0.00	0.00	0.00	0.00
0.125	0.18	0.19	0.29	-1.46	-2.63	-3.07	0.47	0.42	1.19
0.250	2.45	2.67	2.65	-2.38	-5.11	-5.62	1.48	1.40	2.16
0.375	5.39	7.54	8.72	-1.79	-4.84	-5.29	2.51	2.81	1.17
0.500	6.18	8.38	9.66	-0.56	-3.93	-4.32	2.77	3.52	0.00
	S	S	S	S	S	S	S	S	A

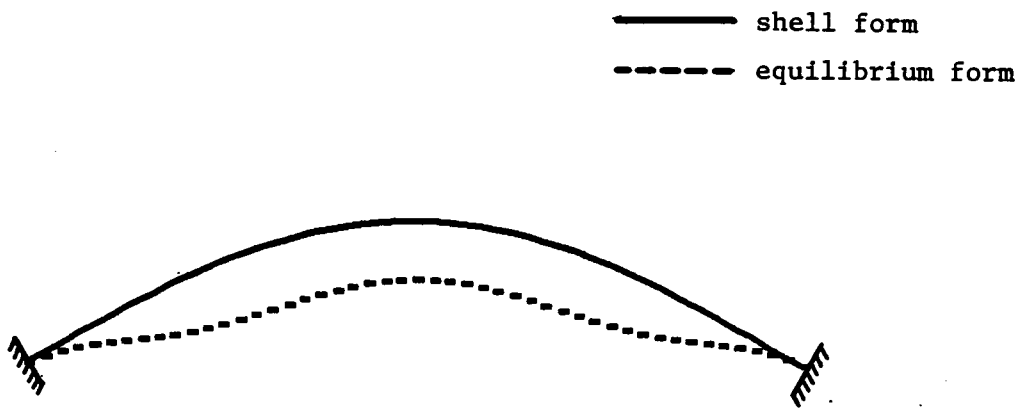

(a) Shell Form and Equilibrium Form Prior to Buckling

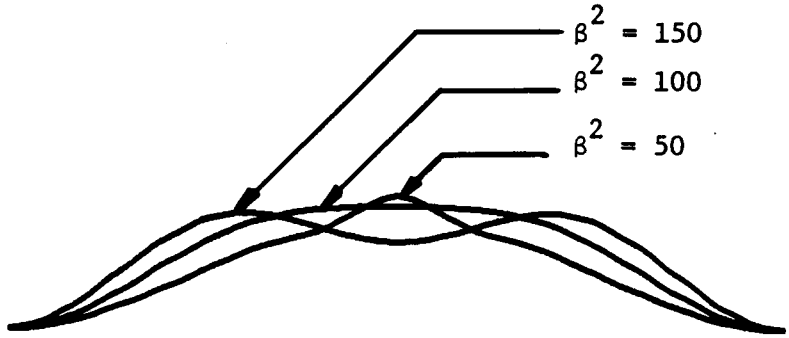

(b) Buckling Modes

Figure 5.5: Results at x = 0.5 for the Reference Form of a Rectangular, Clamped Shell Under Full Uniform Load

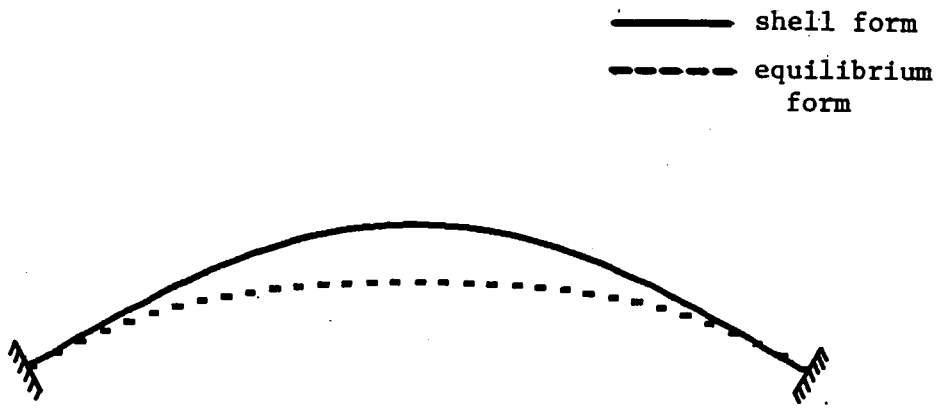

(a) Shell Form and Equilibrium Form Prior to Buckling

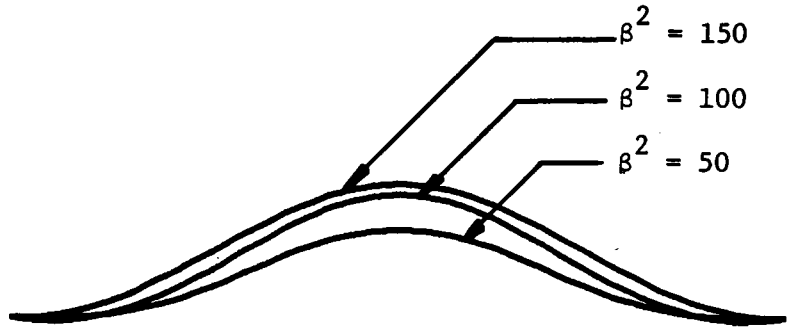

(b) Buckling Modes

Figure 5.6: Results at y = 0.75 for the Reference Form of a Rectangular, Clamped Shell Under Full Uniform Load

modes. All cases of $\beta^2 = 100$ and $\beta^2 = 150$ exhibit anti-symmetric buckling along the y-axis, except the case of the reference form subject to partial uniform load in which all values of β^2 lead to doubly-symmetric buckling.

The behavior of the square, simply supported shells may be described as follows:

(1) For a given β^2 and for uniform loading, the optimal form has a lower apex and has a steeper slope at the boundaries than the reference form.

(2) For a given β^2 and for partial loading, the optimal form has a higher apex and is lower near the boundaries than the reference form.

(3) For full uniform load, the ratio of the height of the apex of the optimal form to the height of the apex of the reference form decreases as β^2 increases. For partial uniform load, this ratio is approximately the same for all β^2 values.

(4) The displacement, w, of the reference form prior to buckling decreases as β^2 increases, whereas the displacement, w, of the optimal form prior to buckling does not follow any pattern.

(5) For a given β^2, the optimal form for full uniform load undergoes more displacement, w, prior to buckling than the reference form, and the optimal form for partial uniform load undergoes less displacement prior to buckling than the reference form.

(6) For a given β^2, the optimal form for partial loading undergoes more displacement prior to buckling than the optimal form for full loading.

(7) For the reference forms, the equilibrium forms are "flatter" for the partial loading cases than for the full loading cases.

(8) For the optimal forms, the equilibrum forms are "flatter" in the full loading cases than in the partial loading cases.

(9) The optimal forms under full uniform loading show an increase in buckling load of between 4 and 8 percent.

(10) The optimal forms under partial uniform loading show an increase in buckling load of between 5 and 19 percent.

The determination of the optimal forms required between 3 and 7 iterations. Although the problem of multiple eigenvalues was present again during some of the iterations for the cases of $\beta^2 = 150$, slight modifications to the shell form permitted the solution process to continue. Even though for most cases the two lowest eigenvalues were relatively close together and during the iterative process many of the forms exhibited anti-symmetric buckling, the optimal forms were obtained quickly. This success can be attributed partially to the fact that the reference forms were good approximations of the optimal forms. Therefore, fewer iterations were required, but a smaller increase in buckling load was achieved and less change in form was noticed.

Table 5.7: Results at x = 0.5 for Square, Simply Supported Shells Under Full Uniform Load

y	Shell Form			Equilibrium Form			Buckling Mode		
	$\beta^2 = 50$	$\beta^2 = 100$	$\beta^2 = 150$	$\beta^2 = 50$	$\beta^2 = 100$	$\beta^2 = 150$	$\beta^2 = 50$	$\beta^2 = 100$	$\beta^2 = 150$
Reference Form									
0.0	0.00	0.00	0.00	0.00	0.00	0.00	0.00	0.00	0.00
0.1	1.41	2.00	2.45	0.58	1.00	1.30	0.74	1.43	1.65
0.2	2.70	3.80	4.66	1.30	2.35	3.13	1.26	2.08	2.21
0.3	3.70	5.24	6.42	2.07	3.83	5.12	1.51	1.81	1.72
0.4	4.35	6.16	7.54	2.67	4.97	6.61	1.57	1.00	0.85
0.5	4.57	6.47	7.93	2.89	5.39	7.15	1.57	0.00	0.00
	S	S	S	S	S	S	S	A	A
Optimal Form									
0.0	0.00	0.00	0.00	0.00	0.00	0.00	0.00	0.00	0.00
0.1	1.49	2.17	2.92	0.75	1.42	2.55	0.64	1.34	1.64
0.2	2.75	3.88	5.06	1.45	2.62	4.30	1.19	2.15	2.38
0.3	3.65	5.00	6.27	2.01	3.44	5.03	1.59	2.14	2.05
0.4	4.18	5.61	6.81	2.37	3.92	5.15	1.82	1.31	1.12
0.5	4.36	5.80	6.96	2.50	4.08	5.12	1.87	0.00	0.00
	S	S	S	S	S	S	S	A	A

Table 5.8: Results at x = 0.5 for Square, Simply Supported Shells Under Partial Uniform Load

y	Shell Form			Equilibrium Form			Buckling Mode		
	$\beta^2 = 50$	$\beta^2 = 100$	$\beta^2 = 150$	$\beta^2 = 50$	$\beta^2 = 100$	$\beta^2 = 150$	$\beta^2 = 50$	$\beta^2 = 100$	$\beta^2 = 150$
Reference Form									
0.0	0.00	0.00	0.00	0.00	0.00	0.00	0.00	0.00	0.00
0.1	1.41	2.00	2.45	0.92	1.79	2.36	0.46	0.15	0.04
0.2	2.70	3.80	4.65	1.55	2.98	4.00	1.04	0.70	0.55
0.3	3.70	5.23	6.40	1.81	3.37	4.61	1.70	1.70	1.65
0.4	4.35	6.15	7.54	1.89	3.41	4.77	2.24	2.71	2.87
0.5	4.57	6.47	7.93	1.90	3.40	4.79	2.45	3.14	3.40
	S	S	S	S	S	S	S	S	S
Optimal Form									
0.0	0.00	0.00	0.00	0.00	0.00	0.00	0.00	0.00	0.00
0.1	1.31	1.87	2.22	0.66	1.50	1.72	0.63	1.27	1.38
0.2	2.59	3.66	4.32	1.29	2.67	3.16	1.19	2.14	2.30
0.3	3.74	5.24	6.25	1.84	3.47	4.42	1.62	2.24	2.35
0.4	4.55	6.37	7.74	2.29	4.10	5.75	1.86	1.43	1.44
0.5	4.34	6.79	8.35	2.47	4.37	6.40	1.94	0.00	0.00
	S	S	S	S	S	S	S	A	A

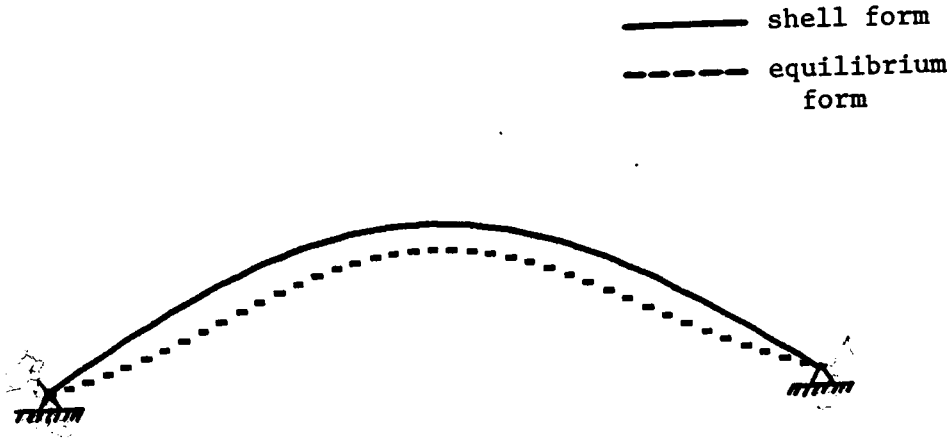

(a) Shell Form and Equilibrium Form Prior to Buckling

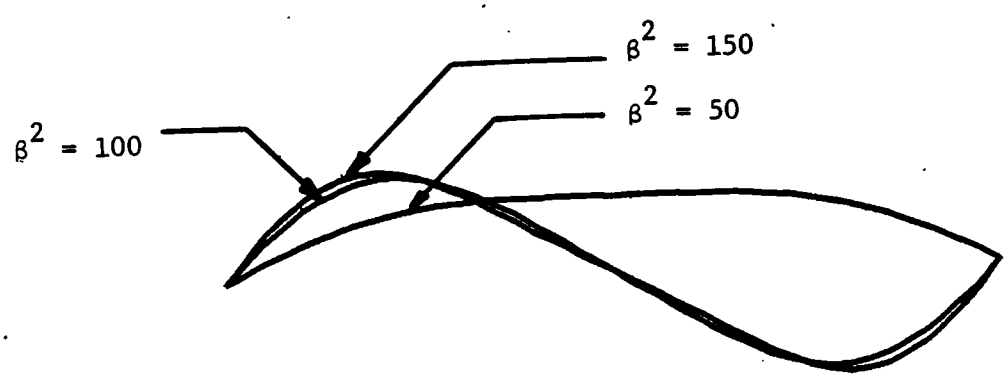

(b) Buckling Modes

Figure 5.7: Results at x = 0.5 for the Reference Form of a Square, Simply Supported Shell Under Full Uniform Load

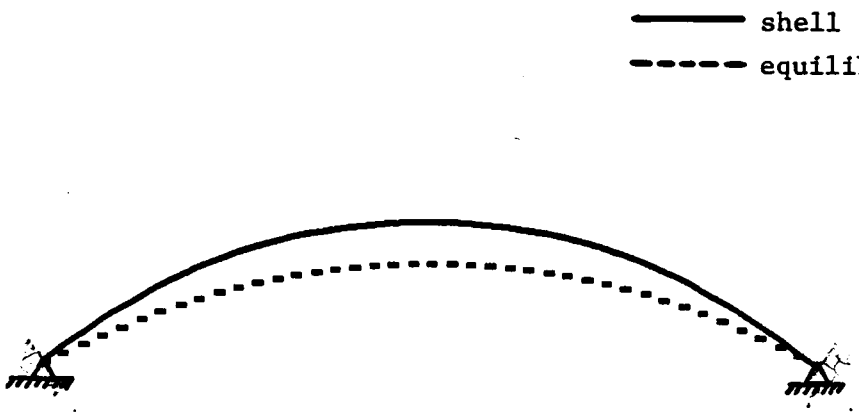

(a) Shell Form and Equilibrium Form Prior to Buckling

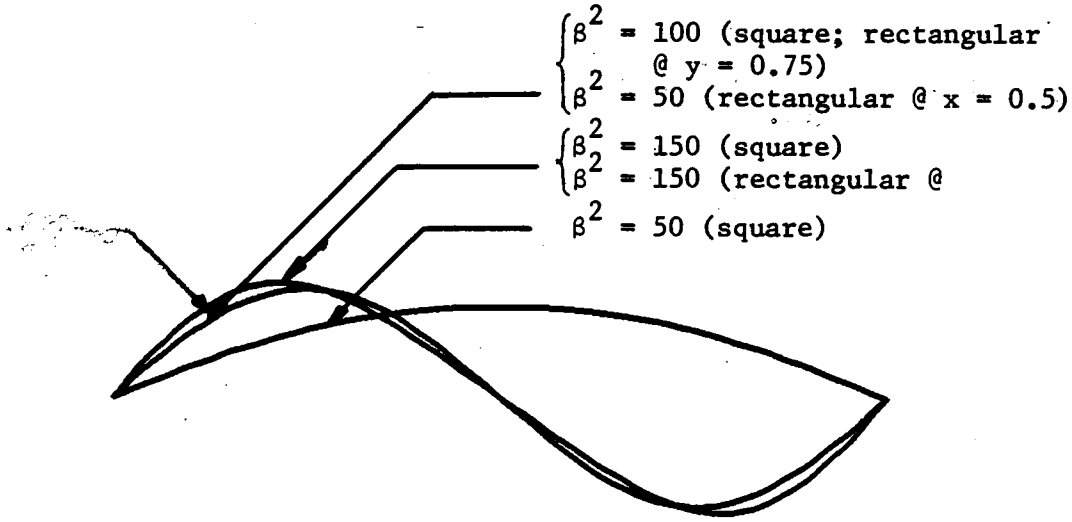

(b) Buckling Modes

Figure 5.8: Results for the Optimal Form of Simply Supported Shells Under Full Uniform Load

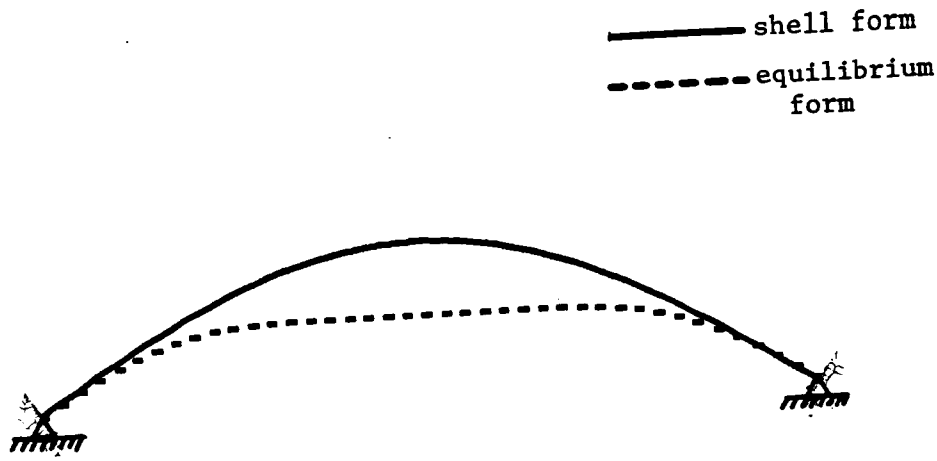

(a) Shell Form and Equilibrium Form Prior to Buckling

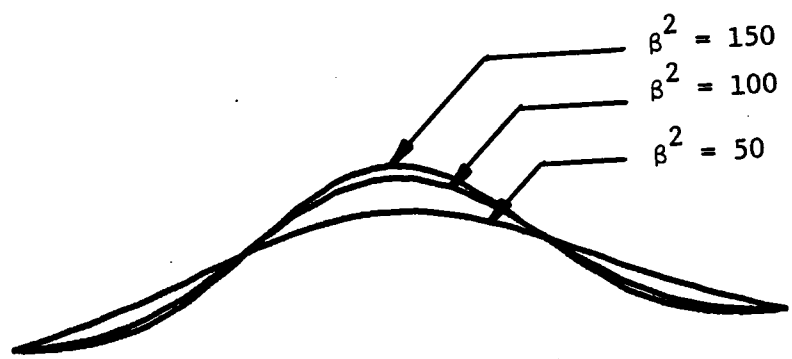

(b) Buckling Modes

Figure 5.9: Results at x = 0.5 for the Reference Form of a Square, Simply Supported Shell Under Partial Uniform Load

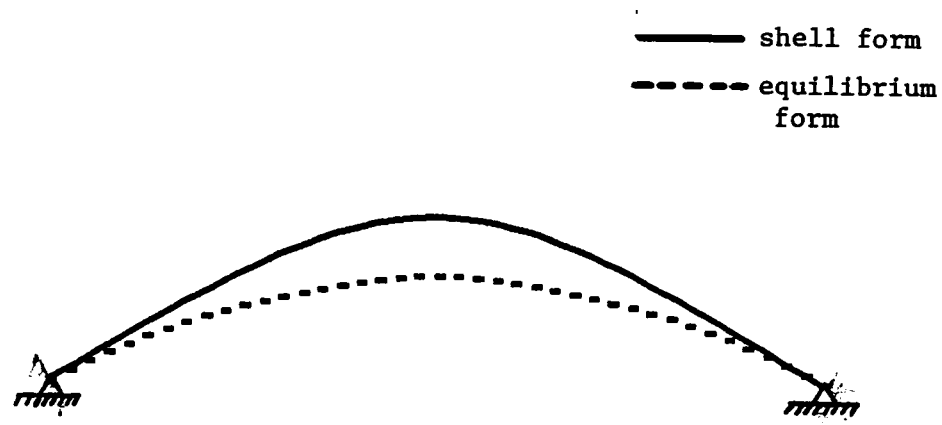

(a) Shell Form and Equilibrium Form Prior to Buckling

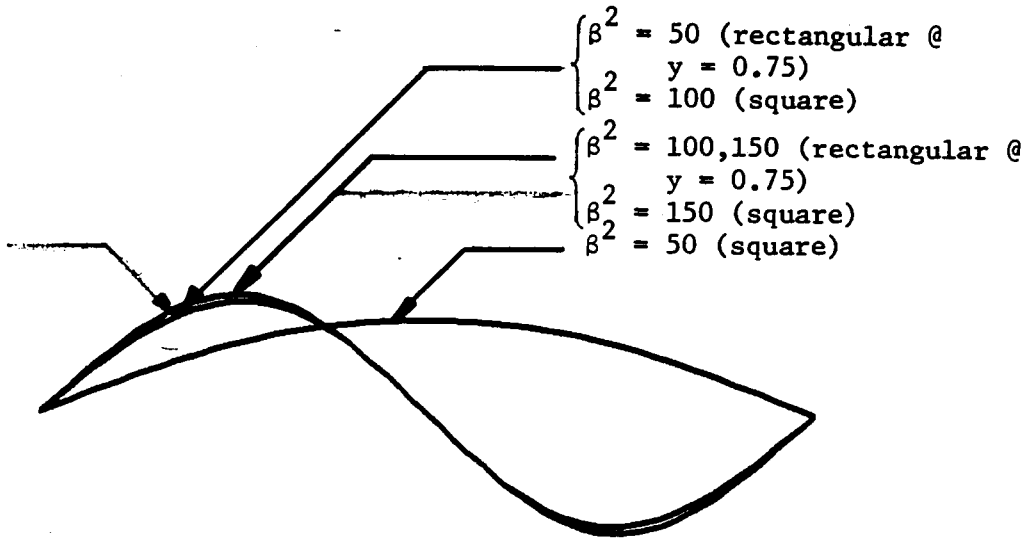

(b) Buckling Modes

Figure 5.10: Results for the Optimal Form of Simply Supported Shells Under Partial Uniform Load

5.4 Simply Supported, Rectangular Shells

Results for shells having rectangular boundaries and simply supported boundary conditions are presented for full uniform load in Table 5.9 (at x = 0.5) and in Table 5.10 (at y = 0.75). Results for partial uniform load are presented in Table 5.11 (at x = 0.5) and in Table 5.12 (at y = 0.75). Cross sections of the reference form under full uniform load are given in Figure 5.11 (at x = 0.5) and in Figure 5.12 (at y = 0.75). Cross sections in each direction of the optimal form under full uniform load, of the reference form under partial uniform load, and of the optimal form under partial uniform load are similar to those given in Figures 5.8, 5.9, and 5.10, respectively.

As discussed in Section 5.3 for square shells, the optimal forms and corresponding equilibrium forms are plotted in Figures 5.8a - 5.12a for $\beta^2 = 100$ only. The buckling modes are presented in Figures 5.8b - 5.12b, and many of the cases exhibit anti-symmetric buckling in the x-direction. The behavior of the rectangular, simply supported shells is characterized by the first 8 items listed for square shells in Section 5.3. Additional points worth noting include:

(1) The optimal forms under full uniform load show an increase in buckling load of between 22 and 50 percent.

(2) The optimal forms under partial uniform load show an increase in buckling load of between 13 and 18 percent.

The determination of the optimal forms required between 3 and 7 iterations, where, as in the case of the square shells, the fewer iterations resulted from the fact that the reference form was a good initial guess for the optimal shape. Once again, during the iterative

procedure many of the forms (especially those with $\beta^2 = 150$) produced multiple eigenvalues, but in spite of this problem, optimal forms were obtained after a few iterations.

Table 5.9: Results at x = 0.5 for Rectangular, Simply Supported Shells Under Full Uniform Load

y	Shell Form			Equilibrium Form			Buckling Mode		
	$\beta^2 = 50$	$\beta^2 = 100$	$\beta^2 = 150$	$\beta^2 = 50$	$\beta^2 = 100$	$\beta^2 = 150$	$\beta^2 = 50$	$\beta^2 = 100$	$\beta^2 = 150$
Reference Form									
0.000	0.00	0.00	0.00	0.00	0.00	0.00	0.00	0.00	0.00
0.125	1.08	1.52	1.86	0.16	0.30	0.44	0.80	1.23	1.28
0.250	2.08	2.94	3.60	0.57	1.07	1.52	1.38	1.76	1.98
0.375	2.94	4.16	5.09	1.23	2.27	3.15	1.66	1.91	1.94
0.500	3.60	5.09	6.24	1.96	3.54	4.78	1.69	1.52	1.47
0.625	4.02	5.68	6.96	2.52	4.47	5.95	1.60	1.40	1.02
0.750	4.16	5.88	7.21	2.73	4.81	6.35	1.55	1.29	0.84
	S	S	S	S	S	S	S	S	S
Optimal Form									
0.000	0.00	0.00	0.00	0.00	0.00	0.00	0.00	0.00	0.00
0.125	1.32	1.86	2.51	0.49	0.79	1.86	1.09	0.00	0.00
0.250	2.43	3.46	4.47	1.02	1.87	3.50	1.85	0.00	0.00
0.375	3.24	4.63	5.70	1.54	3.06	4.63	2.08	0.00	0.00
0.500	3.74	5.36	6.32	1.94	4.02	5.23	1.75	0.00	0.00
0.625	3.97	5.72	6.62	2.16	4.62	5.53	1.00	0.00	0.00
0.750	4.04	5.84	6.71	2.22	4.82	5.63	0.00	0.00	0.00
	S	S	S	S	S	S	A	S	S

Table 5.10: Results at y = 0.75 for Rectangular, Simply Supported Shells Under Full Uniform Load

x	Shell Form			Equilibrium Form			Buckling Mode		
	$\beta^2 = 50$	$\beta^2 = 100$	$\beta^2 = 150$	$\beta^2 = 50$	$\beta^2 = 100$	$\beta^2 = 150$	$\beta^2 = 50$	$\beta^2 = 100$	$\beta^2 = 150$
Reference Form									
0.000	0.00	0.00	0.00	0.00	0.00	0.00	0.00	0.00	0.00
0.125	1.59	2.25	2.76	0.91	1.65	2.21	0.68	0.56	0.31
0.250	2.94	4.16	5.09	1.80	3.22	4.30	1.19	0.91	0.57
0.375	3.84	5.43	6.65	2.47	4.38	5.80	1.47	1.23	0.77
0.500	4.16	5.88	7.21	2.73	4.81	6.35	1.55	1.29	0.84
	S	S	S	S	S	S	S	S	S
Optimal Form									
0.000	0.00	0.00	0.00	0.00	0.00	0.00	0.00	0.00	0.00
0.125	1.68	2.31	2.91	0.94	1.64	2.36	0.00	1.58	1.66
0.250	2.99	4.19	5.08	1.66	3.20	4.22	0.00	2.14	2.35
0.375	3.78	5.41	6.32	2.09	4.38	5.29	0.00	1.46	1.66
0.500	4.04	5.84	6.71	2.22	4.82	5.63	0.00	0.00	0.00
	S	S	S	S	S	S	S	A	A

Table 5.11: Results at x = 0.5 for Rectangular, Simply Supported Shells Under Partial Uniform Load

y	Shell Form			Equilibrium Form			Buckling Mode		
	$\beta^2 = 50$	$\beta^2 = 100$	$\beta^2 = 150$	$\beta^2 = 50$	$\beta^2 = 100$	$\beta^2 = 150$	$\beta^2 = 50$	$\beta^2 = 100$	$\beta^2 = 150$
Reference Form									
0.000	0.00	0.00	0.00	0.00	0.00	0.00	0.00	0.00	0.00
0.125	1.08	1.52	1.86	0.64	1.26	1.65	0.42	0.00	0.00
0.250	2.08	2.94	3.60	1.14	2.28	2.95	0.88	0.00	0.00
0.375	2.94	4.16	5.09	1.46	2.99	3.83	1.37	0.00	0.00
0.500	3.60	5.09	6.24	1.73	3.63	4.67	1.80	0.00	0.00
0.625	4.02	5.68	6.96	1.93	4.13	5.36	2.09	0.00	0.00
0.750	4.16	5.88	7.21	2.01	4.31	5.62	2.20	0.00	0.00
	S	S	S	S	S	S	S	S	S
Optimal Form									
0.000	0.00	0.00	0.00	0.00	0.00	0.00	0.00	0.00	0.00
0.125	1.04	1.67	2.10	0.57	1.48	1.93	0.00	0.00	0.00
0.250	2.10	3.27	4.05	1.15	2.74	3.43	0.00	0.00	0.00
0.375	2.86	4.67	5.71	1.57	3.66	4.35	0.00	0.00	0.00
0.500	3.87	5.69	6.91	2.21	4.36	5.04	0.00	0.00	0.00
0.625	4.32	6.21	7.53	2.56	4.73	5.38	0.00	0.00	0.00
0.750	4.47	6.24	7.56	2.68	4.70	5.29	0.00	0.00	0.00
	S	S	S	S	S	S	S	S	S

Table 5.12: Results at y = 0.75 for Rectangular, Simply Supported Shells Under Partial Uniform Load

x	Shell Form			Equilibrium Form			Buckling Mode		
	$\beta^2 = 50$	$\beta^2 = 100$	$\beta^2 = 150$	$\beta^2 = 50$	$\beta^2 = 100$	$\beta^2 = 150$	$\beta^2 = 50$	$\beta^2 = 100$	$\beta^2 = 150$
Reference Form									
0.000	0.00	0.00	0.00	0.00	0.00	0.00	0.00	0.00	0.00
0.125	1.59	2.25	2.76	0.84	1.81	2.45	0.78	1.62	1.59
0.250	2.94	4.16	5.09	1.46	3.13	4.15	1.50	2.32	2.33
0.375	3.84	5.43	6.66	1.87	4.00	5.24	2.01	1.64	1.68
0.500	4.16	5.88	7.21	2.01	4.31	5.62	2.20	0.00	0.00
	S	S	S	S	S	S	S	A	A
Optimal Form									
0.000	0.00	0.00	0.00	0.00	0.00	0.00	0.00	0.00	0.00
0.125	1.68	2.45	3.06	1.02	2.03	2.83	1.60	1.66	1.47
0.250	3.16	4.51	5.57	1.90	3.53	4.52	2.25	2.38	2.35
0.375	4.14	5.80	7.08	2.48	4.40	5.16	1.59	1.71	1.84
0.500	4.47	6.24	7.56	2.68	4.69	5.29	0.00	0.00	0.00
	S	S	S	S	S	S	A	A	A

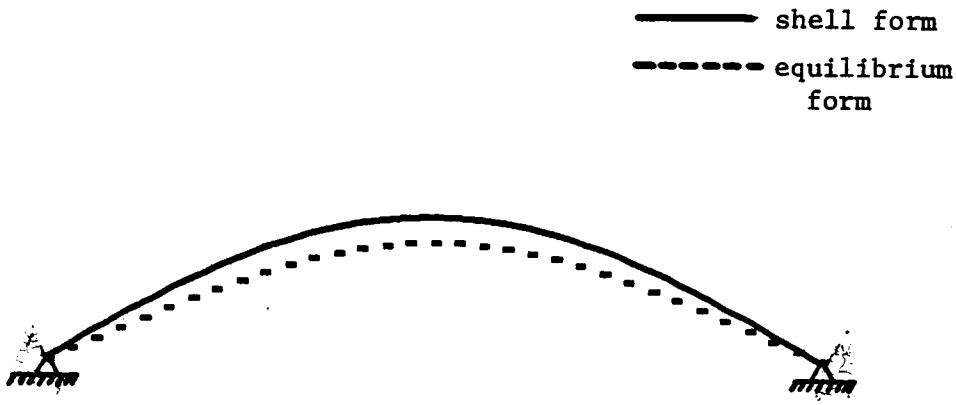

(a) Shell Form and Equilibrium Form Prior to Buckling

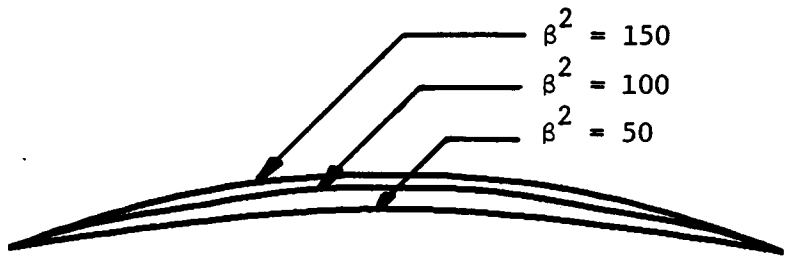

(b) Buckling Modes

Figure 5.11: Results at x = 0.5 and y = 0.75 for the Reference Form of a Rectangular, Simply Supported Shell Under Full Uniform Load

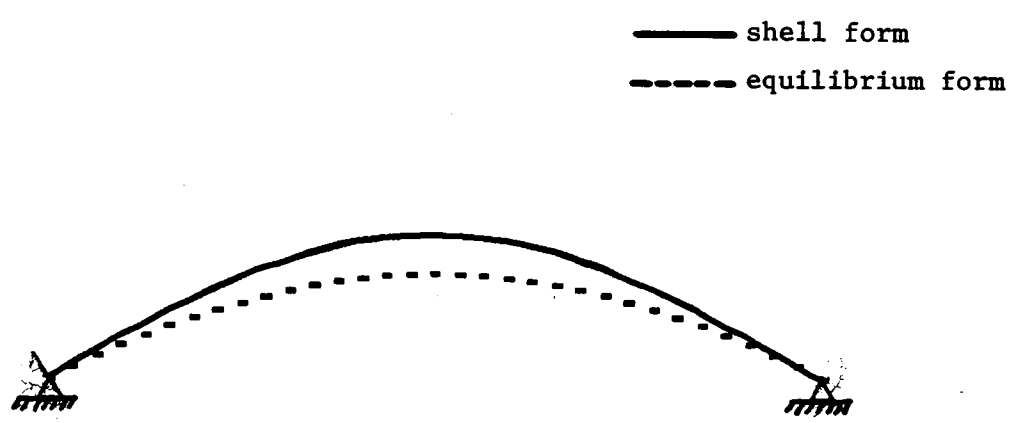

(a) Shell Form and Equilibrium Form Prior to Buckling

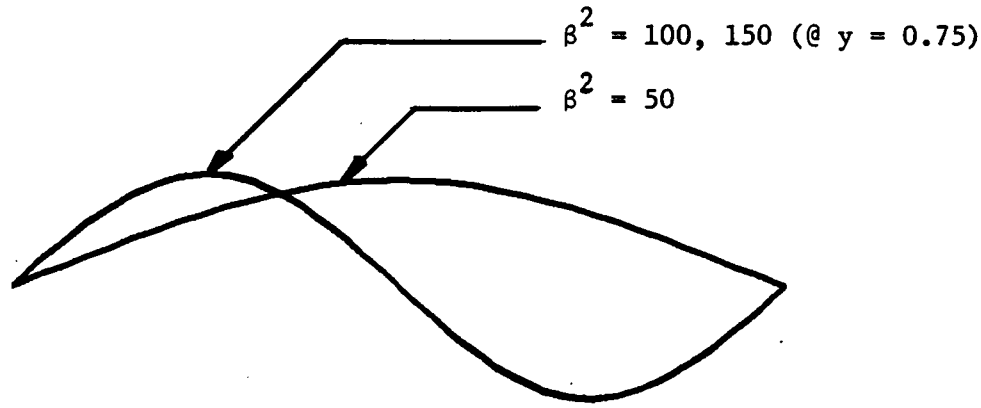

(b) Buckling Modes

Figure 5.12: Results at x = 0.5 and y = 0.75 for the Reference Form of a Rectangular, Simply Supported Shell Under Partial Uniform Load

Chapter 6

CONCLUSIONS

6.1 Conclusions

A recent reception at the University of California at Berkeley honored Dr. Heinz Isler for his design of thin concrete shells. Many of Dr. Isler's works are recognized as structural art forms, and a collection of photographs of his designs were exhibited and considered to be profoundly satisfying by the observers. Dr. Isler stated that although only a small number of structural shapes have been built, the possibilities for design are endless. However, the structures must be designed to get the maximum stability and strength with a minimum of materials.

Numerical results have been presented in this paper which verify the fact that the shell form can have a significant effect on the critical value of the applied load. Shallow shells having a rectangular boundary and a prescribed value of the surface area coefficient β^2 have been investigated. Twenty-four cases have been examined, involving clamped or simply supported boundary conditions, square or rectangular boundaries, full uniform or partial uniform loads, and β^2 values of 50, 100, and 150.

The optimal forms vary significantly between the clamped and simply supported boundary conditions. For clamped boundaries the apex of the optimal form is higher than that of the reference form (double-sine). For the simply supported cases, the apex of the optimal form

is lower than that of the reference form in the cases of full uniform load. In the cases of partial uniform load, the apex of the optimal form is higher than that of the reference form. Regardless of boundary conditions, the apex of the rectangular optimal form is higher than the corresponding square form, and the apex of the optimal form for partial loading is higher than that of the optimal form for full loading. A summary of these form changes is given in Tables 5.15 and 5.16.

The effect of the form changes upon the buckling load is discussed in Sections 5.1 - 5.4, and those results are summarized in Table 5.13. In every case, a form is generated that offers a higher buckling load than the reference form. The percentage increase in buckling load above that of the reference form depends upon the similarity of the reference form to the optimal form. Perspectives of the optimal forms of four test cases are shown in Figures 5.16 - 5.20.

The optimal forms also exhibited a more frequent occurrence of anti-symmetric buckling modes than the reference forms. These changes in buckling mode are summarized in Table 5.14. As indicated, the forms having a β^2 value of 50 have predominantly doubly-symmetric modes, and thus the critical load for these shells is associated with a limit point. These shells do not tend to be sensitive to small imperfections. On the other hand, several of the reference forms and many of the optimal forms having β^2 values of 100 and 150 have anti-symmetric buckling modes. This type of mode indicates a critical load that is associated with a bifurcation point, and the sensitivity of the critical load to small imperfections is dependent upon the branching path at the critical bifurcation point. Thus, the imperfection-

sensitivity of the buckling load in these cases can only be determined by analyzing the post-buckling behavior of the shell.

Many of the reference forms and the forms generated during the iterations exhibited multiple eigenvalues at the lowest frequency of vibration. Because the formulation described in Chapter 3 is a unimodal formulation, multiple eigenvalues could not be accommodated. Therefore, the forms were changed, and the process was repeated until eventually no further steps could be taken. This obstacle, combined with the fact that the critical load was sensitive to changes in design, created computational difficulties and forced a relaxation of the convergence requirements. Therefore, the forms presented in this study (particularly those having $\beta^2 = 150$) are certainly more efficient than the reference form with respect to buckling, but they may not be the exact, globally optimum designs.

6.2 Suggestions for Future Research

As an extension of this work, several topics are mentioned below as possibilities for future research:

(1) Reformulate the problem to incorporate bimodal (multiple eigenvalue) buckling. Such a formulation would permit a more precise analysis of some of the "deeper" shells.

(2) Reformulate the problem to include the post-buckling analysis of the shell, and thus allow the investigation of the imperfection-sensitivity of the buckling load. Such a formulation would require rewriting the finite difference equations in the equilibrium analysis to eliminate symmetry

across the shell centerlines, and thus permit non-symmetric equilibrium configurations.

(3) Reformulate the problem to permit non-zero form along the boundaries. Such work would allow the analysis of a broad class of shells having rectangular planform, but a prescribed form along the boundaries. Cylindrical shells are included in this class of problems, as are shells supported only at four corners. This particular topic would require much effort since the assumption of no form on the boundaries is applied in the early stages of the formulation during which the stress boundary conditions are derived.

Table 5.13: Ratios of Buckling Load of Optimal Forms to Buckling Load of Reference Form

	Full Uniform Load			Partial Uniform Load		
	$\beta^2 = 50$	$\beta^2 = 100$	$\beta^2 = 150$	$\beta^2 = 50$	$\beta^2 = 100$	$\beta^2 = 150$
Clamped, Square	1.50	1.40	1.26	1.43	1.72	1.51
Clamped, Rectangular	1.68	1.56	1.38	1.47	1.63	1.52
Simply Supported, Square	1.04	1.08	1.08	1.05	1.19	1.11
Simply Supported, Rectangular	1.22	1.35	1.50	1.13	1.18	1.17

Table 5.14: Comparison Between Buckling Modes of Reference Forms and Optimal Forms

	Full Uniform Load						Partial Uniform Load					
	$\beta^2 = 50$		$\beta^2 = 100$		$\beta^2 = 150$		$\beta^2 = 50$		$\beta^2 = 100$		$\beta^2 = 150$	
	R	O	R	O	R	O	R	O	R	O	R	O
Clamped, Square	SS	SS	SS	SS	AS	AS	SS	SS	SS	SS	SS	AS
Clamped, Rectangular	SS	SS	SS	SS	SS	AS	SS	SS	SS	SS	SS	AS
Simply Supported, Square	SS	SS	AS	AS	AS	AS	SS	SS	SS	AS	SS	AS
Simply Supported, Rectangular	SS	SA	SS	AS	SS	AS	SS	AS	AS	AS	AS	AS

R = reference form

O = optimal form

Table 5.15: Comparison of Optimal Forms to Reference Forms

	Reference Form	Full Uniform Load			Partial Uniform Load		
		$\beta^2 = 50$	$\beta^2 = 100$	$\beta^2 = 150$	$\beta^2 = 50$	$\beta^2 = 100$	$\beta^2 = 150$
Square, Clamped; at x = 0.5:							
0.0	0.00	0.00	0.00	0.00	0.00	0.00	0.00
0.1	0.31	0.05	0.04	0.04	0.03	0.02	0.03
0.2	0.59	0.34	0.29	0.30	0.29	0.21	0.24
0.3	0.81	0.74	0.70	0.71	0.69	0.62	0.65
0.4	0.95	1.12	1.11	1.06	1.12	1.12	1.08
0.5	1.00	1.26	1.26	1.20	1.28	1.30	1.22
Rectangular, Clamped; at x = 0.5:							
0.000	0.00	0.00	0.00	0.00	0.00	0.00	0.00
0.125	0.26	0.09	0.09	0.08	0.06	0.05	0.04
0.250	0.50	0.28	0.28	0.33	0.25	0.19	0.17
0.375	0.71	0.56	0.61	0.64	0.53	0.45	0.41
0.500	0.87	0.91	1.04	1.01	1.05	0.99	0.96
0.625	0.97	1.24	1.31	1.20	1.38	1.34	1.28
0.750	1.00	1.37	1.40	1.31	1.48	1.43	1.34
Rectangular, Clamped; at y = 0.75:							
0.000	0.00	0.00	0.00	0.00	0.00	0.00	0.00
0.125	0.38	0.11	0.15	0.15	0.04	0.03	0.04
0.250	0.71	0.59	0.68	0.70	0.59	0.45	0.37
0.375	0.92	1.13	1.21	1.17	1.30	1.28	1.21
0.500	1.00	1.37	1.40	1.31	1.48	1.43	1.34

Table 5.16: Comparison of Optimal Forms to Reference Forms

	Reference Form	Full Uniform Load			Partial Uniform Load		
		$\beta^2 = 50$	$\beta^2 = 100$	$\beta^2 = 150$	$\beta^2 = 50$	$\beta^2 = 100$	$\beta^2 = 150$
Square, Simply Supported; at x = 0.5:							
0.0	0.00	0.00	0.00	0.00	0.00	0.00	0.00
0.1	0.31	0.33	0.34	0.37	0.29	0.29	0.28
0.2	0.59	0.60	0.60	0.64	0.57	0.57	0.55
0.3	0.81	0.80	0.77	0.79	0.82	0.81	0.79
0.4	0.95	0.91	0.87	0.86	1.00	0.98	0.98
0.5	1.00	0.95	0.90	0.88	1.06	1.05	1.05
Rectangular, Simply Supported; at x = 0.5:							
0.000	0.00	0.00	0.00	0.00	0.00	0.00	0.00
0.125	0.26	0.32	0.32	0.35	0.25	0.28	0.29
0.250	0.50	0.58	0.59	0.62	0.50	0.56	0.56
0.375	0.71	0.78	0.79	0.79	0.69	0.79	0.79
0.500	0.87	0.90	0.91	0.88	0.93	0.97	0.96
0.625	0.97	0.95	0.97	0.92	1.04	1.06	1.04
0.750	1.00	0.97	0.99	0.93	1.07	1.07	1.05
Rectangular, Simply Supported; at y = 0.75:							
0.000	0.00	0.00	0.00	0.00	0.00	0.00	0.00
0.125	0.38	0.40	0.39	0.40	0.40	0.42	0.42
0.250	0.71	0.72	0.71	0.70	0.76	0.77	0.77
0.375	0.92	0.91	0.92	0.88	1.00	0.99	0.98
0.500	1.00	0.97	0.99	0.93	1.07	1.07	1.05

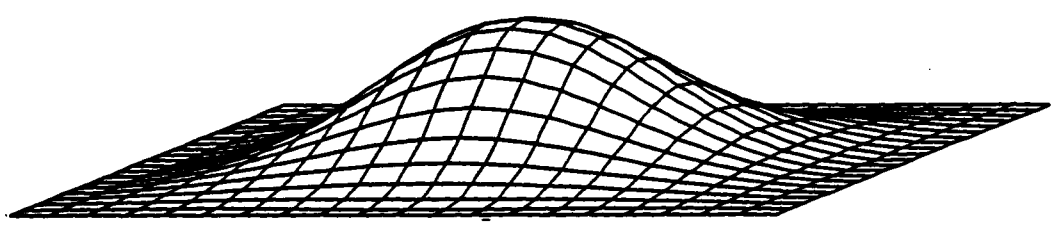

Figure 5.13: Perspective of the Optimal Form of Rectangular, Clamped Shell Under Full Uniform Load ($\beta^2 = 100$)

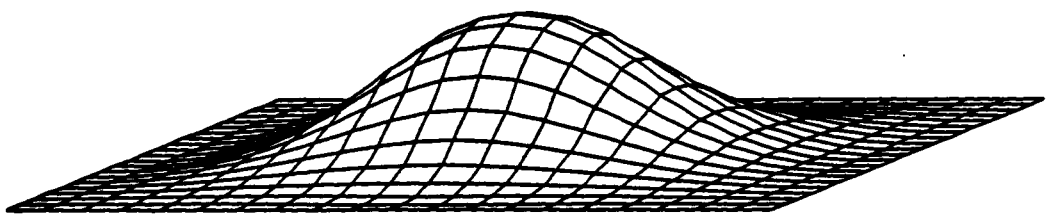

Figure 5.14: Perspective of the Optimal Form of a Rectangular, Clamped Shell Under Partial Uniform Load ($\beta^2 = 100$)

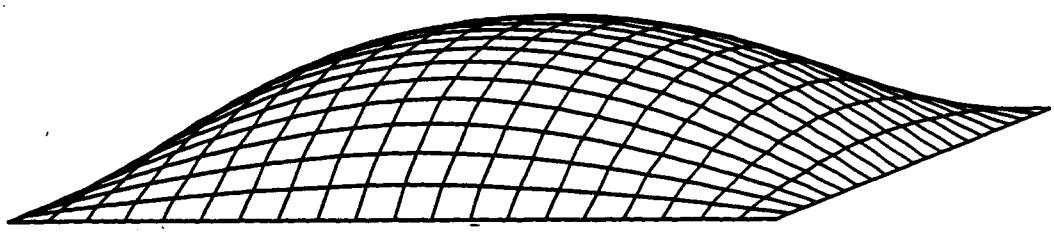

Figure 5.15: Perspective of the Optimal Form of a Rectangular, Simply Supported Shell Under Full Uniform Load ($\beta^2 = 100$)

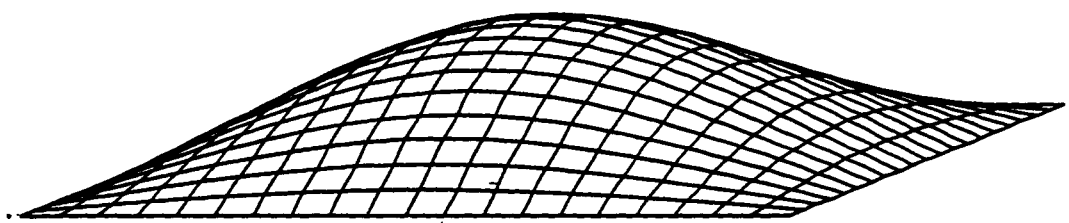

Figure 5.16: Perspective of the Optimal Form of a Rectangular, Simply Supported Shell Under Partial Uniform Load ($\beta^2 = 100$)

REFERENCES

1. Popov, E.P. and Medwadowski, S.J., "Stability of Reinforced Concrete Shells, State-of-the-Art Overview", Proceedings, ACI Symposium on Stability of Concrete Shells, Washington, D.C., 1979.

2. Medwadowski, S.J., "The Interrelation Between the Theory and the Form of Shells", Bulletin of the IASS, No. 70, Vol. 20, 1979.

3. Plaut, R.H. and Johnson, L.W., "Optimal Forms of Shallow Shells with Circular Boundary. Part 3: Maximum Enclosed Volume", Journal of Applied Mechanics, Vol. 51, No. 3, 1984, pp. 536-539.

4. Deel, C.C., Johnson, E.R. and Plaut, R.H., "Load-Frequency Relationships for Shallow Elastic Structures", Recent Advances in Structural Dynamics, Papers Presented at an International Conference, Vol. 2, Southampton, England, July 7-11, 1980. Publ. by Univ. of Southampton, Institute of Sound and Vibration Research, England, 1980, pp. 611-620.

5. Johnson, E.R. and Plaut, R.H., "Load-Frequency Relationships for Shallow Elastic Arches", 1980 Virginia Polytechnic Institute and State University, College of Engineering Technical Report VPI-E-80-4.

6. Bushnell, D., "Buckling of Shells--Pitfall for Designers", AIAA Journal, Vol. 19, No. 9, Sept., 1981, pp. 1183-1226.

7. Brush, D.O. and Almroth, B.O., Buckling of Bars, Plates and Shells, McGraw-Hill Book Co., New York, 1975.

8. Timoshenko, S.P., Theory of Elastic Stability, 2nd Ed., McGraw-Hill Book Co., New York, 1961.

9. Thompson, J.M.T. and Hunt, G.W., A General Theory of Elastic Stability, Wiley, New York, 1973.

10. Medwadowski, S.J., "Stability of Shells and Spatial Structures", Bulletin of the International Association of Shell Structures, No. 70, 1979, pp. 39-51.

11. Medwadowski, S.J., "Conceptual Design of Shells", Proceedings, ACI Symposium on Concrete Thin Shells, ACI Publication SP-28, Detroit, 1971, pp. 15-39.

12. Medwadowski, S.J. et al., Recommendations for Reinforced Concrete Shells and Folded Plates, IASS, Madrid, 1979.

13. ACI Committee 334, "Concrete Shell Structures—Practice and Commentary", ACI Journal, Vol. 61, 1964, pp. 1091-1108.

14. Friedrichs, K.O., "On the Minimum Buckling Load for Spherical Shells", Theodore von Karman Anniv. Vol., 1941, pp. 258-272.

15. VonWillich, T., "The Elastic Stability of Thin Spherical Shells", Proc. ASCE, Vol. 85, 1959, pp. 51-65.

16. Carlson, R.L., Sendlebeck, R.L., and Hoff, N.J., "Experimental Studies of the Buckling of Complete Spherical Shells", Experimental Mechanics, Vol. 7, 1967, pp. 281-288.

17. Huang, N.C., "Unsymmetrical Buckling of Thin Shallow Spherical Shells", Journal of Applied Mechanics, Vol. 31, 1964, pp. 447-457.

18. Bushnell, D., "Bifurcation Phenomena in Spherical Shells under Concentrated and Ring Loads", AIAA Journal, Vol. 5, No. 11, Nov. 1967, pp. 2034-2040.

19. Chien, W.Z. and Hu, H.C., "On the Snapping of a Thin, Spherical Cap", IX International Congress on Applied Mechanics, Brussels, Belgium, Sept. 1956, p. 309.

20. Weinitschke, H.J., "On the Stability Problem for Shallow Spherical Shells", Journal of Mathematics and Physics, Vol. 38, Jan. 1960, pp. 209-231.

21. Weinitschke, H.J., "On the Non-Linear Theory of Shallow Spherical Shells", Journal of the Society for Industrial and Applied Mathematics, Vol. 6, 1958, pp. 209-232.

22. Archer, R.R. and Lange, C.G., "Non-linear Dynamic Behavior of Shallow Spherical Shells", AIAA Journal, Vol. 3, No. 12, 1965, pp. 2312-2319.

23. Archer, R.R., "On the Numerical Solution of the Non-linear Equations for Shells of Revolution", Journal of Mathematics and Physics, Vol. 41, 1962, pp. 165-178.

24. Keller, H.B. and Reiss, E.L., "Spherical Cap Snapping", Journal of the Aerospace Sciences, Vol. 26, 1959, pp. 643-652.

25. Reiss, E.L., Greenberg, H.J. and Keller, H.B., "Non-linear Deflections of Shallow Spherical Shells", Journal of the Aeronautical Sciences, Vol. 24, 1957, pp. 533-543.

26. Reiss, E.L., "On the Non-linear Buckling of Shallow Spherical Domes", Journal of the Aeronautical Sciences, Vol. 23, No. 10, 1956, pp. 973-975.

27. Kaplan, A. and Fung, Y.C., "A Nonlinear Theory of Bending and Buckling of Thin, Elastic Shallow Spherical Shells", NACA TN 3212, 1954.

28. Haydl, H.M., "Buckling of Doubly Curved Shallow Thin Shells", AIAA Journal, Vol. 6, No. 5, 1968, pp. 982-984.

29. Rushton, K.R., "Buckling of Laterally Loaded Plates Having Initial Curvature", International Journal of Mechanical Sciences, Vol. 14, 1972, pp. 667-680.

30. Leicester, R.H., "Finite Deformations of Shallow Shells", Journal of the Engineering Mechanics Division, ASCE, Vol. 94, Dec. 1968, pp. 1409-1423.

31. Archer, R.R. and Hsueh, P.K., "On the Large Deflection of Shallow Rectangular Shell Panels", TR-EM68-3, Aug. 1968, Engineering Research Institute, Univ. of Massachusetts, Amherst.

32. Archer, R.R. and Hsueh, P.K., "Large Deflection of Shallow Rectangular Shell Panels", AIAA Journal, Vol. 8, No. 2, Feb. 1970, pp. 241-245.

33. Marshall, H. and Rhodes, J., "Snap-through Buckling of Thin Shells of Rectangular Planform", in Stability Problems in Engineering Structures and Components, T. H. Richards and P. Stanley, eds., Applied Science Publishers Ltd., 1979, pp. 249-264.

34. Volmir, A.S., "A Translation of Flexible Plates and Shells", TR AFFDL-TR-66-216, April 1967, Air Force Flight Dynamics Lab.

35. Gallagher, R.H., "Finite Element Representations for Thin Shell Instability Analysis", in Buckling of Structures (Ed. B. Budiansky), Springer-Verlag, New York, 1976, pp. 40-52.

36. Bergan, P.G. and Clough, R.W., "Large Deflection Analysis of Plates and Shallow Shells Using the Finite Element Method", International Journal for Numerical Methods in Engineering, Vol. 5, 1973, pp. 543-556.

37. Matsui, T. and Matsuoka, O., "A New Finite Element Scheme for Instability Analysis of Thin Shells", International Journal for Numerical Methods in Engineering, Vol. 10, 1976, pp. 145-170.

38. Noor, A.K. and Hartley, S.J., "Non-linear Shell Analysis via Mixed Isoparametric Elements", Computers and Structures, Vol. 7, No. 5, 1977, pp. 615-626.

39. Noor, A.K. and Andersen, C.M., "Mixed Models and Reduced/ Selective Integration Displacement Models for Nonlinear Shell Analysis", International Journal for Numerical Methods in Engineering, Vol. 18, 1982, pp. 1429-1454.

40. Carnoy, E. and Sander, G., "Stability and Postbuckling Analysis of Nonlinear Structures", Computer Methods in Applied Mechanics and Engineering, Vol. 32, 1982, pp. 329-363.

41. Knight, N.F., Jr., "Nonlinear Structural Dynamics Analysis Using a Modified Modal Method", Proceedings of the 24th Structures, Structural Dynamics and Materials Conference, Lake Tahoe, Part 2, 1983, pp. 111-128.

42. Buckland, J. and Wennerström, H., "Finite Element Analysis of Elasto-Plastic Shells", International Journal for Numerical Methods in Engineering, Vol. 8, No. 2, 1974, pp. 415-424.

43. Sabir, A.B. and Lock, A.C., "The Application of Finite Elements to Large Deflection Geometrically Non-linear Behaviour of Cylindrical Shells", Variational Methods in Engineering by Brebbia, C.A. and Tottenham, H. (Editors), Southampton University Press, 1973, pp. 7166-7175.

44. Crisfield, M.A., "A Fast Incremental/Iterative Solution Procedure that Handles 'Snap-Through'", Computers and Structures, Vol. 13, 1981, pp. 55-62.

45. Thomas, G.R. and Gallagher, R.H., "A Triangular Thin Shell Finite Element: Non-linear Analysis", NASA CR-2483, July, 1975.

46. Wennerström, H., "Non-linear Shell Analysis Performed with Flat Elements", Finite Elements in Non-linear Mechanics, eds., P.G. Bergan, et al., Tapir Publishers, Trondheim, Norway, 1978, pp. 285-299.

47. Gass, N. and Tabarrok, B., "Large Deformation Analysis of Plates and Cylindrical Shells by a Mixed Finite Element Method", International Journal for Numerical Methods in Engineering, Vol. 10, 1976, pp. 731-746.

48. Dhatt, G.S., "Instability of Thin Shells by the Finite Element Method", AISS Symposium for Folded Plates and Prismatic Structures, Vienna, 1970.

49. Batoz, J.L., Chattopadhyay, A. and Dhatt, G., "Finite Element Large Deflection Analysis of Shallow Shells", International Journal for Numerical Methods in Engineering, Vol. 10, No. 1, 1976, pp. 39-58.

50. Marshall, I.H., Rhodes, J. and Banks, W.M., "Experimental Snap-buckling Behaviour of Thin GRP Curved Panels Under Lateral Loading", Composites, Vol. 8, April 1977, pp. 81-86.

51. Marshall, I.H., Rhodes, J. and Banks, W.M., "General Investigation of Snap-through Buckling of Orthotropic Shells", International Colloquium of Discrete Systems, Hungary, April, 1977.

52. Rhodes, J. and Marshall, I.H., "Unsymmetrical Buckling of Laterally Loaded Reinforced Plastics Shells", Second International Conference on Composite Materials, Toronto, Canada, April, 1978.

53. Marshall, I.H., Rhodes, J. and Banks, W.M., "Snap-buckling of Composite Shells", Paper presented to Institution of Mechanical Engineers Meeting, National Engineering Laboratory, Feb., 1978.

54. Noor, A.K. and Andersen, C.M., "Mixed Isoparametric Finite Element Models of Laminated Composite Shells", Computer Methods in Applied Mechanics and Engineering, Vol. 11, 1977, pp. 255-280.

55. Marshall, I.H., Rhodes, J. and Banks, W.M., "The Non-linear Behaviour of Thin, Orthotropic, Curved Panels Under Lateral Loading", Journal of Mechanics and Engineering Science, Vol. 19, No. 1, 1977, pp. 30-37.

56. Wasiutynski, Z. and Brandt, A., "The Present State of the Art in the Field of Optimum Design of Structures", Applied Mechanics Reviews, Vol. 16, No. 5, May 1963, pp. 341-350.

57. Sheu, C.Y. and Prager, W., "Recent Developments in Optimal Structural Design", Applied Mechanics Reviews, Vol. 21, No. 10, October 1968, pp. 985-992.

58. Niordson, F.I. and Pedersen, P., "A Review of Optimal Structural Design", Theoretical and Applied Mechanics, Proceedings of the Thirteenth International Congress of Theoretical and Applied Mechanics, Moscow University, August 21-26, 1972, pp. 264-278.

59. Structural Optimization Symposium, ASME, Vol. 7, Nov. 17-21, 1974, New York, N.Y.

60. Haug, E.J., "A Review of Distributed Parameter Structural Optimization Literature", Optimization of Distributed Parameter Structures, Haug, E.J. and Cea, J., eds., Sijthoff & Noordhoff, Alphen aan den Rijn, The Netherlands, 1981, pp. 3-74.

61. Lev, O.E., ed., Structural Optimization: Recent Developments and Applications, American Society of Civil Engineers, New York, 1981.

62. Stadler, W., "Evolution as an Optimization Process: An Hypothesis and Some of Its Implications", Proceedings of the Euromech-Colloquium 164 Entitled "Optimization Methods in Structural Design", Siegen, Germany, October 12-14, B. I. Wissenschaftsverlag, 1983, pp. 196-203.

63. Haug, E.J. and Cea, J., eds., Optimization of Distributed Parameter Structures, Vols. I and II, Sijthoff & Noordhoff, Alphen aan den Rijn, The Netherlands, 1981.

64. Optimum Structural Design, Proceedings of the 11th ONR Naval Structural Mechanics Symposium, University of Arizona, October 19-22, 1981.

65. Stroud, W.J. and Sykes, N.P., "Minimum-Weight Stiffened Shells with Slight Meridional Curvature Designed to Support Axial Compressive Loads", AIAA Journal, Vol. 7, No. 8, August, 1969, pp. 1599-1601.

66. Manevich, A.I. and Kaganov, M.E., "Stability and Weight Optimization of Reinforced Spherical Shells Under External Pressure", Soviet Applied Mechanics, Vol. 9, No. 1, 1973, pp. 16-21.

67. Batterman, S.C. and Pavicic, N.J., "Optimum Design of Fiber Reinforced Shells of Revolution", in Optimization in Structural Design, A. Sawczuk and Z. Mróz, eds., Springer-Verlag, Berlin, 1975, pp. 372-394.

68. Leonard, R.W., Anderson, M.S. and Heard, Jr., W.L., "Design of a Mars Entry 'Aeroshell'", in Buckling of Structures, B. Budiansky, ed., Springer-Verlag, Berlin, 1976, pp. 346-364.

69. Kalinin, I.N., "A New Approach to the Design of Minimum-Weight Shells of Revolution", Soviet Applied Mechanics, Vol. 12, No. 1, January, 1976, pp. 31-36.

70. Eimer, Cz. and Maczynski, J., "On Optimal Shell Prestressing", Journal of Structural Mechanics, Vol. 4, No. 3, 1976, pp. 289-305.

71. Kunoo, K. and Yang, T.Y., "Minimum Weight Design of Cylindrical Shells with Multiple Stiffener Sizes", AIAA Journal, Vol. 16, No. 1, January, 1978, pp. 35-40.

72. Simitses, G.J., Giri, J. and Sheinman, I., "Optimization of Imperfect Stiffened Cylinders Under Destabilizing Loads", Acta Astronautica, Vol. 7, 1980, pp. 197-207.

73. Rikards, R.B., "Convexity of Some Classes of Optimization Problems for Multilayer Shells Under Conditions of Stability and Vibration", Mechanics of Solids, Vol. 15, No. 1, 1980, pp. 130-137.

74. Freiberger, W., "Minimum Weight Design of Cylindrical Shells", Journal of Applied Mechanics, Vol. 23, No. 4, December, 1956, pp. 576-580.

75. Ziegler, H., "Kuppeln gleicher Festigkeit", Ingenieur-Archiv, Vol. 26, 1958, pp. 378-382.

76. Novozhilov, V.V., The Theory of Thin Shells, P. Noordhoff, Ltd., Groningen, The Netherlands, 1959, pp. 130-134.

77. Issler, W., "Eine Kuppel gleicher Festigkeit", Zeitschrift für angewandte Mathematik und Physik, Vol. 10, 1959, pp. 576-578.

78. Shield, R.T., "On the Optimum Design of Shells", Journal of Applied Mechanics, Vol. 27, No. 2, June, 1960, pp. 316-322.

79. Brown, E.H., "The Minimum Weight Design of Closed Shells of Revolution", Quarterly Journal of Mechanics and Applied Mathematics, Vol. 15, 1962, pp. 109-128.

80. Issler, W., "Membranschalen gleicher Festigkeit", Ingenieur-Archiv, Vol. 33, 1964, pp. 330-345.

81. Shamiyev, F.G., "Designing Minimum-Weight Shells", FTD-TT-64-953, U.S.A.F., February, 1965.

82. Dokmeci, M.C., "A Shell of Constant Strength", Zeitschrift für angewandte Mathematik und Physik, Vol. 17, 1966, pp. 545-547.

83. Lukasiewicz, S., "On the Optimum Design of Shells Loaded by Concentrated Forces", in Theory of Thin Shells, F.I. Niordson, ed., Springer-Verlag, Berlin, 1969, pp. 161-175.

84. Reiss, R. and Megarefs, G.J., "Minimal Design of Axisymmetric Cylindrical Shells Obeying Mises Criterion", Acta Mechanica, Vol. 7, 1969, pp. 72-98.

85. Stroud, W.J., "Minimum Mass Isotropic Shells of Revolution Subjected to Uniform Pressure and Axial Load", NASA TN D-6121, February, 1971.

86. Andreev, L.V., Mossakovsii, V.I. and Obodan, N.I., "On Optimal Thickness of a Cylindrical Shell Loaded by External Pressure", Journal of Applied Mathematics and Mechanics, Vol. 36, No. 4, 1972, pp. 677-685.

87. Schumann, W. and Wuthrich, W., "Über Schalen gleicher Festigkeit", Acta Mechanica, Vol. 14, 1972, pp. 189-197.

88. Save, M.A. and Massonet, C.E., Plastic Analysis and Design of Plates, Shells and Disks, North-Holland Publishing Company, Amsterdam, 1972.

89. Sayir, M. and Schumann, W., "Zu den anisotropen Membranschalen mit gegebenenfalls gleicher Festigkeit", Zeitschrift für angewandte Mathematik und Physik, Vol. 23, 1972, pp. 815-827.

90. Reiss, R., "Minimal Weight Design for Conical Shells", Journal of Applied Mechanics, Vol. 41, No. 3, September, 1974, pp. 599-603.

91. Varvak, P.M., Dekhtyar', A.S. and Kotova, L.B., "Extremal Analysis and Optimal Design of Shallow Shells", Soviet Applied Mechanics, Vol. 12, No. 12, December, 1976, pp. 1277-1281.

92. Dekhtyar', A.S., "Optimization of Rigidly Plastic Shells of Revolution", Soviet Applied Mechanics, Vol. 13, No. 5, May, 1977, pp. 473-477.

93. Kalinin, I.N. and Lenkin, I.B., "Optimization of Shells with Piecewise Constant Thickness for a Given Strength Distribution", Mechanics of Solids, Vol. 13, No. 6, 1978, pp. 77-82.

94. Kruzelecki, J., "Axially Symmetric Shells of Uniform Membrane Strength as Optimal Shells", Bulletin de l'Académie Polonaise des Sciences, Série des Sciences techniques, Vol. 27, No. 8-9, 1979, pp. 683-690.

95. Prager, W. and Rozvany, G.I.N., "Optimal Spherical Cupola of Uniform Strength", Ingenieur-Archiv, Vol. 49, No. 5-6, 1980, pp. 287-293.

96. Reiss, R., "A Note on Optimal Conical Shells", Journal of Applied Mechanics, Vol. 47, No. 3, September, 1980, pp. 669-671.

97. Rozvany, G.I.N., "Optimality Criteria for Grids, Shells, and Arches", in [2], pp. 112-151.

98. Nakamura, H., Dow, M. and Rozvany, G.I.N., "Optimal Spherical Cupola of Uniform Strength: Allowance for Self-weight", Ingenieur-Archiv, Vol. 51, No. 3/4, 1981, pp. 159-181.

99. Wang, H. and Worley, W.J., "An Approach to Optimum Shape Determination for a Class of Thin Shells of Revolution", Journal of Applied Mechanics, Vol. 35, No. 3, September, 1968, pp. 524-529.

100. Hamada, M., "On the Optimum Shapes of Some Axisymmetric Shells", in Optimization in Structural Design, A. Sawczuk and Z. Mróz, eds., Springer-Verlag, Berlin, 1975, pp. 248-262.

101. Gura, N.M., "Shell of Revolution of Maximum Stiffness in Torsion", Mechanics of Solids, Vol. 14, No. 1, 1979, pp. 123-128.

102. Hoffman, G.A., "Minimum-Weight Proportions of Pressure-Vessel Heads", Journal of Applied Mechanics, Vol. 29, No. 4, December, 1962, pp. 662-668.

103. Hoffman, G.A., "Optimal Proportions of Pressure Vessel Heads", Journal of the Aerospace Sciences, Vol. 29, No. 12, December, 1962, pp. 1471-1475.

104. Bert, C.W., "Ellipsoidal Closures for Minimum-Weight Pressure Vessels", Canadian Aeronautics and Space Journal, Vol. 9, No. 5, May, 1963, pp. 133-136.

105. Ramakrishnan, C.V., "Structural Shape Optimization Using Penalty Functions", Journal of Structural Mechanics, Vol. 3, No. 4, 1974-75, pp. 403-422.

106. Middleton, J. and Owen, D.R.J., "Automated Design Optimization to Minimize Shearing Stress in Axisymmetric Pressure Vessels", Nuclear Engineering and Design, Vol. 44, 1977, pp. 357-366.

107. Oda, J. and Yamazaki, K., "On a Technique to Obtain an Optimum Strength Shape of an Axisymmetric Body by the Finite Element Method", Bulletin of the JSME, Vol. 20, No. 150, December, 1977, pp. 1524-1532.

108. Queau, J.P. and Trompette, P., "Two-Dimensional Shape Optimal Design by the Finite Element Method", International Journal for Numerical Methods in Engineering, Vol. 15, 1980, pp. 1603-1612.

109. Middleton, J., "Optimal Shape Design to Minimize Stress Concentration Factors in Pressure Vessel Components", in [3], pp. 5-23 to 5-29.

110. Mansfield, E.H., "An Optimum Surface of Revolution for Pressurised Shells", International Journal of Mechanical Sciences, Vol. 23, No. 1, 1981, pp. 57-62.

111. Zyczkowski, M. and Kruzelecki, J., "Optimal Design of Shells with Respect to Their Stability", in Optimization in Structural Design, A. Sawczuk and Z. Mróz, eds., Springer-Verlag, Berlin, 1975, pp. 229-247.

112. Brinkmann, G., "Die optimierte flache Schale: Formfindung, Tragverhalten, und Stabilität", Ingenieur-Archiv, Vol. 47, No. 4, 1978, pp. 197-206.

113. Solodovnikov, V.N., "Optimization of Elastic Shells of Revolution", Journal of Applied Mathematics and Mechanics, Vol. 42, No. 3, 1978, pp. 535-544.

114. Kruzelecki, J., "Optimization of Shells Under Combined Loadings via the Concept of Uniform Stability", in [2], pp. 929-950.

115. Gould, P.L., "Minimum Weight Design of Hyperbolic Cooling Towers", Journal of the Structural Division, ASCE, Vol. 95, No. ST2, February, 1969, pp. 203-208.

116. Reinschmidt, K.F., "The Optimum Shape of Cooling Towers", Computers & Structures, Vol. 5, 1975, pp. 321-325.

117. Parbery, R.D. and Karihaloo, B.L., "Minimum-Weight Design of Thin-Walled Cylinders Subject to Flexural and Torsional Stiffness Constraints", Journal of Applied Mechanics, Vol. 47, No. 1, March, 1980, pp. 106-110.

118. Gol'dshtein, Yu.B. and Solomeshch, M.A., "Determination of the Optimal Rod and Shell Shape by Using a Variational Principle", Soviet Applied Mechanics, Vol. 14, No. 12, December, 1978, pp. 1293-1297.

119. Starnes, J.H. and Haftka, R.T., "Preliminary Design of Composite Wings for Buckling, Strength, and Displacement Constraints", AIAA/ASME Nineteenth Conference, Bethesda, Md., April, 1978.

120. Torroja, E., Philosophy of Structures (English version by J. J. Plivka and Milos Polivka), University of California Press, 1958.

121. Andres, O.A., "Experimental Design of Shell Structures", Proceedings, 1971 IASS Pacific Symposium, Tension Structures and Space Frames, Architectural Institute of Japan, Tokyo, 1972, pp. 845-854.

122. Torroja, E., The Structures of Eduardo Torroja, F. W. Dodge Corporation, New York, 1958.

123. Isler, H., "The Shapes of Shells", Bulletin of the International Association of Shell Structures, No. 8, Sept., 1959.

124. Isler, H., "New Shapes for Shells--Twenty Years After", Bulletin of the International Association of Shell Structures, No. 71/72, 1979, pp. 9-26.

125. Candela, F., "Shell Construction in Mexico", Proceedings, World Conference on Shell Structures, San Francisco, 1962., S.J. Medwadowski et al., editors, National Academy of Sciences-National Research Council, Publication No. 1187, Washington, D.C., 1964, pp. 27-34.

126. Faber, C., Candela: The Shell Builder, Reinhold Publishing Corporation, New York, 1963.

127. Stadler, W., "Natural Shapes of Shallow Arches", Journal of Applied Mechanics, Vol. 44, No. 2, June 1977, pp. 291-298.

128. Stadler, W., "Stability Implications, and the Equivalence of Stability and Optimality Conditions in the Optimal Design of Uniform Shallow Arches", Proceedings of the International Symposium on Optimal Structural Design, The 11th ONR Naval Structural Mechanics Symposium, Tucson, Arizona, October 19-22, 1981, pp. 3.3-3.10.

129. Olhoff, N. and Plaut, R.H., "Optimal Forms of Shallow Arches with Respect to Vibration and Stability", Journal of Structural Mechanics, Vol. 11, No. 1, 1983, pp. 81-100.

130. Farshad, M., "On Optimal Form of Arches", Journal of the Franklin Institute, Vol. 302, No. 2, Aug. 1976, pp. 187-194.

131. Stadler, W., "Uniform Shallow Arches of Minimum Weight and Minimum Maximum Deflection", Journal of Optimization Theory and Applications, Vol. 23, No. 1, Sept. 1977, pp. 137-165.

132. Mohr, G.A., "Design of Shell Shape Using Finite Elements", Computers & Structures, Vol. 10, 1979, pp. 745-749.

133. Alpa, G., Bozzo, E., Corsanego, A. and Del Grosso, A., "Shape Determination for Shell Structures on Pointlike Supports", Bulletin of the International Association of Shell Structures, Vol. 67, 1978, pp. 3-9.

134. Stadler, W., "Natural Structural Shapes in Shell Theory, An Application of Multicriteria Optimization", presented at the Euromech-Colloquium 165, Munich, Germany, May 17-20, 1983.

135. Haug, E. and Powell, G., "Finite Element Analysis of Nonlinear Membrane Structures", Proceedings, 1971 IASS Pacific Symposium, Tension Structures and Space Frames, Architectural Institute of Japan, Tokyo, 1972, pp. 165-175.

136. Day, A., "A General Computer Technique for Form Finding for Tension Structures", Proceedings, IASS.

137. Plaut, R.H., Johnson, L.W. and Parbery, R., "Optimal Forms of Shallow Shells with Circular Boundary. Part 1: Maximum Fundamental Frequency", Journal of Applied Mechanics, Vol. 51, No. 3, 1984, pp. 526-530.

138. Plaut, R.H. and Johnson, L.W., "Optimal Forms of Shallw Shells with Circular Boundary. Part 2: Maximum Buckling Load", Journal of Applied Mechanics, Vol. 51, No. 3, 1984, pp. 531-535.

139. Timoshenko, S. and Woinowsky-Krieger, S., Theory of Plates and Shells, 2nd Ed., McGraw-Hill Book Co., New York, 1959.

140. Szilard, R., Theory and Analysis of Plates, Prentice Hall, 1974, pp. 340-347.

141. Ugural, A.C., Stresses in Plates and Shells, McGraw-Hill Book Co., New York, 1981, Chapter 8, "Large Deflections of Plates", pp. 174-184.

142. Donnell, L.H., Beams, Plates, and Shells, McGraw-Hill Book Co., New York, 1976.

143. Flügge, W.I., Stresses in Shells, 2nd Ed., Springer-Verlag, New York, 1973.

144. Vlasov, V. Z., "General Theory of Shells and Its Applications in Engineering", NASA TTF-99, Washington, D.C., April, 1964.

145. Muster, D., ed., Symposium on Theory of Shells, University of Houston, 1966.

146. Reissner, E., "On Some Problems in Shell Theory", Proceedings of the 1st Symposium on Naval Structural Mechanics", Permagon Press, New York, 1960, pp. 71-114.

147. Reissner, E. and Johnson, M.W., "On the Foundations of the Theory of Thin Elastic Shells", Journal of Mathematics and Physics, Vol. 37, 1959, pp. 371-392.

148. Reissner, E., "On the Derivation of the Theory of Thin Elastic Shells", Journal of Mathematics and Physics, Vol. 42, 1963, pp. 263-277.

149. Reissner, E., "On Bending of Elastic Plates", Quarterly of Applied Mathematics, Vol. 5, 1947, pp. 55-68.

150. Way, S., "Uniformly Loaded Clamped, Rectangular Plates with Large Deflections", Proceedings of the 5th International Congress on Applied Mechanics, John Wiley & Sons, New York, 1938, pp. 123-128.

151. Timoshenko, S.P., "Bending in Rectangular Plates with Clamped Edges", Proceedings of the 5th International Congress on Applied Mechanics, Cambridge, Mass., 1938, John Wiley & Sons, Inc., 1939, pp. 40-43.

152. Levy, S., "Large Deflection Theory for Rectangular Plate", Proceedings of the 1st Symposium on Applied Mathematics, No. 1, 1947, pp. 197-210.

153. Levy S., "Square Plate with Clamped Edges Under Normal Pressure Producing Large Deflections", NACA Report No. 740, 1942.

154. Stanek, F.J., "Uniformly Loaded Square Plate with No Lateral or Tangential Edge Displacement", Proceedings of the 3rd U.S. National Congress on Applied Mechanics, ASME, 1958, pp. 461-466.

155. Colville, J., Becker, E.B. and Furlong, R.W., "Large Displacement Analysis of Thin Plates", Journal of the Structural Division, Proceedings ASCE, Vol. 99, No. ST3, 1973, pp. 349-364.

156. Bauer, L. and Reiss, E.L., "Nonlinear Buckling of Rectangular Plates", Journal of the Society for Industrial and Applied Mathematics, Vol. 13, 1965, pp. 603-626.

157. Abdomigid, S.B. and Williamson, N.W., "A Grid Analogy for the Non-linear Behavior of Elastic Flat Plates", International Journal of Mechanics and Science, Vol. 9, 1967, pp. 257-269.

158. Banerjee, M.M., "Note on the Large Deflections of Irregular Shaped Plates by the Method of Conformal Mapping", Journal of Applied Mechanics, Vol. 43, 1976, pp. 356-357.

159. Green, J.R. and Southwell, R.V., "Relaxation Methods Applied to Engineering Problems, VIIIA. Problems Relating to Large Transverse Displacements of Thin Elastic Plates", Series C, Vol. I, No. 6, Feb. 1944, pp. 137-176, Phil. Trans. Roy. Soc. (L).

160. Berger, H.M., "A New Approach to the Analysis of Large Deflections of Plates", Journal of Applied Mechanics, Vol. 22, 1955, pp. 465-472.

161. Hooke, R. and Rawlings, B., "An Experimental Investigation of the Behavior of Clamped, Rectangular, Mild Steel Plates Subjected to Uniform Transverse Pressure", Proceedings of the Institute of Civil Engineers, No. 42, 1969, pp. 75-103.

162. Wang, C.T., "Bending of Rectangular Plates with Large Deflections", NACA-TN 1462, National Advisory Committee for Aeronautics, Washington, D.C., 1948.

163. Wang, C.T., "Non-linear Deflection Boundary Value Problems of Rectangular Plates", NACA TN No. 1425, 1948.

164. Stein, M., "Loads and Deformations of Buckled Rectangular Plates", NASA TR No. R-40, 1959.

165. Levy S., "Bending of Rectangular Plates with Large Deflections", NACA TR No. 737, 1942, p. 139.

166. Chien, W. Z. and Yeh, K.Y., "On the Large Deflection of Rectangular Plates", Proceedings of the 9th International Congress on Applied Mechanics", No. 6, 1957, University of Brussels (Belgium), pp. 403-412.

167. Berger, M.S., "On von Karman's Equations and the Buckling of a Thin Elastic Plate, I - The Clamped Plate", Communications on Pure and Applied Mathematics, Vol. 20, 1967, pp. 678-719.

168. Berger, M.S. and Fife, P.C., "Von Karman's Equations and the Buckling of a Thin Elastic Plate, II - Plate with General Edge Conditions", Communications on Pure and Applied Mathematics, Vol. 21, 1968, pp. 227-241.

169. Berger, M. and Fife, P., "On von Karman's Equations and the Buckling of a Thin Elastic Plate", Bulletin of American Mathematics Society, No. 72, 1966, pp. 1006-1011.

170. Knightly, G.H. and Sather, D., "Non-linear Buckled States of Rectangular Plates", Archive for Rational Mechanics and Analysis, Vol. 54, 1965, pp. 356-372.

171. Chia, C.Y., Non-Linear Analysis of Plates, McGraw-Hill Book Co., New York, 1980.

172. Rushton, K.R., "Large Deflections of Plates with Initial Curvature", International Journal of Mechanical Sciences, Vol. 12, 1970, pp. 1037-1051.

173. Nylander, H., "Initially Deflected Thin Plate with Initial Deflection Affine to Additional Deflection", International Association of Bridge and Structural Engineers, No. 11, 1951, pp. 347-374.

174. Parisch, H., "Geometrically Non-linear Analysis of Shells", Computer Methods in Applied Mechanics and Engineering, Vol. 14, 1978, pp. 159-178.

175. Marshall, I.H., "The Non-linear Behavior of Thin, Initially Curved, Orthotropic Plates", Ph.D. Thesis, University of Strathclyde, 1976.

176. Hudson, J., "The Non-linear Behavior of Thin Curved Panels", Ph.D. Thesis, University of Strathclyde, 1971.

177. Bucco, D., Mazumdar, J. and Ived, G., "Static Analysis of Shallow Shells of Arbitrary Shape—A New Approach", International Journal for Numerical Methods in Engineering, Vol. 18, 1982, pp. 967-1979.

178. Nash, W.A. and Modeer (eds.), Proceedings of the Symposium on the Theory of Thin Elastic Shells, New York, 1959.

179. Marguerre, K., "The Apparent Width of the Plate in Compression", NACA TM No. 833, 1937.

180. Huang, N.C., "Unsymmetrical Buckling of Thin Shallow Spherical Shells", ASME Journal of Applied Mechanics, Vol. 31, 1964, pp. 447-457.

181. Shyh-ning, L., "On a Generalized Variational Principle and Some of its Applications in the Theory of Elastic Shallow Shells", Scientia Sinica, Vol. 12, No. 10, 1963.

182. Langhaar, H.L., Energy Methods in Applied Mechanics, John Wiley and Sons, New York, 1962.

183. Forray, M.J., Variational Calculus in Science and Engineering, McGraw-Hill Book Co., New York, 1968.

184. Sokolnikoff, I.S. and Sokolnikoff, E.S., Higher Mathematics for Engineers and Physicists, McGraw-Hill Book Co., New York, 1934.

185. Kirsch, U., Optimum Structural Design, McGraw-Hill Book Co., New York, 1981.

186. Reissner, E., "On a Variational Theorem for Finite Elastic Deformations", Journal of Mathematics and Physics, Vol. 32, 1953, pp. 129-135.

187. Reissner, E., "On a Variational Theorem in Elasticity", Journal of Mathematics and Physics, No. 29, 1950, pp. 90-95.

188. Washizu, K., Variational Methods in Elasticity and Plasticity, Pergamon Press, New York, 1968.

189. Berger, M., "An Application of the Calculus of Variations in the Large to the Equations of Non-linear Elasticity", Bulletin of the American Mathematical Society, No. 73, 1967, pp. 520-525.

190. Friedrichs, K.O., "On the Boundary Value Problems of the Theory of Elasticity and Korn's Inequality", Annals of Mathematics, 1947, No. 48, pp. 441-471.

191. Wang, C.T., "Principle and Application of Complementary Energy Method for Thin, Homogeneous and Sandwich Plates and Shells with Finite Deformations", NACA TN No. 2620, 1952.

192. Naghdi, P.M., "On a Variational Theorem in Elasticity and Its Application to Shell Theory", Journal of Applied Mechanics, No. 3, 1964, pp. 647-653.

193. Reissner, E., "On the Form of Variationally Derived Shell Equations", Journal of Applied Mechanics, Vol. 31, 1964, pp. 233-238.

194. Soare, M., "Application of Finite Difference Equations to Shell Analysis", Pergamon Press, Inc., Elmsford, New York, 1967.

195. Johnson, L.W. and Riess, R.D., Numerical Analysis, 2nd Ed., Addison-Wesley Publishing Co., Reading, Mass., 1982.

196. Ali, R., "Finite Difference Methods in Vibration Analysis", Shock and Vibration Digest, Vol. 15, No. 3, March, 1983, pp. 3-8.

197. Fried, I., Numerical Solution of Differential Equations, Academic Press, New York, 1979.

198. Collatz, L., The Numerical Treatment of Differential Equations, 3rd Ed., Springer-Verlag, Berlin, 1966.

199. Forsythe, G.E. and Wasow, W.R., Finite Difference Methods for Partial Differential Equations, John Wiley & Sons, Inc., New York, 1960.

200. Hsueh, P.S. and Charles, A., "Buckling of Axially Loaded Cylindrical Panels", Journal of the Engineering Mechanics Division, Vol. 97, June 1971, pp. 919-933.

201. Leissa, A.W., Vibration of Shells, NASA Report NASA-SP-288, Ohio State University, 1973.

202. Warburton, G.B., The Dynamical Behavior of Structures, 2nd Ed., Pergamon Press, 1976, pp. 260-303.

203. Szechenyi, E., "Approximate Methods for the Determination of the Natural Frequencies of Stiffened and Curved Plates", Journal of Sound and Vibration, Vol. 14, No. 3, 1971, pp. 401-418.

204. Singh, P.N., Sundararajan, V. and Das, Y.C., "Large Amplitude Vibration of Some Moderately Thick Structural Elements", Journal of Sound and Vibration, Vol. 36, No. 3, 1974, pp. 375-387.

205. Chauhan, A.P. and Ashwell, D.G., "Small- and Large-Amplitude Free Vibrations of Square Shallow Shells", International Journal of Mechanical Sciences, Vol. 11, 1969, pp. 337-349.

206. Chu, H.N. and Herrmann, G., "Influence of Large Amplitudes on Free Flexural Vibrations of Rectangular Elastic Plates", Journal of Applied Mechanics, Vol. 23, 1956, pp. 532-540.

207. Palmer, P.J., "The Natural Frequency Vibration of Curved Rectangular Plates", Aeronautical Quarterly, Vol. V, Pt. 2, July, 1954, pp. 101-110.

208. Leissa, A., Vibration of Plates, NASA-SP-160, Office of Technology Utilization, NASA, Washington, D.C., 1969.

209. Gorman, D.J., Free Vibration Analysis of Rectangular Plates, Elsevier North Holland, Inc., New York, 1982.

210. Reissner, E., "On Transverse Vibrations of Thin, Shallow Elastic Shells", Quarterly of Applied Mathematics, Vol. 13, No. 2, 1955, pp. 169-176.

211. Blevins, R.D., Formulae for Natural Frequency and Mode Shape, Van Nostrand Reinhold, New York, 1979.

212. Webster, J.J., "Free Vibrations of Rectangular Curved Panels", International Journal of Mechanical Sciences, Vol. 10, 1961, pp. 571-582.

APPENDIX A

Integration by Parts for the Derivation of the Variational Principle

Integration by Parts for the Derivation of the Variational Principle

Equation (3.43) can be rewritten as

$$\int_0^1\int_0^c (g\cdot g_{xxxx})dxdy + 2\cdot\int_0^1\int_0^c (g\cdot g_{xxyy})dxdy + \int_0^1\int_0^c (g\cdot g_{yyyy})dxdy$$

$$- \int_0^1\int_0^c (g\cdot g_{xx}\cdot\chi_{yy})dxdy - \int_0^1\int_0^c (g\cdot g_{yy}\cdot\chi_{xx})dxdy$$

$$- \int_0^1\int_0^c (g\cdot f_{yy}\cdot\theta_{xx})dxdy - \int_0^1\int_0^c (g\cdot f_{xx}\cdot\theta_{yy})dxdy$$

$$+ 2\cdot\int_0^1\int_0^c (g\cdot g_{xy}\cdot\chi_{xy})dxdy + 2\cdot\int_0^1\int_0^c (g\cdot f_{xy}\cdot\theta_{xy})dxdy$$

$$- \Omega^2\cdot\int_0^1\int_0^c g^2\,dxdy - \int_0^1\int_0^c (f\cdot f_{xxxx})dxdy - 2\cdot\int_0^1\int_0^c (f\cdot f_{xxyy})dxdy$$

$$- \int_0^1\int_0^c (f\cdot f_{yyyy})dxdy + 2\cdot\int_0^1\int_0^c (f\cdot g_{xy}\cdot\theta_{xy})\,dxdy$$

$$- \int_0^1\int_0^c (f\cdot g_{xx}\cdot\theta_{yy})dxdy - \int_0^1\int_0^c (f\cdot g_{yy}\cdot\theta_{xx})dxdy = 0\ . \qquad (A.1)$$

In order to reduce the order of differentiation, integration by parts is performed on each integral term in (A.1) as shown below:

$$\int_0^1\int_0^c (g\cdot g_{xxxx})dxdy = \int_0^c \left\{[g\cdot g_{xxx}]_{x=0}^{x=1} - \int_0^1 (g_{xxx}\cdot g_x)dx\right\} dy$$

$$= - \int_0^1\int_0^c (g_{xxx}\cdot g_x)dxdy + \int_0^c [g\cdot g_{xxx}]_{x=0}^{x=1}\,dy \qquad (A.2)$$

and then

$$-\int_0^1\int_0^c (g_{xxx}\cdot g_x)\,dxdy = -\int_0^c \left\{[g_x\cdot g_{xx}]_{x=0}^{x=1} + \int_0^1 (g_{xx}\cdot g_{xx})\,dx\right\} dy$$

$$= \int_0^1\int_0^c (g_{xx})^2\,dxdy - \int_0^c [g_x\cdot g_{xx}]_{x=0}^{x=1}\,dy \qquad (A.3)$$

Substituting (A.3) into (A.2) yields

$$\int_0^1\int_0^c (g\cdot g_{xxxx})\,dxdy = \int_0^1\int_0^c (g_{xx})^2\,dxdy - \int_0^c [g_x\cdot g_{xx}]_{x=0}^{x=1}\,dy$$

$$+ \int_0^c [g\cdot g_{xxx}]_{x=0}^{x=1}\,dy \qquad (A.4)$$

The remaining terms in (A.1) are integrated in a similar manner to yield

$$2\cdot\int_0^1\int_0^c (g\cdot g_{xxyy}) = 2\cdot\int_0^1\int_0^c (g_{xx}\cdot g_{yy})\,dxdy - \int_0^c [g_x\cdot g_{yy}]_{x=0}^{x=1}\,dy$$

$$+ \int_0^c [g\cdot g_{xyy}]_{x=0}^{x=1}\,dy - \int_0^1 [g_y\cdot g_{xx}]_{y=0}^{y=c}\,dx$$

$$+ \int_0^1 [g\cdot g_{xxy}]_{y=0}^{y=c}\,dx \qquad (A.5)$$

$$\int_0^1\int_0^c (g\cdot g_{yyyy})\,dxdy = \int_0^1\int_0^c (g_{yy})^2\,dxdy - \int_0^1 [g_y\cdot g_{yy}]_{y=0}^{y=c}\,dx$$

$$+ \int_0^1 [g\cdot g_{yyy}]_{y=0}^{y=c}\,dx \qquad (A.6)$$

$$-\int_0^1\int_0^c (g\cdot g_{xx}\cdot\chi_{yy})\,dxdy = \int_0^1\int_0^c \left\{(\chi_{yy}\cdot g)_x\cdot\ g_x\right\} dxdy$$

$$-\int_0^c [\chi_{yy}\cdot g\cdot g_x]_{x=0}^{x=1}\,dy$$

$$=\int_0^1\int_0^c (\chi_{yyx}\cdot g\cdot g_x)\,dxdy + \int_0^1\int_0^c (\chi_{yy}$$

$$\cdot (g_x)^2)\,dxdy - \int_0^c [\chi_{yy}\cdot g\cdot g_x]_{x=0}^{x=1}\,dy$$

(A.7)

$$-\int_0^1\int_0^c (g\cdot g_{yy}\cdot\chi_{xx})\,dxdy = \int_0^1\int_0^c (\chi_{xxy}\cdot g\cdot g_y)\,dxdy + \int_0^1\int_0^c (\chi_{xx}$$

$$\cdot (g_y)^2)\,dxdy - \int_0^1 [\chi_{xx}\cdot g\cdot g_y]_{y=0}^{y=c}\,dx$$

(A.8)

$$-\int_0^1\int_0^c (g\cdot f_{yy}\cdot\theta_{xx})\,dxdy = \int_0^1\int_0^c (g\cdot f_y\cdot\theta_{xxy})\,dxdy + \int_0^1\int_0^c (g_y\cdot f_y\cdot\theta_{xx})$$

$$dxdy - \int_0^1 [g\cdot f_y\cdot\theta_{xx}]_{y=0}^{y=c}\,dx \qquad (A.9)$$

$$-\int_0^1\int_0^c (g\cdot f_{xx}\cdot\theta_{yy})\,dxdy = \int_0^1\int_0^c (g\cdot f_x\cdot\theta_{xyy})\,dxdy + \int_0^1\int_0^c (g_x\cdot f_x$$

$$\cdot\ \theta_{yy})\,dxdy - \int_0^c [g\cdot f_x\cdot\theta_{yy}]_{x=0}^{x=1}\,dy \qquad (A.10)$$

$$2 \cdot \int_0^1\int_0^c (g \cdot g_{xy} \cdot \chi_{xy})\,dxdy = - \int_0^1\int_0^c (g \cdot g_y \cdot \chi_{xxy})\,dxdy$$

$$- 2 \cdot \int_0^1\int_0^c (g_x \cdot g_y \cdot \chi_{xy})\,dxdy$$

$$- \int_0^1\int_0^c (g \cdot g_x \cdot \chi_{xyy})\,dxdy + \int_0^c [g \cdot g_y$$

$$\cdot \chi_{xy}]_{x=0}^{x=1}\,dy + \int_0^1 [g \cdot g_x \cdot \chi_{xy}]_{y=0}^{y=c}\,dx \qquad (A.11)$$

$$2 \cdot \int_0^1\int_0^c (g \cdot f_{xy} \cdot \theta_{xy})\,dxdy = - \int_0^1\int_0^c (g \cdot f_y \cdot \theta_{xxy})\,dxdy - \int_0^1\int_0^c (g_x \cdot f_y$$

$$\cdot \theta_{xy})\,dxdy - \int_0^1\int_0^c (g \cdot f_x \cdot \theta_{xyy})\,dxdy$$

$$- \int_0^1\int_0^c (g_y \cdot f_x \cdot \theta_{xy})\,dxdy + \int_0^c [g \cdot f_y$$

$$\cdot \theta_{xy}]_{x=0}^{x=1}\,dy + \int_0^1 [g \cdot f_x \cdot \theta_{xy}]_{y=0}^{y=c}\,dx \qquad (A.12)$$

$$\Omega^2 \cdot \int_0^1\int_0^c g^2\,dxdy = \Omega^2 \int_0^1\int_0^c g^2\,dxdy \qquad (A.13)$$

$$\int_0^1\int_0^c (f \cdot f_{xxxx})\,dxdy = \int_0^1\int_0^c (f_{xx})^2\,dxdy - \int_0^c [f_x \cdot f_{xx}]_{x=0}^{x=1}\,dy$$

$$+ \int_0^c [f \cdot f_{xxx}]_{x=0}^{x=1}\,dy \qquad (A.14)$$

$$2 \cdot \int_0^1\int_0^c (f \cdot f_{xxyy})dxdy = 2 \cdot \int_0^1\int_0^c (f_{xx} \cdot f_{yy})dxdy - \int_0^c [f_x \cdot f_{yy}]_{x=0}^{x=1} dy$$

$$+ \int_0^c [f \cdot f_{xyy}]_{x=0}^{x=1} dy - \int_0^1 [f_y \cdot f_{xx}]_{y=0}^{y=c} dx$$

$$+ \int_0^1 [f \cdot f_{xxy}]_{y=0}^{y=c} dx \qquad (A.15)$$

$$\int_0^1\int_0^c (f \cdot f_{yyyy})dxdy = \int_0^1\int_0^c (f_{yy})^2 dxdy - \int_0^1 [f_y \cdot f_{yy}]_{y=0}^{y=c} dx$$

$$+ \int_0^1 [f \cdot f_{yyy}]_{y=0}^{y=c} dx \qquad (A.16)$$

$$2 \cdot \int_0^1\int_0^c (f \cdot g_{xy} \cdot \theta_{xy})dxdy = - \int_0^1\int_0^c (f \cdot g_y \cdot \theta_{xxy})dxdy - \int_0^1\int_0^c (f_x \cdot g_y$$

$$\cdot \theta_{xy})dxdy - \int_0^1\int_0^c (f \cdot g_x \cdot \theta_{xy})dxdy$$

$$- \int_0^1\int_0^c (f_y \cdot g_x \cdot \theta_{xy})dxdy + \int_0^c [f \cdot g_y$$

$$\cdot \theta_{xy}]_{x=0}^{x=1} dy + \int_0^1 [f \cdot g_x \cdot \theta_{xy}]_{y=0}^{y=c} dx \qquad (A.17)$$

$$- \int_0^1\int_0^c (f \cdot g_{xx} \cdot \theta_{yy})dxdy = \int_0^1\int_0^c (f \cdot g_x \cdot \theta_{xyy})dxdy$$

$$+ \int_0^1\int_0^c (f_x \cdot g_x \cdot \theta_{yy})dxdy$$

$$- \int_0^c [f \cdot g_x \cdot \theta_{yy}]_{x=0}^{x=1} dy \qquad (A.18)$$

$$-\int_0^1\int_0^c (f\cdot g_{yy}\cdot\theta_{xx})dxdy = \int_0^1\int_0^c (f\cdot g_y\cdot\theta_{xxy})dxdy$$

$$+\int_0^1\int_0^c (f_y\cdot g_y\cdot\theta_{xx})dxdy$$

$$-\int_0^1 [f\cdot g_y\cdot\theta_{xx}]_{y=0}^{y=1}\,dx \qquad (A.19)$$

Eliminating the double integral terms in equations (A.4) through (A.19) that are identical but have opposite signs, and substituting the remaining double integral terms into (A.1) produces equation (3.44). Since the same boundary conditions exist on g that exist on w, applying the conditions shown in Figure 2.3 to equations (A.4) - (A.19) causes all but the following boundary terms to vanish:

$$\int_0^c [f_x\cdot f_{xx}]_{x=0}^{x=1}\,dy - \int_0^c [f\cdot f_{xxx}]_{x=0}^{x=1}\,dy + \int_0^c [f_x\cdot f_{yy}]_{x=0}^{x=1}\,dy$$

$$-\int_0^c [f\cdot f_{xyy}]_{x=0}^{x=1}\,dy \qquad (A.20)$$

and

$$\int_0^1 [f_y\cdot f_{yy}]_{y=0}^{y=c}\,dx - \int_0^1 [f\cdot f_{yyy}]_{y=0}^{y=c}\,dx + \int_0^1 [f_y\cdot f_{xx}]_{y=0}^{y=c}\,dx$$

$$-\int_0^1 [f\cdot f_{xxy}]_{y=0}^{y=c}\,dx \qquad (A.21)$$

In order to reduce the order of differentiation, integration by parts is performed on each term in (A.20) and (A.21) as follows:

$$\int_0^c [f_x \cdot f_{xx}]_{x=0}^{x=1} dy = \int_0^c \left\{ f_x(1,y) \cdot f_{xx}(1,y) \right\} dy$$

$$- \int_0^c \left\{ f_x(0,y) \cdot f_{xx}(0,y) \right\} dy$$

$$= - \int_0^c \left\{ f_{xx}(1,y) \cdot f_x(1,y) \right\} dy + [f_x(1,c)]^2$$

$$- [f_x(1,0)]^2 + \int_0^c \left\{ f_{xx}(0,y) \cdot f_x(0,y) \right\} dy$$

$$- [f_x(0,c)]^2 + [f_x(0,0)]^2 \qquad \text{(A.22)}$$

$$- \int_0^c [f \cdot f_{xxx}]_{x=0}^{x=1} dy = \int_0^c \left\{ f_x(1,y) \cdot f_{xx}(1,y) \right\} dy - f(1,c) \cdot f_{xx}(1,c)$$

$$+ f(1,0) \cdot f_{xx}(1,0) - \int_0^c \left\{ f_x(0,y) \cdot f_{xx}(0,y) \right\} dy$$

$$+ f(0,c) \cdot f_{xx}(0,c) - f(0,0) \cdot f_{xx}(0,0) \qquad \text{(A.23)}$$

Each integral term in (A.22) has a matching term in (A.23) that has the opposite sign, and, therefore, all of the integral terms vanish. The remaining terms are functions of "f" and its derivatives at the corners. Since "f" represents the dynamic equivalent of the non-dimensionalized stress function, χ, it is equivalent to a second integral of the actual stress (equation 3.5). Some constants of integration are free to be chosen, and f and its first derivatives will be assumed to vanish at the corners. Thus, all of the boundary terms in (A.22) and (A.23) are eliminated. The remaining six terms in

equations (A.20) and (A.21) can be integrated in a manner similar to that shown in equations (A.22) and (A.23), and the same procedure is used for eliminating the integral terms along the boundaries and the corner boundary terms. Thus the final result consists of the double integral expression (equation 3.44), and all boundary terms vanish.

APPENDIX B

Application of Variational Calculus to the Augmented Objective Function

Application of Variational Calculus to the Augmented Objective Function

Equation (3.57) is evaluated eleven times, once for each variable upon which p* is dependent, and the eleven governing equations are produced. The substitution of each variable into equation (3,57) is discussed in the paragraphs that follow.

Substituting "wo + εη" for "wo" in equation (3.55) and recognizing that only the terms containing "ε" need to be retained results in

$$
\begin{aligned}
p^* = \int_0^1\int_0^c \Big\{ & \lambda_1 \cdot [2 \cdot w_{xy} \cdot (wo+\varepsilon\eta)_{xy} - w_{xx} \cdot (wo+\varepsilon\eta)_{yy} \\
& - w_{yy} \cdot (wo+\varepsilon\eta)_{xx}] \Big\} dxdy - \int_0^1\int_0^c \Big\{ \lambda_2 \cdot [- \chi_{yy} \cdot (w_{xx} - (wo+\varepsilon\eta)_{xx}) \\
& - \chi_{xx} \cdot (w_{yy} - (wo+\varepsilon\eta)_{yy}) + 2 \cdot \chi_{xy} \cdot (w_{xy} - (wo+\varepsilon\eta)_{xy})] \Big\} dxdy \\
& - \lambda_3 \cdot \Big\{ \Omega^2 - \int_0^1\int_0^c [2 \cdot f_x \cdot g_x \cdot (w_{yy} - (wo+\varepsilon\eta)_{yy}) \\
& + 2 \cdot f_y \cdot g_y \cdot (w_{xx} - (wo+\varepsilon\eta)_{xx}) - 2 \cdot f_y \cdot g_x \cdot (w_{xy} - (wo+\varepsilon\eta)_{xy}) \\
& - 2 \cdot f_x \cdot g_y \cdot (w_{xy} - (wo+\varepsilon\eta)_{xy})] dxdy \Big\} - \lambda_4 \cdot \Big\{ \frac{1}{2} \cdot \int_0^1\int_0^c [(wo+\varepsilon\eta)_x^2 \\
& + (wo+\varepsilon\eta)_y^2] \, dxdy - \beta^2 \Big\} \qquad \text{(B.1)}
\end{aligned}
$$

Substituting (B.1) into (3.57) gives

$$- \int_0^1\int_0^c \left\{\lambda_1 \cdot [2 \cdot w_{xy} \cdot \eta_{xy} - w_{xx} \cdot \eta_{yy} - w_{yy} \cdot \eta_{xx}]\right\}dxdy$$

$$- \int_0^1\int_0^c \left\{\lambda_2 \cdot [\chi_{yy} \cdot \eta_{xx} + \chi_{xx} \cdot \eta_{yy} - 2 \cdot \chi_{xy} \cdot \eta_{xy}]\right\}dxdy$$

$$- \lambda_3 \cdot \left\{\int_0^1\int_0^c [2 \cdot f_x \cdot g_x \cdot \eta_{yy} + 2 \cdot f_y \cdot g_y \cdot \eta_{xx} - 2 \cdot f_x \cdot g_y \cdot \eta_{xy}\right.$$

$$\left. - 2 \cdot f_y \cdot g_x \cdot \eta_{xy}]dxdy\right\}$$

$$- \lambda_4 \cdot \left\{\int_0^1\int_0^c [wo_x \cdot \eta_x + wo_y \cdot \eta_y]dxdy\right\} = 0 \qquad \text{(B.2)}$$

Each term in (B.2) must be expressed in terms of η and not in terms of the derivatives of η. Therefore integration by parts is performed on each term as shown below:

$$- 2 \cdot \int_0^1\int_0^c (\lambda_1 \cdot w_{xy} \cdot \eta_{xy})dxdy = - 2 \cdot \int_0^1\int_0^c [(\lambda_1 \cdot w_{xy})_{xy} \cdot \eta]dxdy$$

$$+ \int_0^1 [(\lambda_1 \cdot w_{xy})_x \cdot \eta]_{y=0}^{y=c} dx$$

$$- \int_0^c [\lambda_1 \cdot w_{xy} \cdot \eta_y]_{x=0}^{x=1} dy$$

$$+ \int_0^c [\lambda_1 \cdot w_{xy})_y \cdot \eta]_{x=0}^{x=1} dy$$

$$- \int_0^1 [\lambda_1 \cdot w_{xy} \cdot \eta_x]_{y=0}^{y=c} dx \qquad \text{(B.3)}$$

$$\int_0^1\int_0^c (\lambda_1 \cdot w_{xx} \cdot \eta_{yy})dxdy = \int_0^1\int_0^c [(\lambda_1 \cdot w_{xx})_{yy} \cdot \eta]dxdy$$

$$- \int_0^1 [(\lambda_1 \cdot w_{xx})_y \cdot \eta]_{y=0}^{y=c} dx$$

$$+ \int_0^1 [\lambda_1 \cdot w_{xx} \cdot \eta_y]_{y=0}^{y=c} dx \qquad (B.4)$$

$$\int_0^1\int_0^c (\lambda_1 \cdot w_{yy} \cdot \eta_{xx})dxdy = \int_0^1\int_0^c [\lambda_1 \cdot w_{yy})_{xx} \cdot \eta]dxdy$$

$$- \int_0^c [(\lambda_1 \cdot w_{yy})_x \cdot \eta]_{x=0}^{x=1} dy$$

$$- \int_0^c [\lambda_1 \cdot w_{yy} \cdot \eta_x]_{x=0}^{x=1} dy \qquad (B.5)$$

$$- \int_0^1\int_0^c (\lambda_2 \cdot \chi_{yy} \cdot \eta_{xx})dxdy = - \int_0^1\int_0^c [(\lambda_2 \cdot \chi_{yy})_{xx} \cdot \eta]dxdy$$

$$+ \int_0^c [(\lambda_2 \cdot \chi_{yy})_x \cdot \eta]_{x=0}^{x=1} dy$$

$$- \int_0^c [\lambda_2 \cdot \chi_{yy} \cdot \eta_x]_{x=0}^{x=1} dy \qquad (B.6)$$

$$- \int_0^1\int_0^c (\lambda_2 \cdot \chi_{xx} \cdot \eta_{yy})dxdy = - \int_0^1\int_0^c [(\lambda_2 \cdot \chi_{xx})_{yy} \cdot \eta]dxdy$$

$$+ \int_0^1 [(\lambda_2 \cdot \chi_{xx})_y \cdot \eta]_{y=0}^{y=c} dx$$

$$- \int_0^1 [\lambda_2 \cdot \chi_{xx} \cdot \eta_y]_{y=0}^{y=c} dx \qquad (B.7)$$

$$2 \cdot \int_0^1\int_0^c (\lambda_2 \cdot \chi_{xy} \cdot \eta_{xy})dxdy = 2 \cdot \int_0^1\int_0^c [(\lambda_2 \cdot \chi_{xy})_{xy} \cdot \eta]dxdy$$

$$- \int_0^1 [(\lambda_2 \cdot \chi_{xy})_x \cdot \eta]_{y=0}^{y=c} dx$$

$$+ \int_0^c [\lambda_2 \cdot \chi_{xy} \cdot \eta_y]_{x=0}^{x=1} dy$$

$$- \int_0^c [\lambda_2 \cdot \chi_{xy}]_y \cdot \eta]_{x=0}^{x=1} dy$$

$$+ \int_0^1 [\lambda_2 \cdot \chi_{xy} \cdot \eta_x]_{y=0}^{y=c} dx \qquad (B.8)$$

$$- 2 \cdot \lambda_3 \cdot \int_0^1\int_0^c (f_x \cdot g_x \cdot \eta_{yy})dxdy = - 2 \cdot \lambda_3 \cdot \int_0^1\int_0^c [(f_x \cdot g_x)_{yy} \cdot \eta]dxdy$$

$$+ 2 \cdot \lambda_3 \cdot \int_0^1 [(f_x \cdot g_x)_y \cdot \eta]_{y=0}^{y=c} dx$$

$$- 2 \cdot \lambda_3 \cdot \int_0^1 [f_x \cdot g_x \cdot \eta_y]_{y=0}^{y=c} dx \qquad (B.9)$$

$$- 2 \cdot \lambda_3 \cdot \int_0^1\int_0^c (f_y \cdot g_y \cdot \eta_{xx})dxdy = - 2 \cdot \lambda_3 \cdot \int_0^1\int_0^c [(f_y \cdot g_y)_{xx} \cdot \eta]dxdy$$

$$+ 2 \cdot \lambda_3 \cdot \int_0^1 [f_x \cdot g_x)_y \cdot \eta]_{y=0}^{y=1} dx$$

$$- 2 \cdot \lambda_3 \cdot \int_0^c [f_y \cdot g_y \cdot \eta_x]_{x=0}^{x=1} dy \qquad (B.10)$$

$$2 \cdot \lambda_3 \cdot \int_0^1\int_0^c (f_y \cdot g_x \cdot \eta_{xy})dxdy = 2 \cdot \lambda_3 \cdot \int_0^1\int_0^c [f_y \cdot g_x)_{xy} \cdot \eta]dxdy$$

$$- \lambda_3 \cdot \int_0^1 [f_y \cdot g_x)_x \cdot \eta]_{y=0}^{y=c} dx + \lambda_3 \cdot \int_0^c [f_y \cdot g_x \cdot \eta_y]_{x=0}^{x=1} dy$$

$$- \lambda_3 \cdot \int_0^c [f_y \cdot g_x)_y \cdot \eta]_{x=0}^{x=1} dy + \lambda_3 \cdot \int_0^1 [f_y \cdot g_x \cdot \eta_x]_{y=0}^{y=c} dx \qquad (B.11)$$

$$2 \cdot \lambda_3 \cdot \int_0^1\int_0^c (f_x \cdot g_y \cdot \eta_{xy})dxdy = 2 \cdot \lambda_3 \cdot \int_0^1\int_0^c [(f_x \cdot g_y)_{xy} \cdot \eta]dxdy$$

$$- \lambda_3 \cdot \int_0^1 [f_x \cdot g_y)_x \cdot \eta]_{y=0}^{y=c} dx + \lambda_3 \cdot \int_0^c [f_x \cdot g_y \cdot \eta_y]_{x=0}^{x=1} dy$$

$$- \lambda_3 \cdot \int_0^c [(f_x \cdot g_y)_y \cdot \eta]_{x=0}^{x=1} dy + \lambda_3 \cdot \int_0^1 [f_x \cdot g_y \cdot \eta_x]_{y=0}^{y=c} dx \qquad (B.12)$$

$$- \lambda_4 \cdot \int_0^1\int_0^c (wo_x \cdot \eta_x)dxdy = \lambda_4 \cdot \int_0^1\int_0^c (wo_{xx} \cdot \eta)dxdy$$

$$- \lambda_4 \cdot \int_0^c [wo_x \cdot \eta]_{x=0}^{x=1} dy \qquad (B.13)$$

$$- \lambda_4 \cdot \int_0^1\int_0^c (wo_y \cdot \eta_y)dxdy = \lambda_4 \cdot \int_0^1\int_0^c (wo_{yy} \cdot \eta)dxdy$$

$$- \lambda_4 \cdot \int_0^1 [wo_y \cdot \eta]_{y=0}^{y=c} dx \qquad (B.14)$$

When the integrated expressions in equations (B.3) - (B.14) are substituted into equation (B.2), the result is an integral expression and boundary terms. The integral expression contains an Euler

(governing) equation multiplied by a constant, and is given below:

$$\int_0^1\int_0^c \eta\,[-2\cdot(\lambda_1\cdot w_{xy})_{xy} + (\lambda_1\cdot w_{xx})_{yy} + (\lambda_1\cdot w_{yy})_{xx}$$
$$- (\lambda_2\cdot \chi_{yy})_{xx} - (\lambda_2\cdot \chi_{xx})_{yy} + 2\cdot(\lambda_2\cdot \chi_{xy})_{xy}$$
$$- 2\cdot\lambda_3\cdot(f_x\cdot g_x)_{yy} - 2\cdot\lambda_3\cdot(f_y\cdot g_y)_{xx} + 2\cdot\lambda_3\cdot(f_y\cdot g_x)_{xy}$$
$$+ 2\cdot\lambda_3\cdot(f_x\cdot g_y)_{xy} + \lambda_4\cdot wo_{xx} + \lambda_4\cdot wo_{yy}]dxdy = 0 \qquad (B.15)$$

By expanding the derivatives on each term and then cancelling, and by realizing that the integrand must be equal to zero since η is an arbitrary function (only restricted by the boundary conditions on wo), the following equation is produced:

$$-2\cdot(\lambda_1)_{xy}\cdot w_{xy} + (\lambda_1)_{yy}\cdot w_{xx} + (\lambda_1)_{xx}\cdot w_{yy} + 2\cdot(\lambda_2)_{xy}\cdot \chi_{xy}$$
$$- (\lambda_2)_{yy}\cdot \chi_{xx} - (\lambda_2)_{xx}\cdot \chi_{yy} - 4\cdot\lambda_3\cdot f_{xy}\cdot g_{xy}$$
$$+ 2\cdot\lambda_3\cdot f_{yy}\cdot g_{xx} + 2\cdot\lambda_3\cdot f_{xx}\cdot g_{yy} + \lambda_4\cdot(wo_{xx} + wo_{yy}) = 0 \qquad (B.16)$$

Equation (B.16) is the same as equation (3.60), and thus the variation of p* with respect to wo produces the optimality condition.

The elimination of the boundary terms from equations (B.3) to (B.14) is accomplished by first expanding the derivatives as required. For instance,

$$
\begin{aligned}
-\int_0^1 [\lambda_1 \cdot w_{xy})_x \cdot \eta]_{y=0}^{y=c}\, dx &= -\int_0^1 [(\lambda_1)_x \cdot w_{xy} \cdot \eta]_{y=0}^{y=c}\, dx \\
&\quad -\int_0^1 [\lambda_1 \cdot w_{xxy} \cdot \eta]_{y=0}^{y=c}\, dx \\
&= -\int_0^1 [\lambda_1(x,c)_x \cdot w(x,c)_{xy} \cdot \eta]_{y=0}^{y=c}\, dx \\
&\quad -\int_0^1 [\lambda_1(x,0)_x \cdot w(x,0)_y \cdot \eta]_{y=0}^{y=c}\, dx \\
&\quad -\int_0^1 [\lambda_1(x,c) \cdot w(x,c)_{xxy} \cdot \eta]_{y=0}^{y=c}\, dx \\
&\quad -\int_0^1 [\lambda_1(x,0) \cdot w(x,0)_{xxy} \cdot \eta]_{y=0}^{y=c}\, dx
\end{aligned}
\tag{B.17}
$$

After the terms are expanded, they vanish by assigning the same boundary conditions to λ_2 that exist on w and g, and by cancelling terms.

Substituting "$\chi + \varepsilon\eta$" for "χ" in equation (3.55) and retaining only the terms containing ε results in

$$
\begin{aligned}
p^* = &-\int_0^1\int_0^c \Big\{\lambda_1 \cdot [(\chi+\varepsilon\eta)_{xxxx} + 2\cdot(\chi+\varepsilon\eta)_{xxyy} \\
&+ (\chi+\varepsilon\eta)_{yyyy}]\Big\}dxdy - \int_0^1\int_0^c \Big\{\lambda_2 \cdot [-(\chi+\varepsilon\eta)_{yy}\cdot\theta_{xx} \\
&- (\chi+\varepsilon\eta)_{xx}\cdot\theta_{yy} + 2\cdot(\chi+\varepsilon\eta)_{xy}\cdot\theta_{xy}]\Big\}dxdy \\
&- \lambda_3 \cdot \Big\{\int_0^1\int_0^c [-(\chi+\varepsilon\eta)_{yy}\cdot(g_x)^2 - (\chi+\varepsilon\eta)_{xx}\cdot(g_y)^2 \\
&+ 2\cdot(\chi+\varepsilon\eta)_{xy}\cdot g_x\cdot g_y]dxdy\Big\}
\end{aligned}
\tag{B.18}
$$

Substituting (B.18) into (3.57) yields

$$- \int_0^1\int_0^c \left\{\lambda_1 \cdot [\eta_{xxxx} + 2 \cdot \eta_{xxyy} + \eta_{yyyy}]\right\}dxdy$$

$$- \int_0^1\int_0^c \left\{\lambda_2 \cdot [- \theta_{xx} \cdot \eta_{yy} - \theta_{yy} \cdot \eta_{xx} + 2 \cdot \theta_{xy} \cdot \eta_{xy}]\right\}dxdy$$

$$- \lambda_3 \cdot \left\{\int_0^1\int_0^c [-(g_x)^2 \cdot \eta_{yy} - (g_y)^2 \cdot \eta_{xx}\right.$$

$$\left. + 2 \cdot \eta_{xy} \cdot g_x \cdot g_y]dxdy\right\} = 0 \qquad \text{(B.19)}$$

Integration by parts is performed in order to express (B.19) in terms of "η" and is accomplished in a manner similar to that done previously for wo. The results of the integration by parts include an integral expression and boundary terms. The integrand must equal zero, and the resulting equation is given by equation (3.59) which, in conjunction with equation (3.58), describes the adjoint problem. The boundary terms are made to vanish by expanding derivatives as required, assigning the same boundary conditions to λ_1 that exist on χ, and cancelling terms.

Substituting "$w+\varepsilon\eta$" for "w" in equation (3.55) and retaining only the terms containing ε results in

$$p^* = - \int_0^1\int_0^c \left\{\lambda_1 \cdot [- (w+\varepsilon\eta)_{xy}^2 + 2 \cdot (w+\varepsilon\eta)_{xy} \cdot wo_{xy}\right.$$

$$+ (w+\varepsilon\eta)_{xx} \cdot (w+\varepsilon\eta)_{yy} - (w+\varepsilon\eta)_{xx} \cdot wo_{yy}$$

$$\left. - (w+\varepsilon\eta)_{yy} \cdot wo_{xx}]\right\}dxdy$$

$$- \int_0^1\int_0^c \left\{\lambda_2 \cdot [(w+\varepsilon\eta)_{xxxx} + 2 \cdot (w+\varepsilon\eta)_{xxyy} + (w+\varepsilon\eta)_{yyyy}\right.$$

$$- \chi_{yy} \cdot ((w+\varepsilon\eta)_{xx} - wo_{xx}) - \chi_{xx} \cdot ((w+\varepsilon\eta)_{yy} - wo_{yy}$$

$$+ 2 \cdot \chi_{xy} \cdot ((w+\varepsilon\eta)_{xy} - wo_{xy})]\Big\}dxdy$$

$$- \lambda_3 \cdot \Big\{\int_0^1\int_0^c [-2 \cdot f_x \cdot g_x \cdot ((w+\varepsilon\eta)_{yy} - wo_{yy}) - 2 \cdot f_y \cdot g_y \cdot ((w+\varepsilon\eta)_{xx}$$

$$- wo_{xx}) + 2 \cdot f_y \cdot g_x \cdot ((w+\varepsilon\eta)_{xy} - wo_{xy}) + 2 \cdot f_x \cdot g_y \cdot ((w+\varepsilon\eta)_{xy}$$

$$- wo_{xy})]dxdy\Big\} \qquad \text{(B.20)}$$

Substituting (B.20) into (3.57) yields

$$- \int_0^1\int_0^c \Big\{\lambda_1 \cdot [-2 \cdot \theta_{xy} \cdot \eta_{xy} + \theta_{xx} \cdot \eta_{yy} + \theta_{yy} \cdot \eta_{xx}]\Big\}dxdy$$

$$- \int_0^1\int_0^c \Big\{\lambda_2 \cdot [\eta_{xxxx} + 2 \cdot \eta_{xxyy} + \eta_{yyyy} - \chi_{yy} \cdot \eta_{xx} - \chi_{xx} \cdot \eta_{yy}$$

$$+ 2 \cdot \chi_{xy} \cdot \eta_{xy}]\Big\}dxdy - \lambda_3 \cdot \Big\{\int_0^1\int_0^c [-2 \cdot f_x \cdot g_x \cdot \eta_{yy}$$

$$- 2 \cdot f_y \cdot g_y \cdot \eta_{xx} + 2 \cdot f_y \cdot g_x \cdot \eta_{xy} + 2 \cdot f_x \cdot g_y \cdot \eta_{xy}]dxdy\Big\} \qquad \text{(B.21)}$$

Integration by parts is performed in order to express (B.21) in terms of "η" and is accomplished in a manner similar to that done previously for wo. The resulting integrand expression is given as equation (3.58) which, in conjunction with equation (3.59), describes the adjoint problem. The boundary terms vanish by expanding the derivatives as required, assigning the same boundary conditions to λ_2 that exist on w, and cancelling terms.

Substituting "$f+\varepsilon\eta$" for "f" in equation (3.55) and retaining only the terms containing ε results in

$$\lambda_3 \cdot \left\{ \int_0^1 \int_0^c [2 \cdot (f+\varepsilon\eta)_x \cdot g_x \cdot \theta_{yy} + 2 \cdot (f+\varepsilon\eta)_y \cdot g_y \cdot \theta_{xx} \right.$$
$$- 2 \cdot (f+\varepsilon\eta)_y \cdot g_x \cdot \theta_{xy} - 2 \cdot (f+\varepsilon\eta)_x \cdot g_y \cdot \theta_{xy}$$
$$- (f+\varepsilon\eta)_{xx}^2 - 2 \cdot (f+\varepsilon\eta)_{xx} \cdot (f+\varepsilon\eta)_{yy}$$
$$\left. - (f+\varepsilon\eta)_{yy}^2] dxdy \right\} \qquad \text{(B.22)}$$

Substituting (B.22) into (3.57) yields

$$\lambda_3 \cdot \left\{ \int_0^1 \int_0^c [2 \cdot g_x \cdot \theta_{yy} \cdot \eta_x + 2 \cdot g_y \cdot \theta_{xx} \cdot \eta_y - 2 \cdot g_x \cdot \theta_{xy} \cdot \eta_y \right.$$
$$- 2 \cdot g_y \cdot \theta_{xy} \cdot \eta_x - 2 \cdot f_{xx} \cdot \eta_{xx} - 2 \cdot f_{xx} \cdot \eta_{yy}$$
$$\left. - 2 \cdot f_{yy} \cdot \eta_{xx} - 2 \cdot f_{yy} \cdot \eta_{yy}] dxdy \right\} \qquad \text{(B.23)}$$

Integration by parts is performed on (B.23) and the resulting integrand expression is given by equation (3.42) which is one of the two vibration equations. Most of the boundary terms are made to vanish by cancelling terms; however, there are several terms that do not vanish, and they are given below:

$$2 \cdot \lambda_3 \cdot \left\{ \int_0^c [f_{xxx} \cdot \eta - f_{xx} \cdot \eta_x + f_{xyy} \cdot \eta - f_{yy} \cdot \eta_x]_{x=0}^{x=1} dy \right\} \qquad \text{(B.24a)}$$

$$2 \cdot \lambda_3 \cdot \left\{ \int_0^1 [f_{xxy} \cdot \eta - f_{xx} \cdot \eta_y + f_{yyy} \cdot \eta - f_{yy} \cdot \eta_y]_{y=0}^{y=c} dx \right\} \qquad \text{(B.24b)}$$

By following a procedure similar to the one used in Appendix A for equation (A.21) the integral terms in (B.24a,b) are made to vanish. Likewise, the resulting boundary terms at the corners are eliminated by assuming that f and its first derivatives are zero at the corners.

Substituting "g+εη" for "g" in equation (3.55) and retaining only the terms containing ε results in

$$p^* = \lambda_3 \cdot \left\{ \int_0^1 \int_0^c [-\Omega^2 \cdot (g+\varepsilon\eta)^2 + \chi_{yy} \cdot (g+\varepsilon\eta)_x^2 + \chi_{xx} \cdot (g+\varepsilon\eta)_y^2 \right.$$
$$- 2 \cdot \chi_{xy} \cdot (g+\varepsilon\eta)_x \cdot (g+\varepsilon\eta)_y + 2 \cdot f_x \cdot (g+\varepsilon\eta)_x \cdot \theta_{yy}$$
$$+ 2 \cdot f_y \cdot (g+\varepsilon\eta)_y \cdot \theta_{xx} - 2 \cdot f_y \cdot (g+\varepsilon\eta)_x \cdot \theta_{xy}$$
$$- 2 \cdot f_x \cdot (g+\varepsilon\eta)_y \cdot \theta_{xy} + (g+\varepsilon\eta)_{xx}^2 + 2(g+\varepsilon\eta)_{xx} \cdot (g+\varepsilon\eta)_{yy}$$
$$\left. + (g+\varepsilon\eta)_{yy}^2] dxdy \right\} - \lambda_5 \cdot \left\{ (g+\varepsilon\eta)^2 \, dxdy \right\} \qquad \text{(B.25)}$$

Substituting (B.25) into (3.57) yields

$$\lambda_3 \cdot \left\{ \int_0^1 \int_0^c [-2 \cdot \Omega^2 \cdot g \cdot \eta + 2 \cdot \chi_{yy} \cdot g_x \cdot \eta_x + 2 \cdot \chi_{xx} \cdot g_y \cdot \eta_y \right.$$
$$- 2 \cdot \chi_{xy} \cdot g_y \cdot \eta_x - 2 \cdot \chi_{xy} \cdot g_x \cdot \eta_y + 2 \cdot f_x \cdot \theta_{yy} \cdot \eta_x$$
$$+ 2 \cdot f_y \cdot \theta_{xx} \cdot \eta_y - 2 \cdot f_y \cdot \theta_{xy} \cdot \eta_x - 2 \cdot f_x \cdot \theta_{xy} \cdot \eta_y$$
$$+ 2 \cdot g_{xx} \cdot \eta_{xx} + 2 \cdot g_{xx} \cdot \eta_{yy} + 2 \cdot g_{yy} \cdot \eta_{xx}$$
$$\left. + 2 \cdot g_{yy} \cdot \eta_{yy}] dxdy \right\} - 2 \cdot \lambda_5 \cdot \int_0^1 \int_0^c (g \cdot \eta) dxdy \qquad \text{(B.26)}$$

Integration by parts is performed, derivatives are expanded, terms are cancelled, and the resulting integrand expression is given by equation (3.41) which is one of the two vibration equations. It should be noted that λ_5 and Ω^2 are assumed to equal zero in order to maintain equation (3.41) as a homogeneous equation. The boundary terms that are generated by the integration by parts are eliminated by cancelling terms.

Taking the variation of p* with respect to p is discussed in Chapter 3 and the results are given by equation (3.63) which represents the normalization of λ_2. Also as discussed in Chapter 3, taking the variation of p* with respect to λ_1, λ_2, λ_3, λ_4, and λ_5 reproduces equations (3.25) (equilibrium), (3.26) (compatibility), (3.44) (vibration functional), (3.53) (surface area), and (3.54) (normalization of g), respectively.

The two page vita has been removed from the scanned document. Page 1 of 2

The two page vita has been removed from the scanned document. Page 2 of 2